FLEXIBLE PZT-POLYMER LAMINATED COMPOSITE ELECTROMECHANICAL SENSORS AND ACTUATORS

by

Zheng Min

Bachelor of Mechanical Engineering, Central South University, 2011

Submitted to the Graduate Faculty of

Swanson School of Engineering in partial fulfillment

of the requirements for the degree of

Master of Science

University of Pittsburgh

2015

UNIVERSITY OF PITTSBURGH

SWANSON SCHOOL OF ENGINEERING

This thesis was presented

by

Zheng Min

It was defended on

November 24, 2015

and approved by

Qing-Ming Wang, Ph.D., Professor,

Department of Mechanical Engineering and Materials Science

William S. Slaughter, Ph.D., Associate Professor,

Department of Mechanical Engineering and Material Science

Patrick Smolinski, Ph.D., Associate Professor,

Department of Mechanical Engineering and Material Science

Thesis Advisor: Qing-Ming Wang, Ph.D., Professor,

Department of Mechanical Engineering and Materials Science

FLEXIBLE PZT-POLYMER LAMINATED COMPOSITE ELECTROMECHANICAL SENSORS AND ACTUATORS

Zheng Min, M.S.

University of Pittsburgh, 2015

Piezoelectric multilayer composite is widely used in piezoelectric devices which can offer a lot of benefits for applications of sensors and actuators. This kind of composite consists of several piezoelectric layers and several polymer layers connected in laminated composite structure in which both the piezoelectric and the polymer layers are continuous in two dimensions. In this thesis, lead zirconium titanate (PZT) film with thickness under 100um is chosen as the piezoelectric layers due to its relatively high piezoelectric charge constant, high electromechanical coupling effect and good mechanical flexibility. Five layers composite with two layers of PZT and three layers of polymer have been analyzed and developed for applications of two different structures of sensors and actuators including cantilever beam and doubly clamped beam. The static constitutive equations in matrix form for each structure under different excitations have been established analytically for theoretical analysis and characterization of the devices. Several dimensions of the polarizations of PZT element in doubly clamped beam are discussed for optimizing the electromechanical coupling performance. The dynamic admittance matrix which relates harmonic external excitations to their response parameters is also derived for cantilever beam. Several experiments have been conducted to partially verify the theoretical model. A cantilever beam actuator is fabricated and studied experimentally to verify the electromechanical

coupling properties under harmonic external voltage under different frequencies. Two vibration sensors with proof masses with different structures are designed and tested as accelerometers.

TABLE OF CONTENTS

LIST OF TABLES

LIST OF FIGURES

ACKNOWLEDGEMENT

I would like to thank first and foremost my these advisor Dr. Qing-Ming Wang, for his invaluable guidance and continuous support during this research work. Our conversations have, and always will be, of great value to me.

Also my committee members Dr. Smolinski and Dr. Slaughter. Thank you for your time and effort in reading and reviewing my thesis.

I am also extremely grateful to my research group members, Hongfei Zu, Huiyan Wu, Rongjie Liang, Qiuyan Li, Xuande Zhang for their help and encouragement in this research. Without you kind people, I would have never accomplished this work.

Special thanks to all the professors who teaches courses for me, the knowledge I have learned laid the solid foundation for this work.

Last, I would like to thank my family and my girlfriend for their unconditional support and love for my graduate studies, work and my life.

1.0 INTRODUCTION

In this chapter, some basic concepts and theories are introduced concerning fundamental properties of piezoelectric material, piezoelectric constitutive equations and elementary beam theory in section 1.1, section 1.2 and section 1.3 respectively. The fabrication process of the PZT-polymer composite will be presented in section 1.4. Section 1.5 involves the objective of the research work.

1.1 FUNDAMENTAL CONCEPTS OF PIEZOELECTRICITY

When we applied an external force on the piezoelectric material, the mechanical deformation will cause some electric charges to appear on its surface. This phenomenon was observed and recorded by the Curies in 1880. This property, which reveals a linear relationship between mechanical strain and electric field, is named as "piezoelectricity" by Hankel [1]. "*Piezo*-" here is derived from the Greek "to squeeze" or "to press." The piezoelectric effect presents the ability of piezoelectric material to generate electric charges under mechanical excitations that can be used to design sensors. The inverse piezoelectric effect, which we use for designing actuators, occurs in the opposite way: If an electric field is applied across a piezoelectric material, mechanical deformation occurs. Piezoelectricity occurs in the crystal whose structure do not have central symmetry [2]. This property, which can transfer energy between mechanical stress and electric field, is

observable in many natural crystalline materials, including quartz, Rochelle salt, and even human bone. Engineered material, such as Barium Titanate ($BaTiO_3$), lead zirconate titanate (PZT) and poly vinylidene (PVDF) exhibit a more pronounced piezoelectric effect. The microscopic origin of piezoelectricity is the displacement of ionic charges within a crystal. For example, α-quartz crystal has piezoelectricity in x-direction. If we look into a projection of a single cell of α-quartz in *xy* plane as shown in Figure 1-1, we can see that the distribution of ion Si^+ and ion O^{2-} make a shape of a regular hexagon under no stress state. In this state, the angles between each pair of dipole moments ($\overrightarrow{p_1}, \overrightarrow{p_2}, \overrightarrow{p_3}$) are all 120°. The summation of these three dipole moment vectors is 0, which means there is no charge generated on the surface of the crystal.

When a force (tension or compression) is applied on the quartz crystal in *y* direction as shown in Figure 1-2, the crystal will deform in this direction. Then the summation of three dipole moments will be a vector along *x* axis, which means charges will be generated on the positive and negative *x* surfaces. The same result occurs when a force is applied along *x* or *y* axis. The charges will accumulated on the x surfaces no matter which direction the mechanical stress is applied along. Thus *x* direction is called the polarization direction for α-quartz crystal.

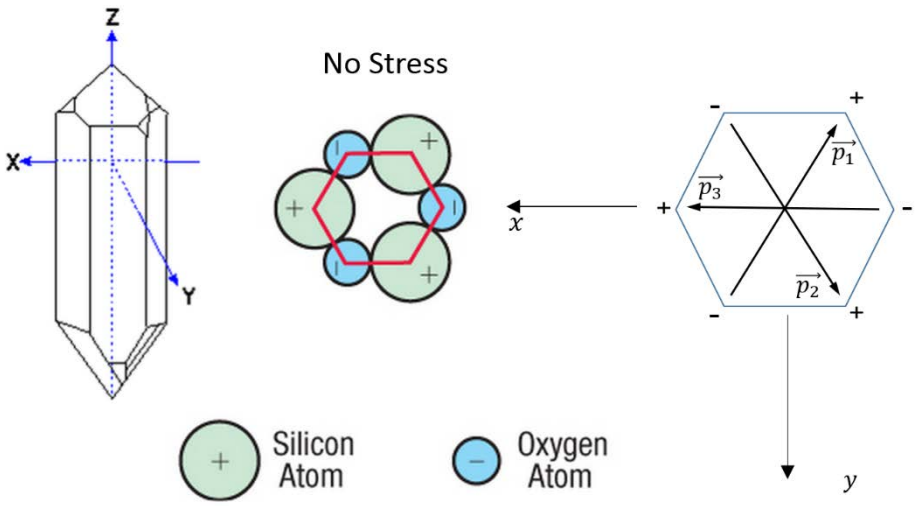

Figure 1-1 The atom distribution and dipole moments of α-quartz crystal in xy-plane

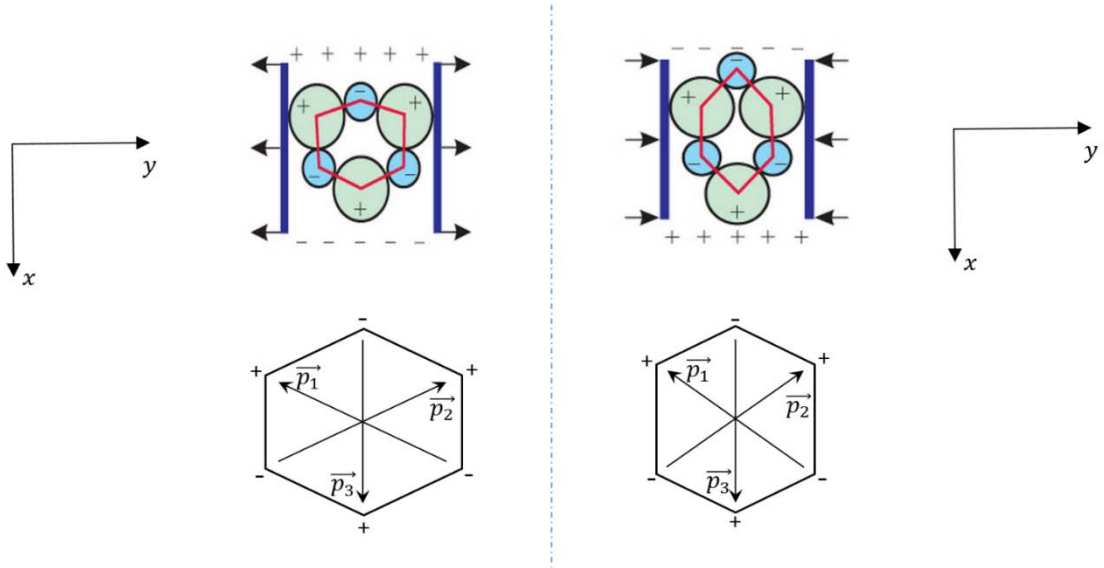

Figure 1-2 The atom distribution and dipole moments under stress in y direction

The polarization of a material is simply the total dipole moment for a unit volume $P = \frac{1}{V}\sum_i \vec{p}_i$, where V is the overall volume of the material. Because $\sum_i \vec{p}_i$ is a vector sum, the net polarization can be zero because the dipole moments can be randomly distributed in the material and cancel out. In the engineered piezoelectric material such as lead zirconate titanate (PZT) ceramics, Barium Titanate ($BaTiO_3$), the dipole moments are generally in randomly oriented when no external electric field is applied as shown in Figure 1-3(a). This kind of material will not present piezoelectricity unless a poling process is conducted. A poling process is an alignment of the dipole moments by applying an external DC electric field normally at a temperature below the Curie temperature. During the poling process, most of dipole moments aligned with the electric field (Figure 1-3(b)). When the external electric field is removed, most of the dipoles are locked into a configuration of near alignment (Figure 1-3(c)). Then the material has a permanent polarization after poling process.

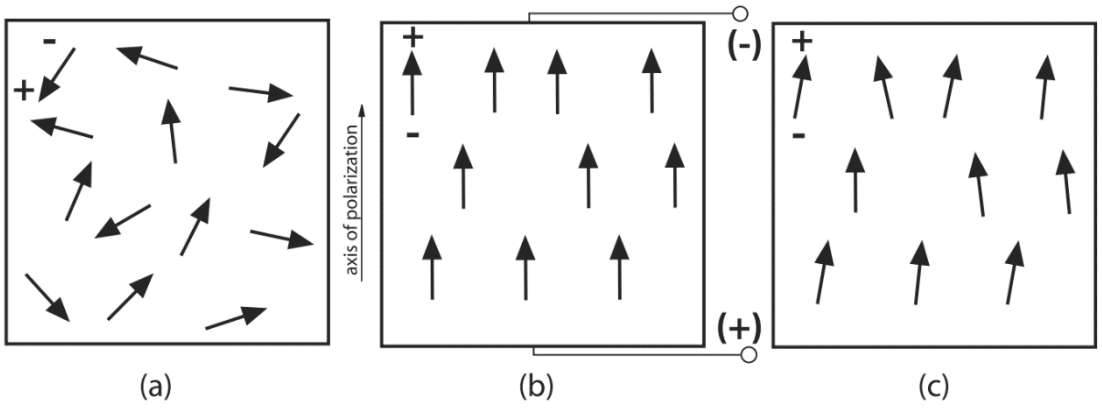

Figure 1-3 Poling process: (a) Unpoled ceramic; (b) During poling; (c) After poling process[3]

1.2 CONSTITUTIVE EQUATIONS OF PZT MATERIAL

In this section, we will introduce the three-dimensional form of the linear piezoelectric constitutive equations of PZT material. We usually consider the polarization axis of the piezoelectric material as *z* axis [4]. A set of linear equations which relate field variables including stress tensor (T_{ij}), strain tensor (S_{ij}), electric field components (E_k), and the electric displacement components (D_k) are introduced to describe the piezoelectric effect which are called as constitutive equations. The standard form of the piezoelectric constitutive equations can be given in four different forms by taking either two of the four field variables as the independent variables. These equations can be written as:

$$\begin{cases} S = s^E T + d^t E \\ D = dT + \varepsilon^T E \end{cases} \tag{1.1}$$

$$\begin{cases} T = c^E S - e^t E \\ D = eS + \varepsilon^S E \end{cases} \tag{1.2}$$

$$\begin{cases} S = s^D T + g^t D \\ E = -gT + \beta^T D \end{cases} \tag{1.3}$$

$$\begin{cases} T = c^D S - h^t D \\ E = -hS + \beta^S D \end{cases} \tag{1.4}$$

Where all the matrixes with superscript *t* are the transpose of the matrix. The superscript *E,D,T,S* indicate the constant electric field, constant electrical displacement, constant stress condition and constant strain condition respectively. The $s, d, \varepsilon, c, e, g, \beta, h$ indicate mechanical compliance coefficient tensor, piezoelectric strain coefficient tensor, permittivity tensor, stiffness coefficient tensor, piezoelectric stress coefficient tensor, piezoelectric voltage coefficient tensor,

reciprocal permittivity tensor and piezoelectric charge coefficient tensor respectively. Consider the form with stress components and electric field as components as independent variables, we usually use form of equation (1.1) as the constitutive equations for piezoelectric material.

The constitutive equations for poled PZT material can be written as[5]:

$$\begin{bmatrix} S_1 \\ S_2 \\ S_3 \\ S_4 \\ S_5 \\ S_6 \end{bmatrix} = \begin{bmatrix} s_{11}^E & s_{12}^E & s_{13}^E & 0 & 0 & 0 \\ s_{21}^E & s_{22}^E & s_{23}^E & 0 & 0 & 0 \\ s_{31}^E & s_{32}^E & s_{33}^E & 0 & 0 & 0 \\ 0 & 0 & 0 & s_{44}^E & 0 & 0 \\ 0 & 0 & 0 & 0 & s_{55}^E & 0 \\ 0 & 0 & 0 & 0 & 0 & s_{66}^E = 2\left(s_{11}^E - s_{12}^E\right) \end{bmatrix} \begin{bmatrix} T_1 \\ T_2 \\ T_3 \\ T_4 \\ T_5 \\ T_6 \end{bmatrix} + \begin{bmatrix} 0 & 0 & d_{31} \\ 0 & 0 & d_{32} \\ 0 & 0 & d_{33} \\ 0 & d_{24} & 0 \\ d_{15} & 0 & 0 \\ 0 & 0 & 0 \end{bmatrix} \begin{bmatrix} E_1 \\ E_2 \\ E_3 \end{bmatrix} \tag{1.5}$$

$$\begin{bmatrix} D_1 \\ D_2 \\ D_3 \end{bmatrix} = \begin{bmatrix} 0 & 0 & 0 & 0 & d_{15} & 0 \\ 0 & 0 & 0 & d_{24} & 0 & 0 \\ d_{31} & d_{32} & d_{33} & 0 & 0 & 0 \end{bmatrix} \begin{bmatrix} T_1 \\ T_2 \\ T_3 \\ T_4 \\ T_5 \\ T_6 \end{bmatrix} + \begin{bmatrix} \varepsilon_{11} & 0 & 0 \\ 0 & \varepsilon_{22} & 0 \\ 0 & 0 & \varepsilon_{33} \end{bmatrix} \begin{bmatrix} E_1 \\ E_2 \\ E_3 \end{bmatrix} \tag{1.6}$$

Where the contracted notation is used so that the vectors and strain and stress components are

$$\begin{bmatrix} S_1 \\ S_2 \\ S_3 \\ S_4 \\ S_5 \\ S_6 \end{bmatrix} = \begin{bmatrix} S_{11} \\ S_{22} \\ S_{33} \\ 2S_{23} \\ 2S_{13} \\ 2S_{12} \end{bmatrix}, \quad \begin{bmatrix} T_1 \\ T_2 \\ T_3 \\ T_4 \\ T_5 \\ T_6 \end{bmatrix} = \begin{bmatrix} T_{11} \\ T_{22} \\ T_{33} \\ T_{23} \\ T_{13} \\ T_{12} \end{bmatrix} \tag{1.7}$$

Now we look into a reduced form of equations for a thin beam which will be the structure model throughout this thesis[6]. Consider the polarization axis is *z* axis (or 3-axis) and electrode pair covers the face perpendicular to polarization direction. Based on the Euler-Bernoulli beam theory, the stress components other than bending normal stress T_1 can be neglected so we have

$$T_2 = T_3 = T_4 = T_5 = T_6 = 0 \tag{1.8}$$

Substituting equation (1.8) into constitutive equations (1.5) and (1.6) for PZT material, the constitutive equations of PZT material for a thin beam can be simplified as

$$\begin{bmatrix} S_1 \\ D_3 \end{bmatrix} = \begin{bmatrix} s_{11}^E & d_{31} \\ d_{31} & \varepsilon_{33}^T \end{bmatrix} \begin{bmatrix} T_1 \\ E_3 \end{bmatrix} \tag{1.9}$$

1.3 ELEMENTARY BEAM THEORY

In this thesis, some PZT-polymer composites will be fabricated to construct some sensors and actuators with different structures including cantilever beam and doubly clamped beam. To establish mathematical models for analyzing the mechanical properties of these structures, the elementary beam theory need to be introduced in this section.

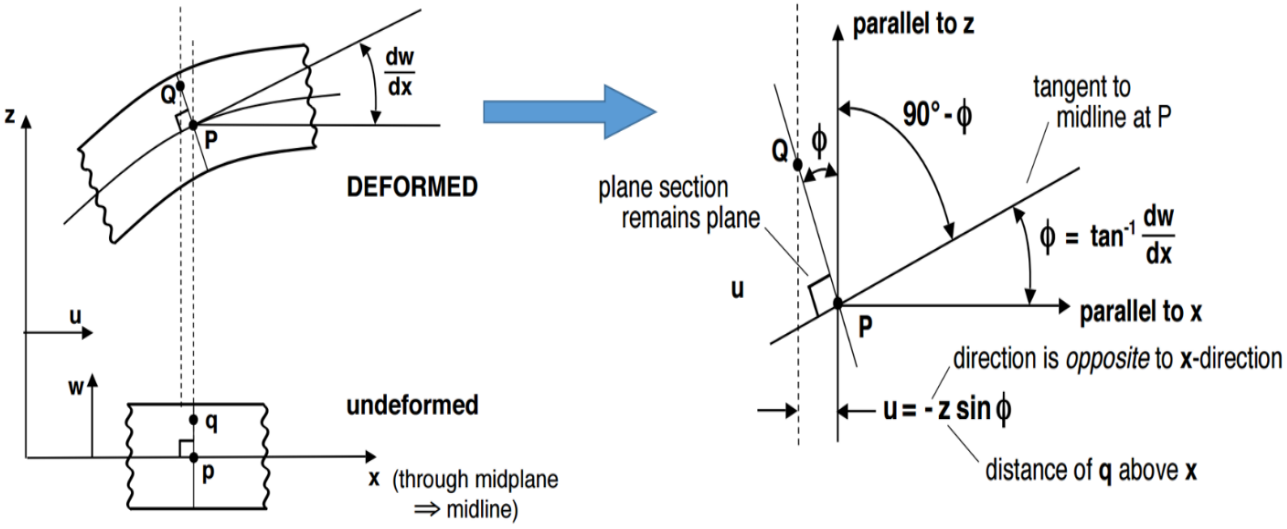

Figure 1-4 Deformation of a beam[7]

The basic assumptions of the elementary theory according to Euler-Bernoulli beam theories of a deformed slender beam as shown in Figure 1-4 whose cross section is symmetrical about the vertical plane of loading are[8]:

1. Cross-sections which are plane and normal to the neutral axis remain plane and normal after deformation.
2. Shear deformations are neglected.
3. Beam deflections are small.

Assumption 1 gives

$$w(x, y, z) = w(x) \tag{1.10}$$

From Figure 1-4 we can obtain the displacement along length direction as follows

$$u(x, y, z) = -z \sin \phi \tag{1.11}$$

If deformation is small, $\sin \phi \approx \phi = \frac{dw}{dx}$, we have

$$u(x, y, z) = -z \frac{dw}{dx} \tag{1.12}$$

The normal strain along x direction is

$$\varepsilon_x = \frac{\partial u}{\partial x} = -z \frac{d^2 w}{dx^2} \tag{1.13}$$

The shear strain

$$\varepsilon_{xz} = \frac{1}{2}\left(\frac{\partial u}{\partial z} + \frac{\partial w}{\partial x}\right) = \frac{1}{2}\left(-\frac{dw}{dx} + \frac{dw}{dx}\right) = 0 \tag{1.14}$$

Equation (1.14) has an agreement with basic assumption 2. Then we can obtain normal stress in length direction as follows:

$$\sigma_{xx} = E\varepsilon_x = -Ez \frac{d^2 w}{dx^2} \tag{1.15}$$

The bending moment caused by internal forces can be written as[9]

$$M = -\int_A \sigma_{xx} z dA = E\frac{d^2w}{dx^2}\int_A z^2 dA = EI\frac{d^2w}{dx^2} \tag{1.16}$$

To gain further insight into the beam problem, consideration is now given to the geometry of the deformed beam. For a beam of symmetrical cross section, the normal strain along length direction can be obtained by substituting equation (1.16) into equation (1.13) which gives

$$\varepsilon_x = -\frac{Mz}{EI} \tag{1.17}$$

In the pure bending case, the deflected axis of the beam is shown deformed with radius of curvature, which is defined by

$$K = \frac{1}{r(x)} = \frac{d\phi}{ds} = \frac{\frac{d^2w}{dx^2}}{[1+(\frac{dw}{dx})^2]^{\frac{3}{2}}} \approx \frac{d^2w}{dx^2} \tag{1.18}$$

Where the approximate form is valid for small deformations ($\frac{dw}{dx} \ll 1$). Therefore, we have relationship between curvature and bending moment as follows

$$K = -\frac{\varepsilon_x}{z} = \frac{M}{EI} \tag{1.19}$$

The elementary beam theory based on the Euler-Bernoulli beam theory relates the beam curvature to the bending moment, which will be used in chapter 2 and chapter 4 to obtain the transverse deflection functions for different structures of beams.

1.4 FABRICATION PROCESS OF PZT-POLYMER LAMINATED COMPOSITE

In the past a few decades, a lot of researches have been conducted to investigate the properties of different types of PZT bending mode sensors and actuators[10]-[14]. The most commonly applied structures of the devices are PZT unimorph and bimorph as shown in Figure 1-5(a) and (b). Figure 1-5(c) shows the structure of triple layer which is similar to the bimorph. Consider three different cantilever beam consisting of these different types of structure, when the electric field is applied across the thickness direction parallel to the poling direction of the PZT element of the beam, the unimorph PZT element will contract and the lower substrate layer will restrict its motion, which will lead to bending deformation. For the bimorph structure and triple layer structure, the voltage parallel to the upper PZT layer and anti-parallel to the lower PZT layer will cause the upper PZT layer contract and lower PZT layer expand, which will also lead to bending deformation. The sensitivity of the structure (b) is the largest and the unmorph (a) is the smallest.

(a) Unimorph PZT with substrate

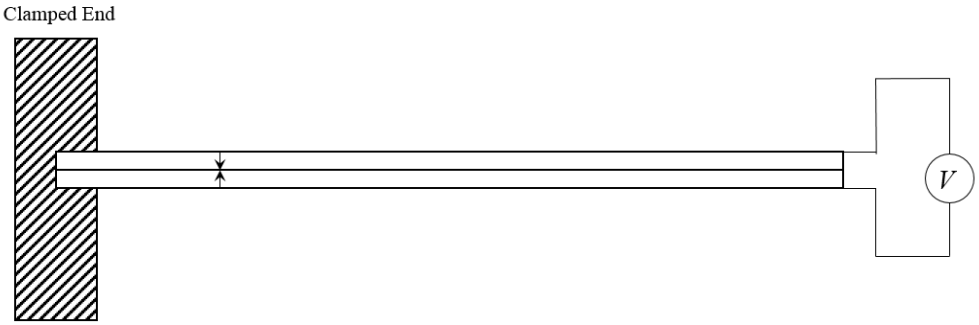

(b) Bimorph PZT

(c) Triple layer with 2 layers of PZT

Figure 1-5 Three different structures of cantilever benders

Although the piezoelectric bimorph and triple layer structures have high sensitivity, it is fragile with PZT ceramic exposed outside. To protect the PZT ceramic from fracture during the vibration and to increase the flexibility of the structure, a five-layer sandwiched composite structure with three layers of polymer and two layers of PZT ceramic is designed in this research.

Figure 1-6 shows the schematic cross section structure of PZT-polyimide composite we used for experiments.

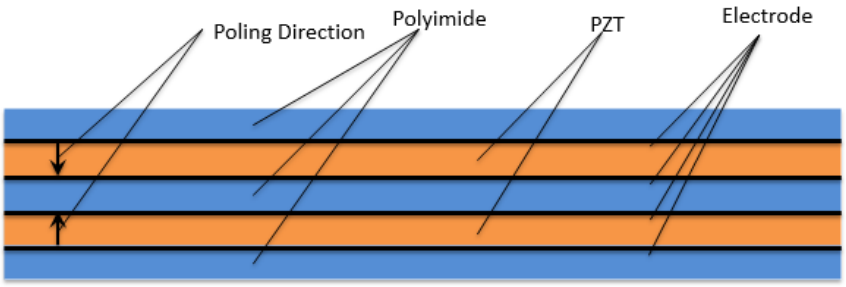

Figure 1-6 Schematic Structure of PZT-polyimide laminated composite

The thin film PZT ceramic in the composite is fabricated by using tape-casting processing by Lifeng Qin et al (2009)[15] as shown in Figure 1-7(a). After cutting process, the rectangular samples of unpoled PZT pieces we used to produce PZT-polymer composite is shown in Figure 1-7(b).

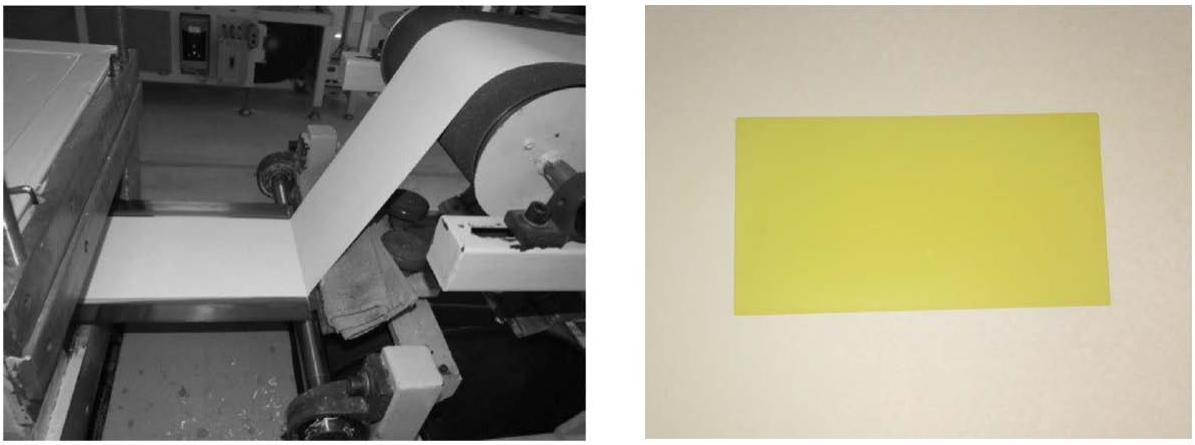

(a) (b)

Figure 1-7 (a) Tape-casting processing for PZT film; (b) Unpoled PZT thin film sample (80um) laid on white paper

After fabrication of soft PZT thin film sample, the second step is to coat electrodes on the two surfaces of the PZT sample. Two types of electrode coverages are used in this research which includes fully covered electrodes and partially covered electrodes. The thin golden electrodes (80-120 nm) are coated by DC sputtering in a sputter coater as shown in Figure 1-8(a). The PZT samples with different electrodes coverage are shown in Figure 1-8(b).

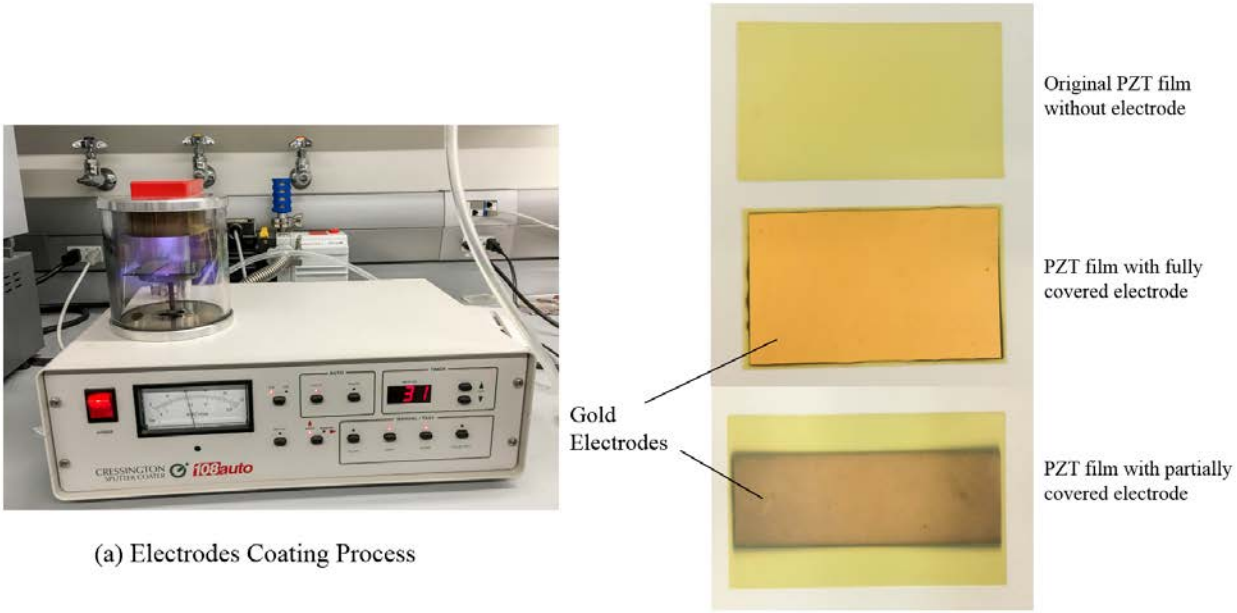

(a) Electrodes Coating Process

(b) Different Types of Electrodes Coverages

Figure 1-8 Coating process of electrodes of PZT film and different electrode coverages

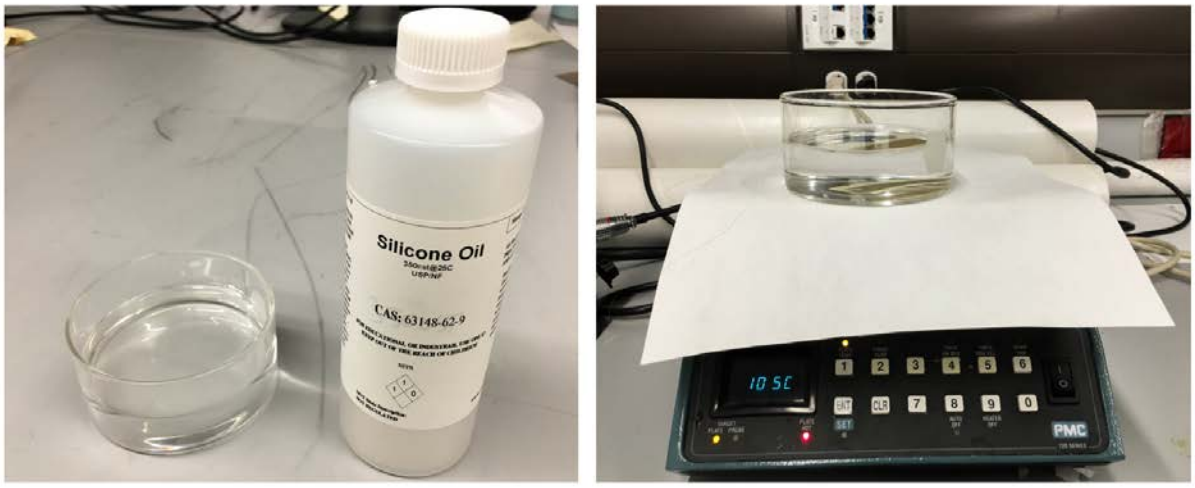

Figure 1-9 The poling process of PZT sample

The following step is poling process: The PZT thin film sample is put in silicone oil at a temperature of 105℃ and a DC electric field 3 kV/mm is applied across the thickness direction for 30 minutes as shown in Figure 1-9.

After poling process, we can cut these poled PZT sheets into desirable shapes such as rectangular plates or circular plates. In this research, some PZT long slices with length 33mm and width 4mm (Figure 1-10(a)) are needed as we utilize PZT-polymer composite construct beam structures. Therefore, some rectangular polyimide film (DoPont Kapton HN) are trimmed and we use epoxy binder to bond the PZT slices and polyimide filmes together to make the five- layer composite. Then the composite sample are put into an oven (47900 Furnace, Barnstead Thermolyne) at temperature 140℃. This baking process will increase the bonding strength and result in compressed thermal stress into PZT film to increase the tensile flexibility. The composite sample for cantilever beam are presented as Figure 1-10(b).

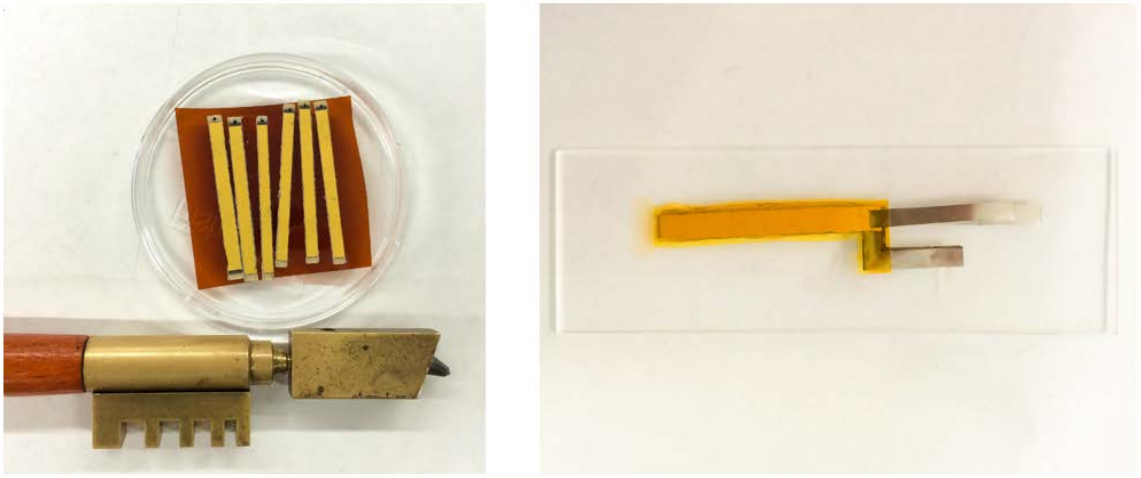

(a) PZT Slices and Diamond Knife (b) PZT-polymer Composite with Electrodes

Figure 1-10 PZT slices and PZT-polyimide laminated composite

1.5 RESEARCH OBJECTIVE

As mentioned in previous sections, the PZT-polymer laminated composite has high electromechanical coupling coefficient, broad bandwidth, great sensitivity and good flexibility. Hence, the composite can be applied as powerful transducers in wide application areas. The research objectives in this thesis contain both the mathematical modeling of constitutive equations for different structures and experimental studies to validate the constitutive equations and to develop some sensors for application. Generally, cantilever beam structure unimorph or bimorph is widely used in bender actuators, vibration sensors, accelerometers and energy harvesting devices, the doubly clamped beam structure is often used in accelerometer designs [16]-[21]. Therefore, constitutive equations for these two typical structures are analyzed in this research. The research work can be divided into four parts:

The first part is theoretical analysis which derives the matrix form constitutive equations for cantilever beam under static and dynamic mechanical or electrical excitations.

The second part is to fabricate and characterize the cantilever beam actuators and sensors to validate the constitutive equations.

The third part is static theoretical analysis of doubly clamped beam which derives the static matrix form constitutive equations under different types of excitations and analyzes the optimal dimension for the polarization areas of the PZT elements used in the composite.

The fourth part of the research work is to fabricate and characterize the doubly clamped beam sensors with partially covered electrodes. The validation works are conducted to verify the theoretical model.

2.0 THEORETICAL ANALYSIS OF PZT-POLYMER COMPOSITE CANTILEVER BEAM

2.1 GENERAL STRUCTURE OF FIVE LAYERS CANTILEVER BEAM

In the previous sections, three different types of cantilever benders were reviewed. In order to increase the flexibility, our device is made of two PZT layers bonded with three thin layers of polyimide. Consider such a cantilever beam consisting of PZT-polymer composite of length L, width w, as shown in Figure 2-1. The two piezoelectric layers have equal thickness h_c and thethickness of each single polymer layer is h_p. The thickness of electrode is so much smaller than the thickness of a single PZT or polymer layer that can be neglected.

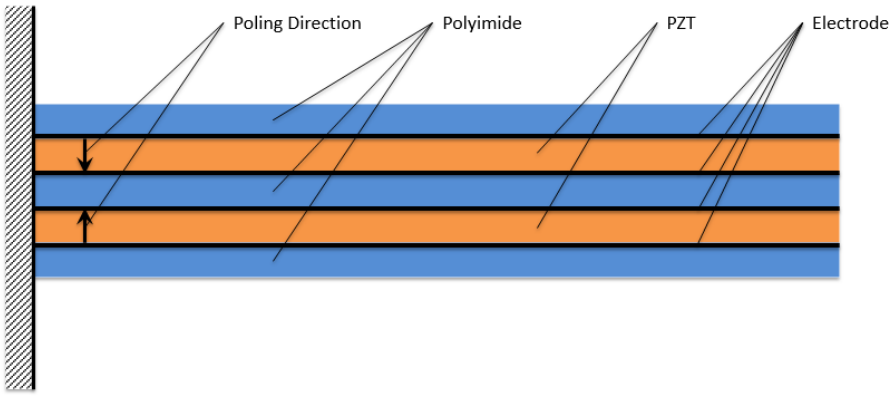

Figure 2-1 A schematic diagram of a PZT-polyimide composite cantilever beam

In this five layers construction, the polarizations of two PZT elements are antiparallel to each other. The two piezoelectric layers are electrically connected in series by conductive wires. In actuation mode, an electric field is applied across the thickness direction which will cause one piezoelectric layer to expand and the other piezoelectric layer to contract. The different motion directions will result in a bending deformation of the composite.

2.2 MATHEMATICAL MODELS FOR THE CANTILEVER BEAM

As introduced in Chapter 1, the equations of motion of a beam element is derived from Euler-Bernoulli beam theory. In this section, we can start from these equations to derive the constitutive equations of the PZT-polymer composite cantilever beam as shown in Figure 2-1.

The constitutive equations represent the electromechanical coupling for the piezoelectric devices. One method to derive these equations which is given by Smits[22] is to obtain a 4×4 matrix that relates the external driving excitations (a moment M, a force F at the tip, surface pressure p and voltage V across the thickness direction) to the beam response parameters (tip rotation angle α, tip vertical deflection δ, volumetric displacement v and electric charge generated Q). The matrix constitutive equations are in the form as shown in equation (2.1).

$$\begin{bmatrix} \alpha \\ \delta \\ v \\ Q \end{bmatrix} = \begin{bmatrix} e_{11} & e_{12} & e_{13} & e_{14} \\ e_{21} & e_{22} & e_{23} & e_{24} \\ e_{31} & e_{32} & e_{33} & e_{34} \\ e_{41} & e_{42} & e_{43} & e_{44} \end{bmatrix} \begin{bmatrix} M \\ F \\ p \\ V \end{bmatrix} \tag{2.1}$$

The matrix containing 16 elements from e_{11} to e_{44} need to be determined for the mathematical model of our device. To obtain these elements, the transverse deflection function of the beam is firstly investigated.

According to the beam theory in Chapter 1, the deflection function $W(x)$ under the effect of different mechanical excitations is derived in the following part of this section. Figure 2-2 shows a free-body diagram of an element of a beam under transverse vibration.

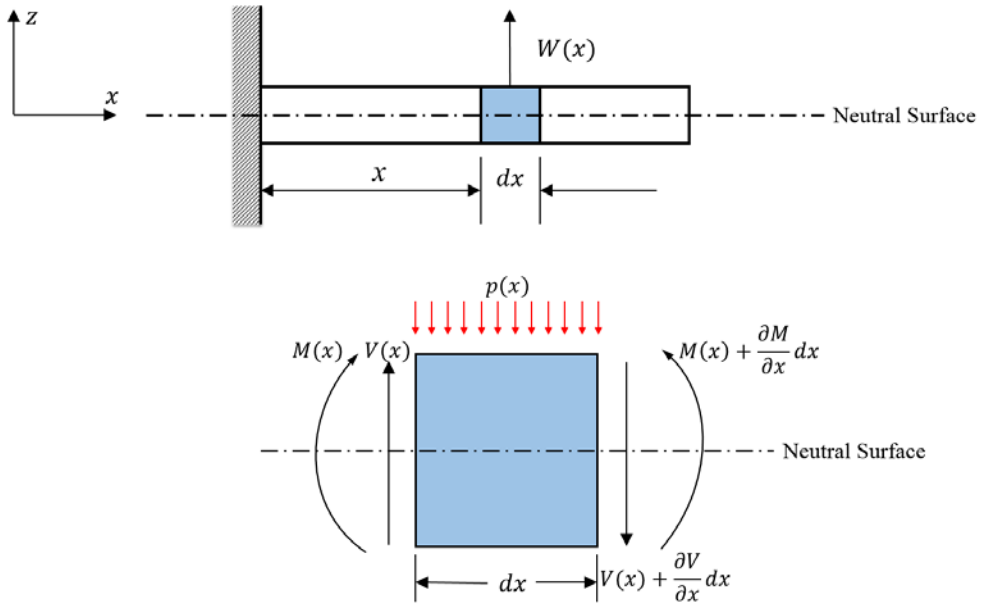

Figure 2-2 Free body diagram of a beam element

The equilibrium of the element in z direction leads to

$$V(x,t) - p(x,t)wdx - [V(x,t) + \frac{\partial V}{\partial x}dx] = \rho dx \frac{\partial^2 W(x,t)}{\partial t^2} \qquad (2.2)$$

Where $V(x)$ is the shear force, $p(x,t)$ is the surface pressure exerted on the beam per unit area, w is the width of the cross section of the beam, ρ is the mass density per unit length of the beam.

The moment equation about y axis gives

$$[M + \frac{\partial M}{\partial x}dx] - [V + \frac{\partial V}{\partial x}dx]dx - pwdx\frac{dx}{2} - M = 0 \qquad (2.3)$$

By neglecting the second order term of infinitesimal dx and dividing by dx on both sides, equation (2.3) can be simplified as

$$\frac{\partial M(x,t)}{\partial x} = V(x,t) \qquad (2.4)$$

In the pure bending case of this composite cantilever, the bending moment can be derived by analyzing the stress state for all five layers.

For the first top polymer layer, the mechanical normal stress along length direction is given by [23]

$$\sigma_x^{(1)} = Y_p \varepsilon_x^{(1)} = -\frac{1}{r(x,t)} Y_p z \qquad (2.5)$$

Where Y_p is Young's modulus for the polymer layer, $r(x,t)$ is local radius of curvature, the superscript (1) represent the first layer.

Similarly, the mechanical normal stresses in *x* direction for other layers are

$$\sigma_x^{(2)} = Y_c \varepsilon_x^{(2)} = -\frac{1}{r(x,t)} Y_c z \qquad (2.6)$$

$$\sigma_x^{(3)} = Y_p \varepsilon_x^{(3)} = -\frac{1}{r(x,t)} Y_p z \qquad (2.7)$$

$$\sigma_x^{(4)} = Y_c \varepsilon_x^{(4)} = -\frac{1}{r(x,t)} Y_c z \qquad (2.8)$$

$$\sigma_x^{(5)} = Y_p \varepsilon_x^{(5)} = -\frac{1}{r(x,t)} Y_p z \tag{2.9}$$

Where subscript *c,p* indicate ceramic layer and polyimide layer respectively. The moment of the internal forces is derived by integrating the product of stress and the distance from neutral axis:

$$M = -\int_{\frac{h_p}{2}+h_c}^{\frac{3h_p}{2}+h_c} \sigma_x^{(1)} zwdz - \int_{\frac{h_p}{2}}^{\frac{h_p}{2}+h_c} \sigma_x^{(2)} zwdz - \int_{-\frac{h_p}{2}}^{\frac{h_p}{2}} \sigma_x^{(3)} zwdz - \int_{-\frac{h_p}{2}-h_c}^{-\frac{h_p}{2}} \sigma_x^{(4)} zwdz - \int_{-\frac{3h_p}{2}-h_c}^{-\frac{h_p}{2}-h_c} \sigma_x^{(5)} zwdz$$

$$= \frac{w\left(8{h_c}^3 Y_c + 27{h_p}^3 Y_p + 12{h_c}^2 h_p \left(Y_c + 2Y_p\right) + 6h_c {h_p}^2 \left(Y_c + 8Y_p\right)\right)}{12r(x,t)} \tag{2.10}$$

Where h_c, h_p is thickness of ceramic layer and polymer layer respectively. To simplify this equation, we can introduce flexural rigidity *R* here as:

$$R = \frac{w\left(8{h_c}^3 Y_c + 27{h_p}^3 Y_p + 12{h_c}^2 h_p \left(Y_c + 2Y_p\right) + 6h_c {h_p}^2 \left(Y_c + 8Y_p\right)\right)}{12} \tag{2.11}$$

Which makes

$$M = \frac{R}{r(x,t)} \tag{2.12}$$

Substituting equation (2.4) and (2.12) into equation (2.2) and recall that $\frac{1}{r(x,t)} = \frac{\partial^2 W(x,t)}{\partial x^2}$, we have

$$R\frac{\partial^4 W(x,t)}{\partial x^4} + \rho \frac{\partial^2 W(x,t)}{\partial t^2} = -p(x,t)w \tag{2.13}$$

For free vibration, $p(x,t) = 0$, the equation (2.13) becomes

$$R\frac{\partial^4 W(x,t)}{\partial x^4} + \rho \frac{\partial^2 W(x,t)}{\partial t^2} = 0 \tag{2.14}$$

We can use the method of separation of variables to solve this equation. Assume that the form of the solution of the vertical deflection function $W(x,t)$ is a product of two functions, one depending only on x and the other depending only on time t; thus

$$W(x,t) = X(x)T(t) \tag{2.15}$$

Substituting from equation (2.15) for W in equation (2.14) yields

$$\frac{R}{\rho}\frac{X''''}{X} = -\frac{T''}{T} \tag{2.16}$$

In which the variables are separated; that is, the left side depends only on x and the right side only on t. It is necessary that both sides of this equation must be equal to the same constant c. Hence we obtained two ordinary differential equations for $X(x)$ and $T(t)$ as follows

$$T'' + cT = 0 \tag{2.17}$$

$$\frac{R}{\rho}X'''' - cX = 0 \tag{2.18}$$

For equation (2.17), we choose a solution of the time dependent equation in anticipation of harmonic excitation of the beam as

$$T = A\cos\omega t + B\sin\omega t \tag{2.19}$$

In which $\omega^2 =$ c, A,B are constants. Then equation (2.18) can be rewritten as

$$\frac{R}{\rho}\frac{X''''}{X} = \omega^2 \tag{2.20}$$

Consider $\frac{R}{\rho} = a^2$, which leads to

$$\frac{X''''}{X} = \frac{\omega^2}{a^2} \tag{2.21}$$

The characteristic equation of equation (2.21) is derived by assuming a solution form of $X(x) = Ae^{rx}$ as follows

$$r^4 - \frac{\omega^2}{a^2} = 0 \tag{2.22}$$

Equation (2.22) gives 4 distinct roots for the characteristic equation:

$$r_1 = \sqrt{\frac{\omega}{a}}, r_2 = -\sqrt{\frac{\omega}{a}}, r_3 = j\sqrt{\frac{\omega}{a}}, r_4 = -j\sqrt{\frac{\omega}{a}} \tag{2.23}$$

Then the general solution of $X(x)$ is the linear combination of the 4 solutions:

$$X(x) = c_1 \cosh \Omega x + c_2 \sinh \Omega x + c_3 \cos \Omega x + c_4 \sin \Omega x \tag{2.24}$$

Where c_i are constants and $\Omega = \sqrt{\frac{\omega}{a}}$. Then the general solution for the deflection equation (2.14) can be derived as

$$W(x,t) = (A\cos\omega t + B\sin\omega t)(c_1 \cos \Omega x + c_2 \sin \Omega x + c_3 \cosh \Omega x + c_4 \sinh \Omega x) \tag{2.25}$$

Where A, B, c_i are constants. We want to determine these coefficients according to different mechanical and electrical excitations. The different types of excitations as shown in Figure 2-3 are introduced in the following sections.

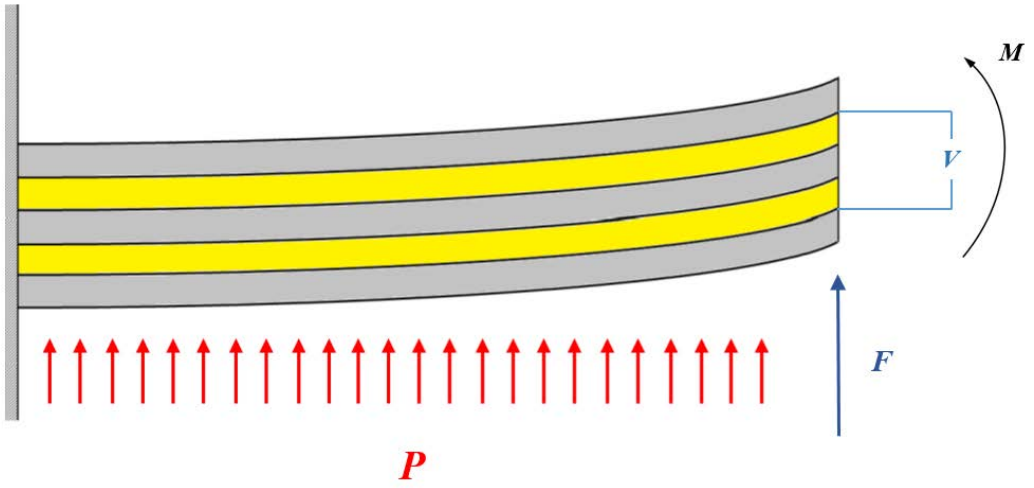

Figure 2-3 Bending deformation of the composite cantilever under different excitation conditions

2.3 STATIC ANALYSIS OF COMPOSITE CANTILEVER BEAM

As described in section 2.2, the governing equation of the transverse deflection function of the cantilever beam is presented in equation (2.13). In this section, we first look into this governing equation for theoretical static analysis of the composite cantilever beam subjected to different external excitations to obtain the constitutive equations.

2.3.1 Cantilever Beam Subjected to an External Bending Moment *M*

In static state, the dynamic terms in equation (2.13) vanishes. Then the governing equations of transverse deflection function only subjected to an external moment can be simplified as

$$R\frac{d^4W}{dx^4} = 0 \tag{2.26}$$

The boundary conditions are imposed as

The displacement of the clamped end is 0:

$$W(0) = 0 \tag{2.27}$$

The slope of the clamped end is 0:

$$\frac{dW(0)}{dx} = 0 \tag{2.28}$$

The moment at the tip is equal to the external moment:

$$\frac{d^2W(L)}{dx^2} = \frac{M}{R} \tag{2.29}$$

The tip force at the free end is 0:

$$\frac{d^3W(L)}{dx^3} = 0 \tag{2.30}$$

Then the transverse deflection function is solved as

$$W(x) = \frac{M}{2R} x^2 \tag{2.31}$$

Therefore, the deflection at the tip of the cantilever under the external moment is given by

$$\delta = W(L) = \frac{M}{2R} L^2 \tag{2.32}$$

This equation leads to the element e_{21} in the matrix in constitutive equation (2.1) which is

$$e_{21} = \frac{L^2}{2R} \tag{2.33}$$

The slope at the tip of the cantilever can be derived from the first order derivative with respect to x at $x=L$:

$$\alpha = \frac{dW(L)}{dx} = \frac{M}{R} L \tag{2.34}$$

$$e_{11} = \frac{L}{R} \tag{2.35}$$

The volume displacement is obtained by integrate the deflection function from $x=0$ to $x=L$:

$$v = \int_{-\frac{w}{2}}^{\frac{w}{2}} \int_0^L W(x) dx dy = \frac{wL^3}{6R} M \tag{2.36}$$

$$e_{31} = \frac{wL^3}{6R} \tag{2.37}$$

Therefore, three elements in the matrix of constitutive equations are derived from the theoretical analysis of the cantilever beam subjected to an external moment.

2.3.2 Cantilever Beam Subjected to an External Tip Force *F*

Consider a force F with positive direction pointing to the positive thickness direction (z-axis) acting at the tip of the cantilever beam as shown in Figure 2-3. The governing equation of the

deflection function of the cantilever is same as equation (2.26). The two boundary conditions at the clamped end are same with the case in which the cantilever is subjected to an external moment as equation (2.27) and (2.28). The two boundary conditions at the tip are given by:

The moment at the tip is 0:

$$\frac{d^2W(L)}{dx^2} = 0 \tag{2.38}$$

The tip force at the tip is the external force *F*:

$$\frac{d^3W(L)}{dx^3} = -\frac{F}{R} \tag{2.39}$$

The solution of the deflection equation can be derived from these boundary conditions:

$$W(x) = \frac{3Lx^2 - x^3}{6R}F \tag{2.40}$$

Therefore, the deflection at the tip of the cantilever is

$$\delta = W(L) = \frac{L^3}{3R}F \tag{2.41}$$

$$e_{22} = \frac{L^3}{3R} \tag{2.42}$$

The slope at the tip is derived by

$$\alpha = \frac{dW(L)}{dx} = \frac{L^2}{2R}F \tag{2.43}$$

$$e_{12} = \frac{L^2}{2R} \tag{2.44}$$

We can see that $e_{12} = e_{21}$. Then the volume displacement can be obtained by integrate the deflection function from *x=0* to *x=L*:

$$v = \int_{-\frac{w}{2}}^{\frac{w}{2}}\int_0^L W(x)dxdy = \frac{wL^4}{8R}F \tag{2.45}$$

$$e_{32} = \frac{wL^4}{8R} \tag{2.46}$$

Therefore, another 3 elements in the second column of the matrix in the constitutive equations are derived from analysis of the cantilever subjected to tip force.

2.3.3 Cantilever Beam Subjected to Uniformly Distributed Pressure *P*

If the cantilever beam is subjected to an external pressure *P* acting on the lower surface with positive direction pointing to the positive *z* direction, the governing equation of the deflection is given by

$$R\frac{d^4W(x)}{dx^4} = wP \tag{2.47}$$

The boundary conditions at the clamped end is same as the previous 2 cases, the two boundary conditions at the tip are

The moment at the tip is 0:

$$\frac{d^2W(L)}{dx^2} = 0 \tag{2.48}$$

The force at the tip is 0:

$$\frac{d^3W(L)}{dx^3} = 0 \tag{2.49}$$

Then the solution of the governing equation can be derived as

$$W(x) = \frac{6L^2x^2 - 4Lx^3 + x^4}{24R}wP \tag{2.50}$$

Then the tip deflection of the cantilever δ, the slope of the tip α and the volumetric displacement *v* can be obtained as follows

$$\delta = W(L) = \frac{wL^4}{8R} P \tag{2.51}$$

$$\alpha = \frac{dW(L)}{dx} = \frac{wL^3}{6R} P \tag{2.52}$$

$$v = \int_{-\frac{w}{2}}^{\frac{w}{2}} \int_0^L W(x) dx dy = \frac{w^2 L^5}{20R} P \tag{2.53}$$

Therefore, another three elements in the third column of the matrix in constitutive equations are derived as

$$e_{23} = \frac{wL^4}{8R} \tag{2.54}$$

$$e_{13} = \frac{wL^3}{6R} \tag{2.55}$$

$$e_{33} = \frac{wL^5}{20R} \tag{2.56}$$

Now we have 9 elements and we can find that $e_{12} = e_{21}$, $e_{13} = e_{31}$, $e_{32} = e_{23}$. In the next subsection we will look into the fourth column of the matrix in constitutive equations.

2.3.4 Cantilever Beam Subjected to an External Voltage *V*

If an external voltage is applied across the cantilever as shown in Figure 2-3, the two layers of piezoelectric elements will have two different deformation: one will expand and the other will contract at the same time. If the electric field is applied across the thickness direction of the cantilever with direction parallel to the upper piezoelectric layer and antiparallel to the lower piezoelectric layer, the upper layer will contract and the lower layer will expand. The constitutive equations for these piezoelectric layers are:

The upper piezoelectric layer:

$$S_x^c = s_{11}^E \sigma_x^c + d_{31} E_3 \tag{2.57}$$

$$D_3^c = d_{31} \sigma_x^c + \varepsilon_{33}^T E_3 \tag{2.58}$$

The lower piezoelectric layer:

$$S_x^c = s_{11}^E \sigma_x^c - d_{31} E_3 \tag{2.59}$$

$$-D_3^c = d_{31} \sigma_x^c - \varepsilon_{33}^T E_3 \tag{2.60}$$

Where the superscript c denotes the ceramic elements, S_x^c is strain in length direction and σ_x^c is mechanical stress in length direction, E_3 is electric field generated by the dynamic voltage in thickness direction. s_{11}^E is mechanical compliance under constant electric field which is equal to $1/Y_c$, d_{31} is transverse piezoelectric coefficient, ε_{33}^T is piezoelectric permittivity. Since the cantilever is subjected to an external voltage only, the strain in the piezoelectric layer is only caused by the electric field as described below:

The upper piezoelectric layer:

$$S_x^c = d_{31} E_3 = d_{31} \frac{V}{h_p + 2h_c} \tag{2.61}$$

The lower piezoelectric layer:

$$S_x^c = -d_{31} E_3 = -d_{31} \frac{V}{h_p + 2h_c} \tag{2.62}$$

These strains will lead to a forced uniform moment in the cantilever. We can consider an equivalent external moment by integrating the product of these stresses and distance from neutral axis throughout the cross section of the beam:

$$M_e = -\int_{\frac{h_p}{2}}^{\frac{h_p}{2}+h_c} Y_c d_{31} \frac{V}{h_p + 2h_c} z w dz - \int_{-\frac{h_p}{2}-h_c}^{-\frac{h_p}{2}} -Y_c d_{31} \frac{V}{h_p + 2h_c} z w dz$$

$$= -wY_c d_{31} V \frac{h_c(h_c + h_p)}{h_p + 2h_c} \tag{2.63}$$

The deflection function subjected an external moment has already been derived as equation (2.31), thus, the deflection function for the equivalent external moment can be written as

$$W(x) = \frac{M_e}{2R} x^2 = -\frac{wY_c d_{31} h_c (h_c + h_p) V}{2R(h_p + 2h_c)} x^2 \tag{2.64}$$

Then the functions of tip deflection, tip slope and volumetric displacement can be obtained as

$$\delta = W(L) = -\frac{wY_c d_{31} h_c (h_c + h_p) L^2}{2R(h_p + 2h_c)} V \tag{2.65}$$

$$\alpha = \frac{dW(L)}{dx} = -\frac{wY_c d_{31} h_c (h_c + h_p) L}{R(h_p + 2h_c)} V \tag{2.66}$$

$$v = \int_{-\frac{w}{2}}^{\frac{w}{2}} \int_0^L W(x) dx dy = -\frac{wY_c d_{31} h_c (h_c + h_p) L^3}{6R(h_p + 2h_c)} V \tag{2.67}$$

Therefore, three elements are obtained as

$$e_{24} = -\frac{wY_c d_{31} h_c (h_c + h_p) L^2}{2R(h_p + 2h_c)} \tag{2.68}$$

$$e_{14} = -\frac{wY_c d_{31} h_c (h_c + h_p) L}{R(h_p + 2h_c)} \tag{2.69}$$

$$e_{34} = -\frac{wY_c d_{31} h_c (h_c + h_p) L^3}{6R(h_p + 2h_c)} \tag{2.70}$$

Then we want to calculate the element e_{44} which can be obtained from the charge generated over the applied voltage. From equation (2.58) we have the electric displacement at the upper surface of the upper piezoelectric layer:

$$D_3 = d_{31}Y_c S_1 + \varepsilon_{33}^T E_3 = -d_{31}Y_c\left(\frac{h_c + \frac{h_p}{2}}{r(x,t)} + d_{31}E_3\right) + \varepsilon_{33}^T E_3$$

$$= -d_{31}Y_c\left(h_c + \frac{h_p}{2}\right)\frac{\partial^2 W(x,t)}{\partial x^2} - d_{31}^2 Y_c E_3 + \varepsilon_{33}^T E_3 \qquad (2.71)$$

The charge can be derived by integrating over the electrode area of the upper surface:

$$Q = \oint_A D_3 dA = w\int_0^L \left(-d_{31}Y_c\left(h_c + \frac{h_p}{2}\right)\frac{\partial^2 W(x,t)}{\partial x^2} - d_{31}^2 Y_c E_3 + \varepsilon_{33}^T E_3\right)dx$$

$$= \frac{wL}{h_p + 2h_c}(\varepsilon_{33}^T - d_{31}^2 Y_c)V + \frac{w^2 L d_{31}^2 h_c (h_c + h_p)Y_c^2}{2R}V \qquad (2.72)$$

The element e_{44} is obtained by dividing Q by V, which is

$$e_{44} = \frac{wL}{h_p + 2h_c}(\varepsilon_{33}^T - d_{31}^2 Y_c) + \frac{w^2 L d_{31}^2 h_c (h_c + h_p)Y_c^2}{2R} \qquad (2.73)$$

2.4 THE SYMMETRIC PROPERTY OF THE MATRIX IN CONSTITUTIVE EQUATIONS

By now we have obtained 13 elements including $e_{11}, e_{12}, e_{13}, e_{14}, e_{21}, e_{22}, e_{23}, e_{24}, e_{31}, e_{32}, e_{33}$, e_{34} and e_{44}. Now we will turn our attention to the symmetric property of the constitutive matrix. If the matrix is symmetric, we will get all the 10 independent elements to complete the constitutive equation.

Consider a linear system without energy dissipation, the work done on the system is equal to the increased internal energy which is the summation of mechanical energy and electric potential energy:

$$U = U_M + U_E = W \qquad (2.74)$$

From Castigliano's Theorem we know that

$$\frac{\partial U}{\partial F} = \frac{\partial U_M}{\partial F} = \delta \tag{2.75}$$

$$\frac{\partial U}{\partial M} = \frac{\partial U_M}{\partial M} = \alpha \tag{2.76}$$

$$\frac{\partial U}{\partial P} = \frac{\partial U_M}{\partial P} = \nu \tag{2.77}$$

And for the electric potential energy in a capacitor, we have:

$$\frac{\partial U}{\partial Q} = \frac{\partial U_E}{\partial Q} = V \tag{2.78}$$

Then we can see that

$$e_{12} = \frac{\partial \alpha}{\partial F} = \frac{\partial^2 U}{\partial M \partial F} = \frac{\partial^2 U}{\partial F \partial M} = \frac{\partial \delta}{\partial M} = e_{21} \tag{2.79}$$

$$e_{13} = \frac{\partial \alpha}{\partial P} = \frac{\partial^2 U}{\partial M \partial P} = \frac{\partial^2 U}{\partial P \partial M} = \frac{\partial \nu}{\partial M} = e_{31} \tag{2.80}$$

$$e_{14} = \frac{\partial \alpha}{\partial V} = \frac{\partial^2 U}{\partial M \partial V} = \frac{\partial^2 U}{\partial V \partial M} = \frac{\partial Q}{\partial M} = e_{41} \tag{2.81}$$

$$e_{23} = \frac{\partial \delta}{\partial P} = \frac{\partial^2 U}{\partial F \partial P} = \frac{\partial^2 U}{\partial P \partial F} = \frac{\partial \nu}{\partial F} = e_{32} \tag{2.82}$$

$$e_{24} = \frac{\partial \delta}{\partial V} = \frac{\partial^2 U}{\partial F \partial V} = \frac{\partial^2 U}{\partial V \partial F} = \frac{\partial Q}{\partial F} = e_{42} \tag{2.83}$$

$$e_{34} = \frac{\partial \nu}{\partial V} = \frac{\partial^2 U}{\partial P \partial V} = \frac{\partial^2 U}{\partial V \partial P} = \frac{\partial Q}{\partial P} = e_{43} \tag{2.84}$$

From these equations we can find that the matrix in the constitutive equation (2.1) is symmetric. Therefore, we have derived the static constitutive equation of the cantilever mounted five layers PZT-polymer composite bender under different excitations.

2.5 DYNAMIC ANALYSIS OF COMPOSITE CANTILEVER BEAM

2.5.1 Theoretical Analysis of a Dynamical Moment

First, we consider a harmonic moment $M = M_0 \sin\omega t$ exerted at the tip of the cantilever which will cause a harmonic motion of the cantilever. The boundary conditions are:

The displacement of the clamped end is 0:

$$W(0,t) = 0 \tag{2.85}$$

The slope of the clamped end is 0:

$$\frac{\partial W(0,t)}{\partial x} = 0 \tag{2.86}$$

The moment at the tip is equal to the external harmonic moment:

$$\frac{\partial^2 W(L,t)}{\partial x^2} = \frac{M}{R} \tag{2.87}$$

The tip force at the free end is 0:

$$\frac{\partial^3 W(L,t)}{\partial x^3} = 0 \tag{2.88}$$

These conditions gives four equations to solve coefficients as follows:

$$(A\cos\omega t + B\sin\omega t)\begin{bmatrix} 1 & 0 & 1 & 0 \\ 0 & \Omega & 0 & \Omega \\ -\Omega^2\cos\Omega L & -\Omega^2\sin\Omega L & \Omega^2\cosh\Omega L & \Omega^2\sinh\Omega L \\ \Omega^3\sin\Omega L & -\Omega^3\cos\Omega L & \Omega^3\sinh\Omega L & \Omega^3\cosh\Omega L \end{bmatrix}\begin{pmatrix} c_1 \\ c_2 \\ c_3 \\ c_4 \end{pmatrix}$$

$$= F_0\cos\omega t\begin{pmatrix} 0 \\ 0 \\ 0 \\ -\dfrac{1}{R} \end{pmatrix}$$

$$= \left(M_0\cos\omega t\right)\begin{pmatrix} 0 \\ 0 \\ \dfrac{1}{R} \\ 0 \end{pmatrix} \tag{2.89}$$

Consider $A = M_0, B = 0$, then solve the matrix equation, we can find

$$\begin{pmatrix} c_1 \\ c_2 \\ c_3 \\ c_4 \end{pmatrix} = \begin{pmatrix} \dfrac{-\cos\Omega L - \cosh\Omega L}{2\Omega^2 R(1+\cos\Omega L\cosh\Omega L)} \\ \dfrac{-\sin\Omega L + \sinh\Omega L}{2\Omega^2 R(1+\cos\Omega L\cosh\Omega L)} \\ \dfrac{\cos\Omega L + \cosh\Omega L}{2\Omega^2 R(1+\cos\Omega L\cosh\Omega L)} \\ \dfrac{\sin\Omega L - \sinh\Omega L}{2\Omega^2 R(1+\cos\Omega L\cosh\Omega L)} \end{pmatrix} \tag{2.90}$$

So the deflection function of the cantilever under the external moment is

$$\begin{aligned} W(x,t) &= -\frac{1}{2\Omega^2 R(1+\cos\Omega L\cosh\Omega L)} M_0\cos\omega t \\ &\times[\left(-\cos\Omega L - \cosh\Omega L\right)\left(\cos\Omega x - \cosh\Omega x\right) \\ &+\left(-\sin\Omega L + \sinh\Omega L\right)\left(\sin\Omega x - \sinh\Omega x\right)] \end{aligned} \tag{2.91}$$

Therefore, the deflection at the tip under the external moment is given by

$$\delta = W(L,t) = \frac{M_0 \cos \omega t}{\Omega^2 R(1+\cos \Omega L \cosh \Omega L)}(\sin \Omega L \sinh \Omega L)$$

$$= \frac{M \sin \Omega L \sinh \Omega L}{R\Omega^2(1+\cos \Omega L \cosh \Omega L)} \tag{2.92}$$

So the element e_{21} in the matrix constitutive equation (2.1) is

$$e_{21} = \frac{\sin \Omega L \sinh \Omega L}{R\Omega^2(1+\cos \Omega L \cosh \Omega L)} \tag{2.93}$$

The element e_{11} can be determined by the slope at the tip of the cantilever which is derived from the first order partial derivative with respect to *x* at *x=L*:

$$\alpha = \frac{\partial W(L,t)}{\partial x} = \frac{M_0 \cos \omega t}{2\Omega^2 R(1+\cos \Omega L \cosh \Omega L)}[2\Omega(\sin \Omega L \cosh \Omega L + \sinh \Omega L \cos \Omega L)]$$

$$= \frac{M(\sin \Omega L \cosh \Omega L + \sinh \Omega L \cos \Omega L)}{\Omega R(1+\cos \Omega L \cosh \Omega L)} \tag{2.94}$$

$$e_{11} = \frac{\sin \Omega L \cosh \Omega L + \sinh \Omega L \cos \Omega L}{\Omega R(1+\cos \Omega L \cosh \Omega L)} \tag{2.95}$$

The volume displacement is obtained by integrate of deflection function from *x=0* to *x=L*, which can give us the element e_{31} as follows

$$v = \int_{-\frac{w}{2}}^{\frac{w}{2}} \int_0^L W(x,t)dxdy = \frac{wM_0 \cos \omega t}{2\Omega^2 R(1+\cos \Omega L \cosh \Omega L)} \frac{2(\sinh \Omega L - \sin \Omega L)}{\Omega}$$

$$= \frac{wM(\sinh \Omega L - \sin \Omega L)}{\Omega^3 R(1+\cos \Omega L \cosh \Omega L)} \tag{2.96}$$

$$e_{31} = \frac{w(\sinh \Omega L - \sin \Omega L)}{\Omega^3 R(1+\cos \Omega L \cosh \Omega L)} \tag{2.97}$$

Therefore, 3 elements e_{11}, e_{21} and e_{31} in the matrix of constitutive equations are found from the theoretical analysis of the external moment above.

2.5.2 Theoretical Analysis of a Harmonic Tip Force

Next we try to find another three elements in the second column of the matrix in the constitutive equations. Consider a dynamic force $F = F_0 cos\omega t$ acting at the tip of the cantilever as shown in Figure 2-3. Since here tip force is acting along the positive *z* axis, the shear force on the left side of a beam element is pointing toward the negative *z* direction. Therefore, the relationship between deflection function and tip force is represented as

$$F = -\frac{\partial M}{\partial x} = -R\frac{\partial^3 W(x,t)}{\partial x^3} \tag{2.98}$$

The boundary conditions are

The deflection at the clamped end is

$$W(0,t) = 0 \tag{2.99}$$

The slope of the clamped end is

$$\frac{\partial W(0,t)}{\partial x} = 0 \tag{2.100}$$

The moment at the tip is

$$\frac{\partial^2 W(L,t)}{\partial x^2} = 0 \tag{2.101}$$

The force at the tip is

$$\frac{\partial^3 W(L,t)}{\partial x^3} = -\frac{F}{R} \tag{2.102}$$

These conditions lead to a matrix form equation as

$$(A\cos\omega t + B\sin\omega t)\begin{bmatrix} 1 & 0 & 1 & 0 \\ 0 & \Omega & 0 & \Omega \\ -\Omega^2\cos\Omega L & -\Omega^2\sin\Omega L & \Omega^2\cosh\Omega L & \Omega^2\sinh\Omega L \\ \Omega^3\sin\Omega L & -\Omega^3\cos\Omega L & \Omega^3\sinh\Omega L & \Omega^3\cosh\Omega L \end{bmatrix}\begin{pmatrix} c_1 \\ c_2 \\ c_3 \\ c_4 \end{pmatrix}$$

$$= F_0\cos\omega t\begin{pmatrix} 0 \\ 0 \\ 0 \\ -\dfrac{1}{R} \end{pmatrix} \qquad (2.103)$$

Consider A $= F_0, B = 0$, we can solve for 4 coefficient c_1, c_2, c_3, c_4 as

$$\begin{pmatrix} c_1 \\ c_2 \\ c_3 \\ c_4 \end{pmatrix} = \begin{pmatrix} -\dfrac{\sin\Omega L + \sinh\Omega L}{2\Omega^3 R(1+\cos\Omega L\cosh\Omega L)} \\ \dfrac{\cos\Omega L + \cosh\Omega L}{2\Omega^3 R(1+\cos\Omega L\cosh\Omega L)} \\ \dfrac{\sin\Omega L + \sinh\Omega L}{2\Omega^3 R(1+\cos\Omega L\cosh\Omega L)} \\ -\dfrac{\cos\Omega L + \cosh\Omega L}{2\Omega^3 R(1+\cos\Omega L\cosh\Omega L)} \end{pmatrix} \qquad (2.104)$$

Thus, the deflection function under the tip force is

$$W(x,t) = \frac{F_0\cos\omega t}{2\Omega^3 R(1+\cos\Omega L\cosh\Omega L)}$$

$$\times[(\sin\Omega L + \sinh\Omega L)(\cosh\Omega x - \cos\Omega x)$$

$$+(\cos\Omega L + \cosh\Omega L)(\sin\Omega x - \sinh\Omega x)] \qquad (2.105)$$

By using the same method as described to find the tip deflection, tip slope and volume displacement excited by the external moment in the section 2.5.1, we can find these three quantities under external harmonic tip force as

The slope α at the tip is

$$\alpha = \frac{\partial W(L,t)}{\partial x} = \frac{F_0 \cos \omega t}{2\Omega^3 R(1+\cos \Omega L \cosh \Omega L)}(2\Omega \sin \Omega L \sinh \Omega L)$$

$$= \frac{F \sin \Omega L \sinh \Omega L}{\Omega^2 R(1+\cos \Omega L \cosh \Omega L)} \tag{2.106}$$

The amplitude of tip deflection is

$$e_{22} = \frac{\cosh \Omega L \sin \Omega L - \cos \Omega L \sinh \Omega L}{\Omega^3 R(1+\cos \Omega L \cosh \Omega L)} \tag{2.107}$$

The volume displacement *v* is

$$v = \int_{-\frac{w}{2}}^{\frac{w}{2}} \int_0^L W(x,t)dxdy = \frac{wF_0 \cos \omega t}{2\Omega^3 R(1+\cos \Omega L \cosh \Omega L)}[\frac{8\sin^2(\frac{\Omega L}{2})\sinh^2(\frac{\Omega L}{2})}{\Omega}]$$

$$= \frac{4wF \sin^2(\frac{\Omega L}{2})\sinh^2(\frac{\Omega L}{2})}{\Omega^4 R(1+\cos \Omega L \cosh \Omega L)} \tag{2.108}$$

Equation (2.106)-(2.108) provide us three elements e_{12}, e_{22} and e_{32} in the matrix of constitutive equation as

$$e_{12} = \frac{\sin \Omega L \sinh \Omega L}{\Omega^2 R(1+\cos \Omega L \cosh \Omega L)} \tag{2.109}$$

$$e_{22} = \frac{\cosh \Omega L \sin \Omega L - \cos \Omega L \sinh \Omega L}{\Omega^3 R(1+\cos \Omega L \cosh \Omega L)} \tag{2.110}$$

$$e_{32} = \frac{4w\sin^2(\frac{\Omega L}{2})\sinh^2(\frac{\Omega L}{2})}{\Omega^4 R(1+\cos \Omega L \cosh \Omega L)} \tag{2.111}$$

2.5.3 Theoretical Analysis of Dynamic Pressure

Now we consider a harmonic pressure $P = P_0 cos\omega t$ acting on the cantilever beam along positive *z* direction. The dynamic governing equation for deflection function is

$$R\frac{\partial^4 W(x,t)}{\partial x^4} + \rho\frac{\partial^2 W(x,t)}{\partial t^2} = wP_0\cos\omega t \qquad (2.112)$$

As introduced in equation (2.15), method of separation of variables is used for this 4-th order partial differential equation. Here we consider the time dependent function $T(t) = \cos\omega t$. Recall that $\frac{R}{\rho} = a^2$, then equation (2.55) can be written as

$$X'''' - \frac{\omega^2}{a^2}X = \frac{wP_0}{R} \qquad (2.113)$$

We have already obtained a general solution for the homogeneous equation (2.21) as equation (2.24), therefore, a specific solution of the nonhomogeneous equation is needed to be added to solution equation (2.24). We seek the nonhomogeneous solution as the form of $X_n = A\cos kx + B$. Then equation (2.113) can be written as

$$A(k^4 - \frac{\omega^2}{a^2})\cos kx - B\frac{\omega^2}{a^2} = \frac{wP_0}{R} \qquad (2.114)$$

Which leads to

$$k^4 - \frac{\omega^2}{a^2} = 0 \qquad (2.115)$$

$$-B\frac{\omega^2}{a^2} = \frac{wP_0}{R} \qquad (2.116)$$

By solving these two equations we can find a particular solution as

$$X_n(x) = A\cos\Omega x - \frac{wP_0}{R\Omega^4} \qquad (2.117)$$

Where A is a constant, $\Omega = \sqrt{\frac{\omega}{a}}$. Therefore, the solution of equation (2.112) is

$$W(x,t) = \cos\omega t(A\cos\Omega x - \frac{wP_0}{R\Omega^4} + c_1\cos\Omega x + c_2\sin\Omega x + c_3\cosh\Omega x + c_4\sinh\Omega x) \quad (2.118)$$

Then we impose the boundary conditions:

The deflection at the clamped end is

$$W(0,t) = 0 \quad (2.119)$$

The slope of the clamped end is

$$\frac{\partial W(0,t)}{\partial x} = 0 \quad (2.120)$$

The moment at the tip is

$$\frac{\partial^2 W(L,t)}{\partial x^2} = 0 \quad (2.121)$$

The force at the tip is

$$\frac{\partial^3 W(L,t)}{\partial x^3} = 0 \quad (2.122)$$

These conditions leads to the matrix equation as follows

$$\begin{bmatrix} 1 & 0 & 1 & 0 \\ 0 & \Omega & 0 & \Omega \\ -\Omega^2\cos\Omega L & -\Omega^2\sin\Omega L & \Omega^2\cosh\Omega L & \Omega^2\sinh\Omega L \\ \Omega^3\sin\Omega L & -\Omega^3\cos\Omega L & \Omega^3\sinh\Omega L & \Omega^3\cosh\Omega L \end{bmatrix} \begin{pmatrix} c_1 \\ c_2 \\ c_3 \\ c_4 \end{pmatrix} = \begin{pmatrix} \frac{wP_0}{R\Omega^4} - A \\ 0 \\ A\Omega^2\cos\Omega L \\ -A\Omega^3\sin\Omega L \end{pmatrix} \quad (2.123)$$

Since A is an arbitrary constant, for convenience we choose $= \frac{wP_0}{2R\Omega^4}$, then we can solve for c_1, c_2, c_3 and c_4 as:

$$\begin{pmatrix} c_1 \\ c_2 \\ c_3 \\ c_4 \end{pmatrix} = \frac{P_0 w}{2R\Omega^4(1+\cos\Omega L\cosh\Omega L)} \begin{pmatrix} -\sin\Omega L\sinh\Omega L \\ \cosh\Omega L\sin\Omega L+\cos\Omega L\sinh\Omega L \\ 1+\cos\Omega L\cosh\Omega L+\sin\Omega L\sinh\Omega L \\ -\cosh\Omega L\sin\Omega L-\cos\Omega L\sinh\Omega L \end{pmatrix} \quad (2.124)$$

Therefore, the deflection function of equation (2.118) can be rewritten as

$$W(x,t) = \frac{P_0 w}{2R\Omega^4}\cos\omega t[\cos\Omega x - 2 - \frac{\sin\Omega L\sinh\Omega L\cos\Omega x}{1+\cos\Omega L\cosh\Omega L}$$

$$+\frac{(\cosh\Omega L\sin\Omega L+\cos\Omega L\sinh\Omega L)\sin\Omega x}{1+\cos\Omega L\cosh\Omega L}$$

$$+\frac{(1+\cos\Omega L\cosh\Omega L+\sin\Omega L\sinh\Omega L)\cosh\Omega x}{1+\cos\Omega L\cosh\Omega L}$$

$$-\frac{(\cosh\Omega L\sin\Omega L+\cos\Omega L\sinh\Omega L)\sinh\Omega x}{1+\cos\Omega L\cosh\Omega L}] \quad (2.125)$$

We want to use this equation to derive the e_{33} element which can be obtained from the volumetric displacement as follows

$$v = \int_{-\frac{w}{2}}^{\frac{w}{2}}\int_0^L W(x,t)dxdy$$

$$= \frac{P_0 w^2(-\Omega L-\Omega L\cosh\Omega L\cos\Omega L+\sin\Omega L\cosh\Omega L+\cos\Omega L\sinh\Omega L)\cos\omega t}{R\Omega^5(1+\cos\Omega L\cosh\Omega L)} \quad (2.126)$$

$$e_{33} = \frac{w^2(-\Omega L-\Omega L\cosh\Omega L\cos\Omega L+\sin\Omega L\cosh\Omega L+\cos\Omega L\sinh\Omega L)}{R\Omega^5(1+\cos\Omega L\cosh\Omega L)} \quad (2.127)$$

2.5.4 Theoretical Analysis of Dynamic Voltage

If we drive the composite cantilever with a dynamic voltage $\mathrm{V} = V_0\cos\omega t$ as shown in Figure 2-3, we will bring this cantilever beam in dynamic motion. Since the poling directions of the two layers of piezoelectric element are opposite, the motions of the two layers will be opposite under

the same applied voltage, which means one layer will expand and the other will contract at the same time. This kind of motion will cause a bending motion with the same frequency of the external dynamic voltage. If the electric field E_3 is applied across the thickness direction of the composite beam with direction parallel to the upper piezoelectric layer and antiparallel to the lower piezoelectric layer, the upper layer will contract and lower layer will expand, the constitutive equations for these two layers are:

The upper piezoelectric layer:

$$S_x^c = s_{11}^E \sigma_x^c + d_{31} E_3 \tag{2.128}$$

$$D_3^c = d_{31} \sigma_x^c + \varepsilon_{33}^T E_3 \tag{2.129}$$

The lower piezoelectric layer:

$$S_x^c = s_{11}^E \sigma_x^c - d_{31} E_3 \tag{2.130}$$

$$-D_3^c = d_{31} \sigma_x^c - \varepsilon_{33}^T E_3 \tag{2.131}$$

Where the superscript *c* denotes the ceramic elements, S_x^c is strain in length direction and σ_x^c is mechanical stress in length direction, E_3 is electric field generated by the dynamic voltage in thickness direction. s_{11}^E is mechanical compliance under constant electric field which is equal to $1/Y_c$, d_{31} is transverse piezoelectric coefficient, ε_{33}^T is piezoelectric permittivity.

Since we only applied voltage across the thickness direction, the strain in each of the piezoelectric layer is only caused by the electric field as described below:

The upper piezoelectric layer:

$$S_x^c = d_{31} E_3 = d_{31} \frac{V}{h_p + 2h_c} \tag{2.132}$$

The lower piezoelectric layer:

$$S_x^c = -d_{31}E_3 = -d_{31}\frac{V}{h_p + 2h_c} \tag{2.133}$$

These strains lead to uniform stress distributed along thickness direction, we can obtain an equivalent external moment by integrate these stresses throughout the cross section of the beam[24]:

$$M_e = -\int_{\frac{h_p}{2}}^{\frac{h_p}{2}+h_c} Y_c d_{31}\frac{V}{h_p + 2h_c} zwdz - \int_{-\frac{h_p}{2}-h_c}^{-\frac{h_p}{2}} -Y_c d_{31}\frac{V}{h_p + 2h_c} zwdz$$

$$= -wY_c d_{31}V\frac{h_c(h_c + h_p)}{h_p + 2h_c} = -wY_c d_{31}\frac{h_c(h_c + h_p)}{h_p + 2h_c}V_0\cos\omega t \tag{2.134}$$

We have already derived the deflection function for a dynamic external moment as equation (2.91). Therefore, the deflection function for the equivalent external moment can be written as

$$W(x,t) = -\frac{1}{2\Omega^2 R(1+\cos\Omega L\cosh\Omega L)}wY_c d_{31}\frac{h_c(h_c + h_p)}{h_p + 2h_c}V_0\cos\omega t$$

$$\times[(-\cos\Omega L - \cosh\Omega L)(\cos\Omega x - \cosh\Omega x)$$

$$+(-\sin\Omega L + \sinh\Omega L)(\sin\Omega x - \sinh\Omega x)] \tag{2.135}$$

Then the expressions for tip slope α, tip deflection δ, and volume displacement v and elements e_{14}, e_{24} and e_{34} are given by

$$\alpha = \frac{\partial W(L,t)}{\partial x} = \frac{M_e}{2\Omega^2 R(1+\cos\Omega L\cosh\Omega L)}[2\Omega(\sin\Omega L\cosh\Omega L + \sinh\Omega L\cos\Omega L)]$$

$$= -\frac{\sin\Omega L\cosh\Omega L + \sinh\Omega L\cos\Omega L}{\Omega R(1+\cos\Omega L\cosh\Omega L)}wY_c d_{31}\frac{h_c(h_c + h_p)}{h_p + 2h_c}V \tag{2.136}$$

$$\delta = W(L,t) = \frac{M_e}{\Omega^2 R(1+\cos\Omega L\cosh\Omega L)}(\sin\Omega L\sinh\Omega L)$$

$$= -\frac{\sin\Omega L\sinh\Omega L}{R\Omega^2(1+\cos\Omega L\cosh\Omega L)} wY_c d_{31}\frac{h_c(h_c+h_p)}{h_p+2h_c}V \tag{2.137}$$

$$v = \int_{-\frac{w}{2}}^{\frac{w}{2}}\int_0^L W(x,t)dxdy = \frac{wM_e}{2\Omega^2 R(1+\cos\Omega L\cosh\Omega L)}\frac{2(\sinh\Omega L-\sin\Omega L)}{\Omega}$$

$$= -\frac{\sinh\Omega L-\sin\Omega L}{\Omega^3 R(1+\cos\Omega L\cosh\Omega L)} w^2 Y_c d_{31}\frac{h_c(h_c+h_p)}{h_p+2h_c}V \tag{2.138}$$

$$e_{14} = -\frac{\sin\Omega L\cosh\Omega L+\sinh\Omega L\cos\Omega L}{\Omega R(1+\cos\Omega L\cosh\Omega L)} wY_c d_{31}\frac{h_c(h_c+h_p)}{h_p+2h_c} \tag{2.139}$$

$$e_{24} = -\frac{\sin\Omega L\sinh\Omega L}{R\Omega^2(1+\cos\Omega L\cosh\Omega L)} wY_c d_{31}\frac{h_c(h_c+h_p)}{h_p+2h_c} \tag{2.140}$$

$$e_{34} = \frac{\sin\Omega L-\sinh\Omega L}{\Omega^3 R(1+\cos\Omega L\cosh\Omega L)} w^2 Y_c d_{31}\frac{h_c(h_c+h_p)}{h_p+2h_c} \tag{2.141}$$

Then we want to calculate the element e_{44} which can be obtained from the charge generated over the applied voltage. From equation (2.129) we have the electric displacement at the upper surface of the upper piezoelectric layer:

$$D_3 = d_{31}Y_c S_1 + \varepsilon_{33}^T E_3 = -d_{31}Y_c\left(\frac{h_c+\frac{h_p}{2}}{r(x,t)} + d_{31}E_3\right) + \varepsilon_{33}^T E_3$$

$$= -d_{31}Y_c\left(h_c+\frac{h_p}{2}\right)\frac{\partial^2 W(x,t)}{\partial x^2} - d_{31}^2 Y_c E_3 + \varepsilon_{33}^T E_3 \tag{2.142}$$

The charge can be derived by integrating over the electrode area of the upper surface:

$$Q = \oint_A D_3 dA = w\int_0^L\left(-d_{31}Y_c\left(h_c+\frac{h_p}{2}\right)\frac{\partial^2 W(x,t)}{\partial x^2} - d_{31}^2 Y_c E_3 + \varepsilon_{33}^T E_3\right)dx$$

$$= \frac{d_{31}^2 h_c (h_c + h_p) w^2 Y_c^2 (\cos \Omega L \sin \Omega L + \cos \Omega L \sinh \Omega L)}{2\Omega R (1 + \cos \Omega L \cosh \Omega L)} V$$

$$+ \frac{wL}{h_p + 2h_c} (\varepsilon_{33}^T - d_{31}^2 Y_c) V \qquad (2.143)$$

The element e_{44} is derived by dividing equation (2.86) by V, which is

$$e_{44} = \frac{d_{31}^2 h_c (h_c + h_p) w^2 Y_c^2 (\cos \Omega L \sin \Omega L + \cos \Omega L \sinh \Omega L)}{2\Omega R (1 + \cos \Omega L \cosh \Omega L)}$$

$$+ \frac{wL}{h_p + 2h_c} (\varepsilon_{33}^T - d_{31}^2 Y_c) \qquad (2.144)$$

Since the matrix in constitutive equation is symmetric, all the elements in the matrix can be obtained by the symmetry.

3.0 EXPERIMENTAL STUDIES OF PZT-POLYMER COMPOSITE CANTILEVER BEAM

3.1 EXPERIMENTAL DESIGN FOR CANTILEVER BEAM ACTUATOR

In chapter 2, the theoretical analysis for composite cantilever beam of static responses and dynamic responses under different excitations have been introduced. In this section, a PZT-polyimide five layers composite is fabricated to construct a cantilever beam and some tests concerning actuating mode are conducted to verify the accuracy of dynamical mathematical models established in previous chapter. The schematic structure of the cantilever with length 33mm and width 4mm is shown in Figure 3-1.

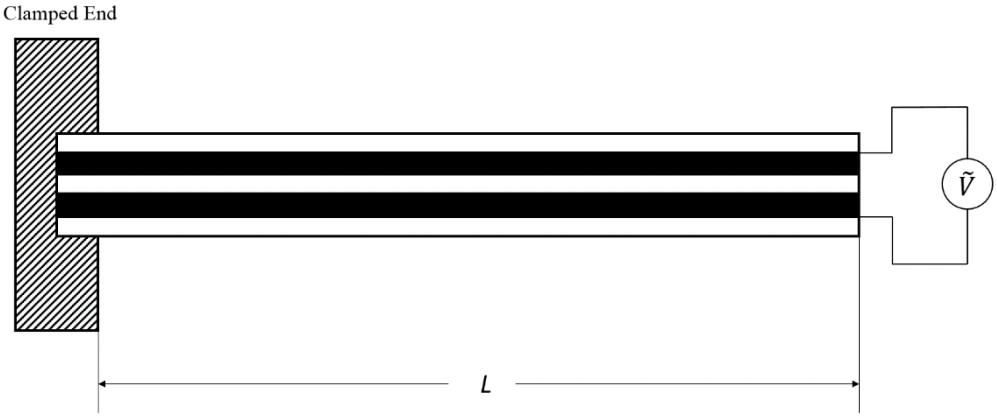

Figure 3-1 The structure of the PZT-polyimide composite cantilever

The experiment setup consists of a function generator, a cantilever actuator, an optical displacement sensor and an oscilloscope. In this experiment, the relationship between input voltage and output tip displacement are studied. In order to provide a sinusoidal signal to drive the cantilever actuator, a signal function generator is used as an external voltage source. The displacement of the cantilever tip is detected by the fiber optical vibrometer. The probe of the fotonic sensor is put above the tip of the cantilever. The displacement measured is transferred to voltage output signal. Both the input and output voltage are finally transferred to an oscilloscope for data recording of the experiment. The illustrative block diagram of the experiment setup is shown in Figure 3-2(a) and the actual experiment setup is shown in Figure 3-2(b).

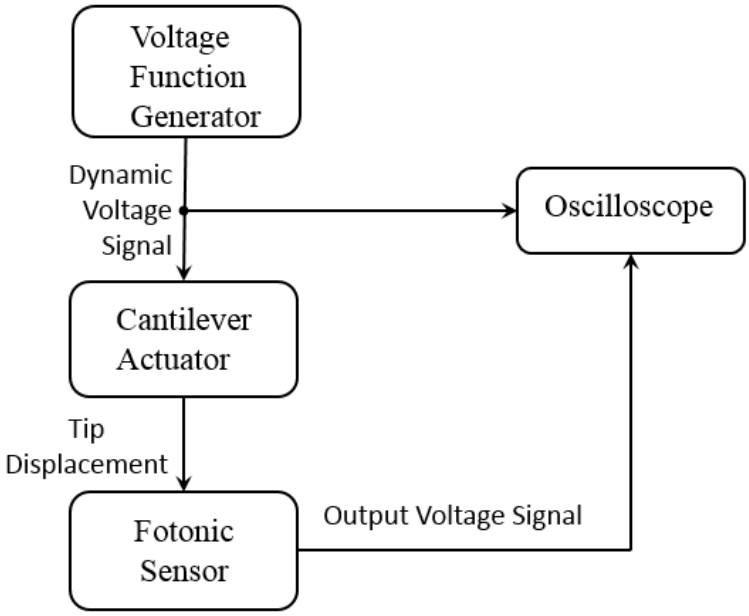

(a)

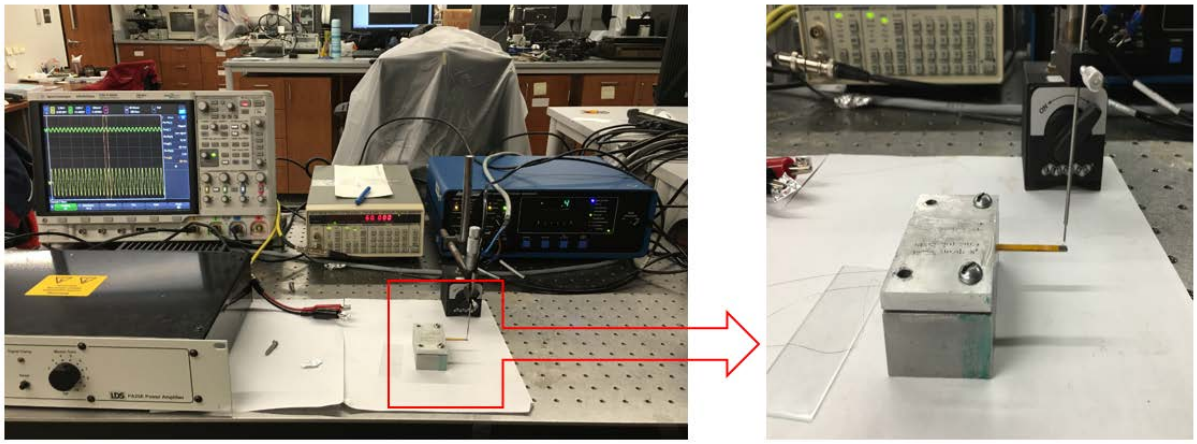

(b)

Figure 3-2 (a) illustrative block diagram of the experiment setup; (b) actual experiment setup for the actuator test

The properties of the cantilever beam actuator are shown in Table 3-1.

Table 3-1 Properties of the cantilever actuator

Parameters	Values
L	30mm
w	4mm
h_c	80μm
h_p	70 μm
Y_c	50GPa
Y_p	2.5GPa
ρ_c	7500kg/m^3
ρ_p	1420 kg/m^3

3.2 RESULTS OF CANTILEVER BEAM ACTUATOR EXPERIMENT

In this section, the first task of the experiment is to find the first natural frequency of the cantilever actuator. In chapter 2, the general solution of the transverse deflection function in free vibration is written as

$$W(x,t) = (A\cos\omega t + B\sin\omega t)(c_1\cos\Omega x + c_2\sin\Omega x + c_3\cosh\Omega x + c_4\sinh\Omega x) \qquad (3.1)$$

The boundary conditions $W(0,t) = 0$, $\frac{\partial W(0,t)}{\partial x} = 0$, $\frac{\partial^2 W(L,t)}{\partial x^2} = 0$ and $\frac{\partial^3 W(L,t)}{\partial x^3} = 0$ leads to

$$\cos(\Omega L)\cosh(\Omega L) = -1 \qquad (3.2)$$

There are infinite values for ΩL to satisfy equation (3.2) which represents the different natural frequencies relate to different shape modes of the cantilever. Then the natural frequency equations can be written as:

$$\omega_n = (\Omega_n L)^2 \sqrt{\frac{R}{\rho L^4}} \tag{3.3}$$

$$f_n = \frac{\omega_n}{2\pi}, n = 1, 2, 3...\infty \tag{3.4}$$

Thus first natural frequency is

$$n = 1 \Rightarrow \Omega_1 L = 1.8751 \Rightarrow \omega_1 = 1.8751^2 \sqrt{\frac{R}{\rho L^4}} \Rightarrow f_1 = \frac{1.8751^2}{2\pi} \sqrt{\frac{R}{\rho L^4}} \tag{3.5}$$

Similarly, the second and third natural frequency is

$$f_2 = \frac{4.6941^2}{2\pi} \sqrt{\frac{R}{\rho L^4}} \tag{3.6}$$

$$f_3 = \frac{7.8547^2}{2\pi} \sqrt{\frac{R}{\rho L^4}} \tag{3.7}$$

Substituting all values for all the parameters in three equations above, we will have f_1=121.656 Hz, f_2=762.404 Hz, f_3=2134.8 Hz. These natural frequencies agrees with the tip deflection function we derived in equation (2.80), which can be rewrite as a function of frequency as follows:

$$\delta = e_{24} V = g(f) V = -\frac{\sin \Omega L \sinh \Omega L}{R\Omega^2 (1 + \cos \Omega L \cosh \Omega L)} w Y_c d_{31} \frac{h_c (h_c + h_p)}{h_p + 2h_c} V \tag{3.8}$$

Where *g(f)* is a function of frequency because $\Omega = \sqrt{2\pi f / \sqrt{R/\rho}}$. Figure 3-3 shows the plot of the function *g(f)* as *f* goes from 0 to 3000 Hz. We can see from the figure the peak values of the function occurs at three points which coincides with the first three natural frequencies

derived above. Therefore, the maximum tip deflection occurs at the first three natural frequencies as expected which are f_1=121.656 Hz, f_2=762.404 Hz, f_3=2134.8 Hz.

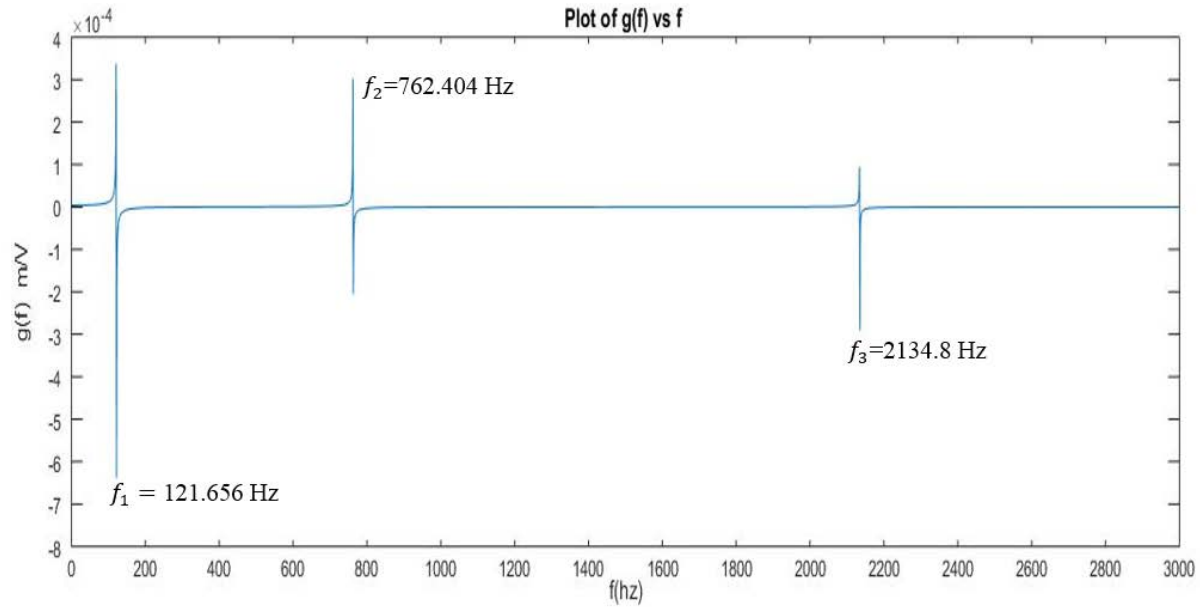

Figure 3-3 g(f) vs f plot

In the experiment, a sinusoidal voltage is generated by the function generator to drive the cantilever actuator to vibrate. We use a linear frequency sweep mode to change the frequency of driven sinusoidal voltage from 10 Hz to 200 Hz. The peak amplitude of driven voltage is 5V. The tip displacement of the cantilever are measured by the fiber optical vibration sensor then converted to output voltage which is transferred to the oscilloscope. Figure 3-4 shows the test result as follows. The signal for channel 1 (yellow waveform) represent the driven sine signal with changing frequency. The signal for channel 2 (green waveform) represent the output voltage from the optical vibration sensor. We can see the peak value of signal 2 occurs at frequency of 123 Hz which means

the tip displacement of the cantilever beam is largest at 123 Hz. This result is close to the previously derived theoretical first natural frequency (121.656 Hz).

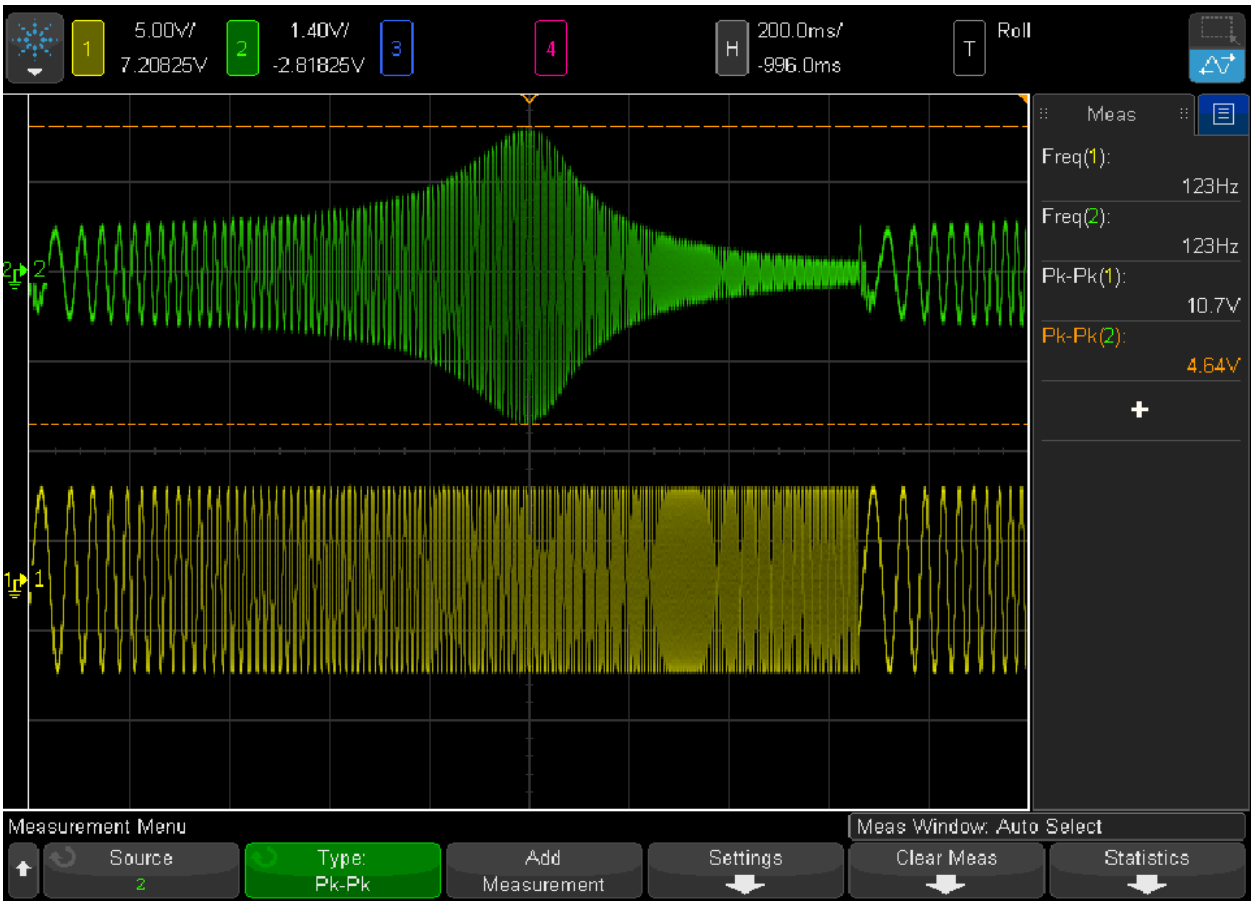

Figure 3-4 Linear Frequency Sweep of Driven Voltage and Response of the Actuator

The second task of the experiment is to test the sensitivity of the actuator. Three groups of tests classified by different peak amplitude of driven voltage (2V, 5V, 10V) are conducted. In each group, we test the tip displacement at different frequency every 10 Hz from 50 Hz to 200 Hz. According to the theoretical analysis in chapter 2, the tip deflection response of the cantilever beam under dynamic voltage is represented by equation (2.80). With same driven voltage in each group

of the experiment, the expected maximum tip deflection becomes a frequency dependent function which can be shown as Figure 3-5. We can see that the theoretical tip deflection at the first natural frequency is very large compared to the beam thickness (370um). Since the theoretical model is based on Euler-Bernoulli beam theory which requires the transverse deflection is relatively small to the beam thickness, we can expect that the model will lose some degree of accuracy around the natural frequency.

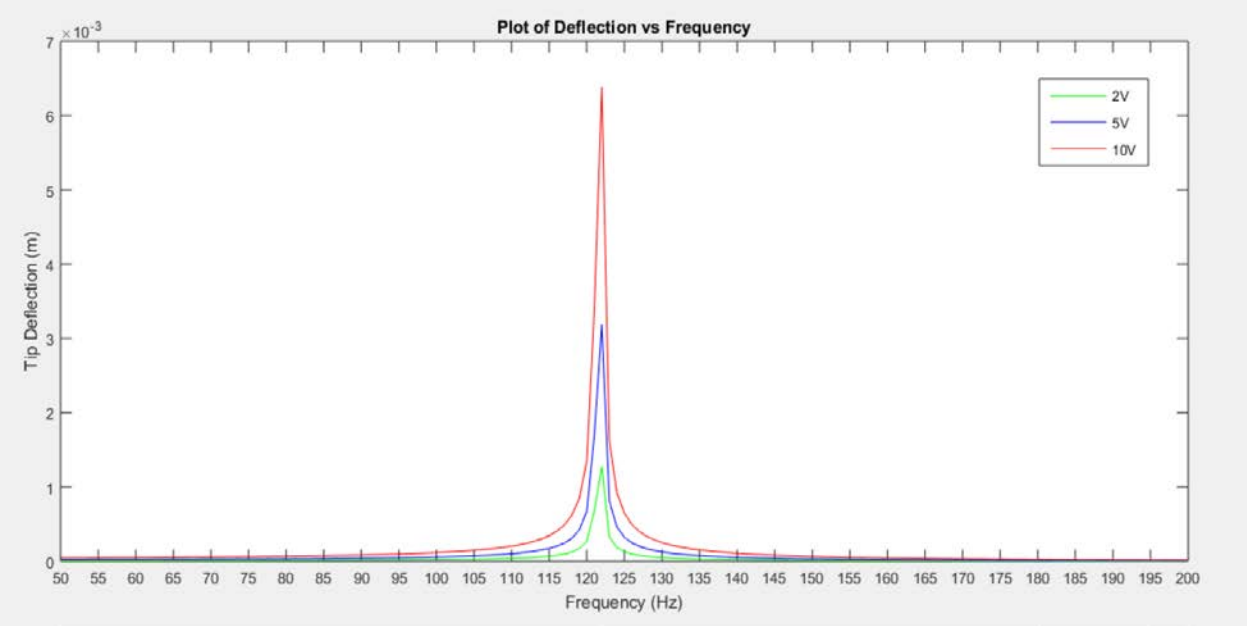

Figure 3-5 Plot of maximum tip deflection vs frequency (50Hz-200Hz) under different drive voltage

In the experiment, by changing the frequency from 50 Hz to 200 Hz in each driven voltage group, the maximum tip deflection is obtained as shown in Table 3-2.

Table 3-2 The experimental data of maximum tip deflections

Peak Driven Voltage / Frequency	2V	5V	10V
50 Hz	8.19 μm	21.14μm	43.56 μm
60 Hz	8.65 μm	23.65 μm	49.30 μm
70 Hz	8.90 μm	25.05 μm	52.45 μm
80 Hz	9.95 μm	30.53 μm	60.62μm
90 Hz	12.32 μm	37.16 μm	76.19 μm
100 Hz	16.36 μm	44.30 μm	96.54 μm
110 Hz	25.58 μm	68.44 μm	145.18 μm
120 Hz	56.34 μm	114.59μm	264.69 μm
130 Hz	29.75 μm	62.70μm	109.31 μm
140 Hz	18.85 μm	40.81 μm	75.59 μm
150 Hz	11.07 μm	27.67 μm	51.31 μm
160 Hz	7.77 μm	19.73 μm	36.04 μm
170 Hz	6.02 μm	14.53 μm	25.83 μm
180 Hz	4.60 μm	10.97 μm	19.12 μm
190 Hz	3.51 μm	8.26 μm	14.53 μm
200 Hz	2.91 μm	6.49 μm	11.13 μm

According to the data recorded in Table 3-2, the plots of maximum value of tip deflections as a function of frequency of driving voltage can be obtained. Figure 3-6 (a), (b) and (c) show the comparison of theoretical simulation and experimental results under different maximum value of driving voltage respectively.

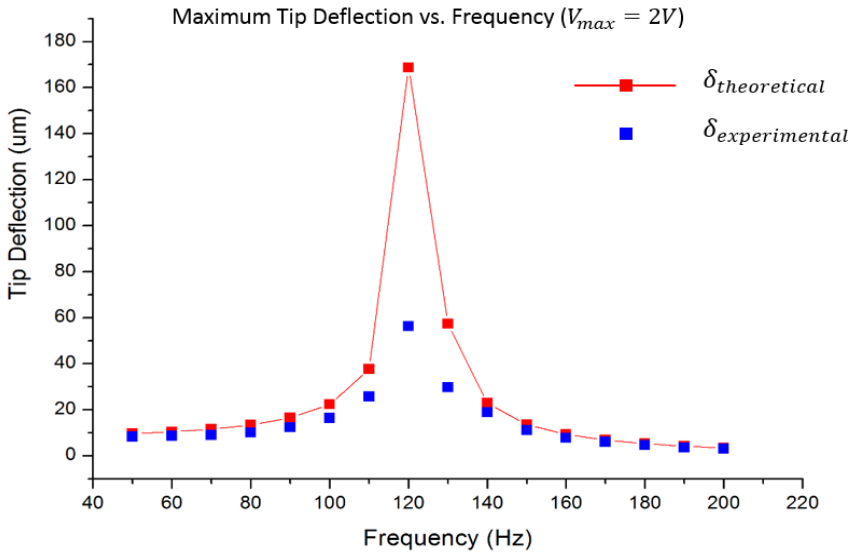

(a)

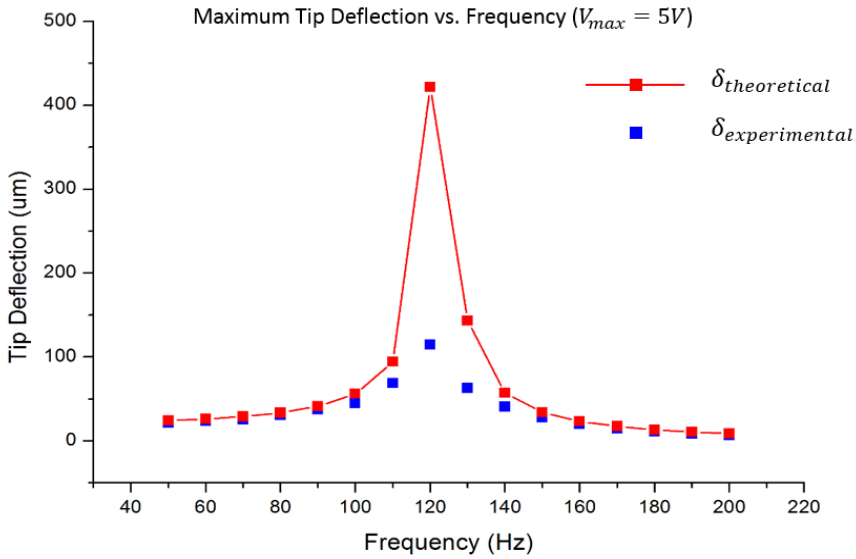

(b)

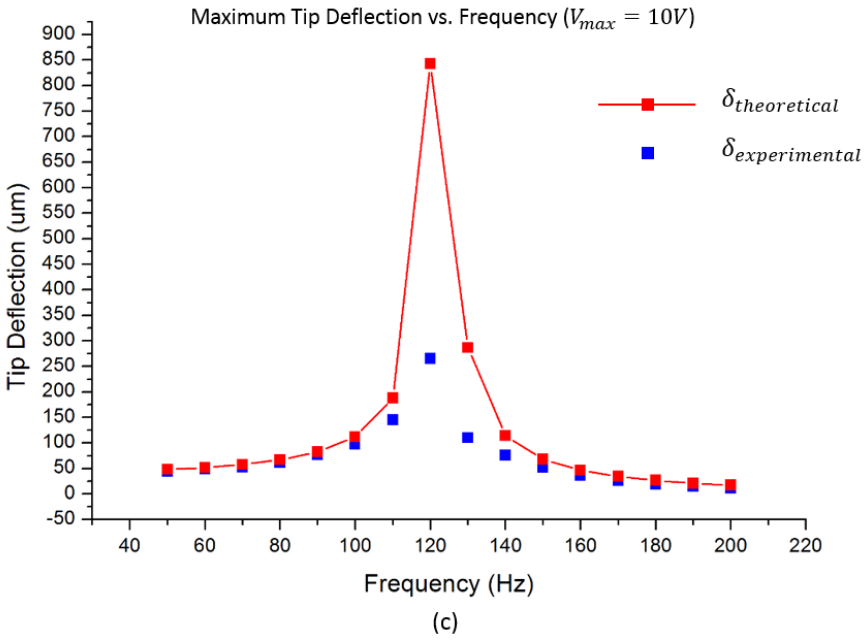

Figure 3-6 Simulated and measured maximum tip deflection versus frequency

From Figure 3-6 we can see the deviations are relatively large near the first natural frequency for all groups of the experiments. The peak value of the tip deflection of the 2V, 5V and 10V maximum driving voltage in experiment only reach 33.42%, 31.39% and 28.57% of the theoretical value. These results are as expected since the transverse deflection is large at the natural frequency which will lead relatively large deviation of the theoretical model.

3.3 EXPERIMENTAL DESIGN FOR CANTILEVER BEAM SENSOR

In this section, a cantilever beam bending sensor is fabricated in base vibration environment working as an accelerometer with proof mass at the tip. Figure 3-7 shows the structure of the sensor. To analyze the sensor vibration, this structure can be modeled as a single degree of freedom system, which consists of a vibration base, a seismic mass M, a spring with spring constant K and a damper with damping coefficient C as shown in Figure 3-8. The effective spring constant can be obtained from the static constitutive equations derived in Chapter 2 as

$$K = \frac{\partial F}{\partial \delta} = \frac{1}{e_{22}} = \frac{3R}{L^3} \tag{3.9}$$

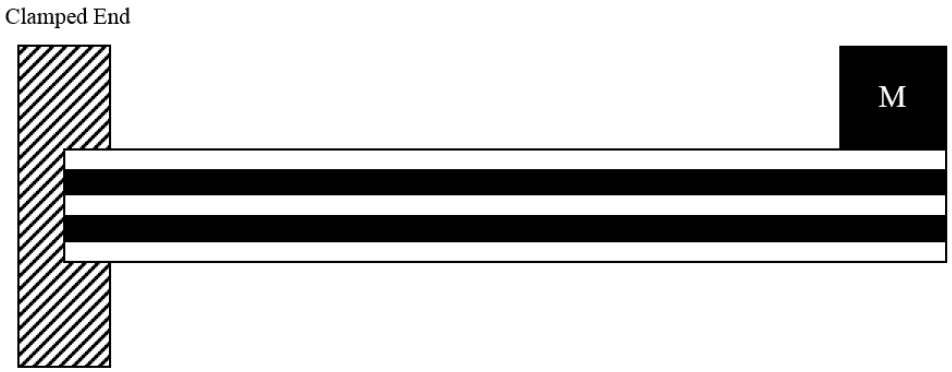

Figure 3-7 The structure of the cantilever accelerometer

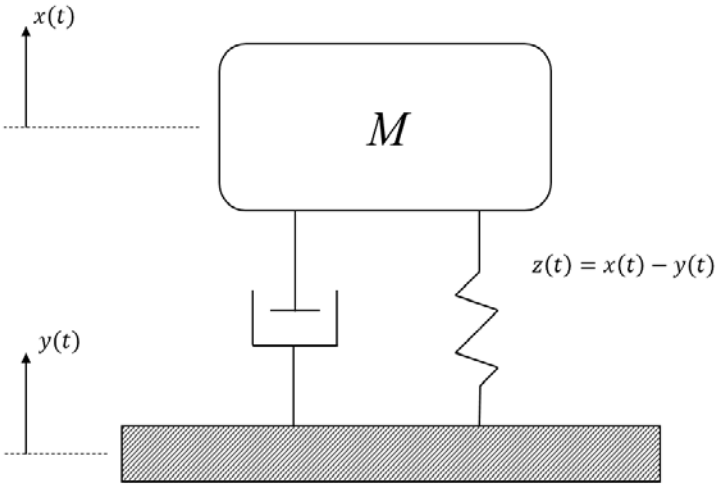

Figure 3-8 Equivalent SDOF model

The seismic mass of the cantilever beam can be calculated as a point mass with equivalent vertical force at the tip of the sensor[25], such that

$$M = m_{eff} + m_{acc} \tag{3.10}$$

Where m_{acc} is the proof mass added at the free end of the beam, m_{eff} is a modeled effective mass of the cantilever beam without tip mass, which can be calculated from the first natural frequency of the cantilever beam as follows:

$$\omega_{n1} = \sqrt{\frac{K}{m_{eff}}} \tag{3.11}$$

Substituting the first natural frequency equation (3.5) and spring constant equation (3.9) into the equation (3.11), the effective mass of the cantilever is derived as follows

$$m_{eff} = \frac{3R}{L^3}\frac{1}{\omega_{n1}^2} = \frac{3R}{L^3}\frac{1}{(1.8751^2\sqrt{\frac{R}{\rho L^4}})^2} \approx \frac{17\rho L}{70} \tag{3.12}$$

The mathematical model of this single degree of freedom mechanical system can be derived by Newton's second law, which is given by

$$M\ddot{x} = -C(\dot{x} - \dot{y}) - K(x - y) \tag{3.13}$$

Where *x* is the displacement of the total mass *M*, *y* is the displacement of the vibration base. We can simplify this equation by introducing the relative displacement *z(t)=x(t)-y(t)*:

$$M\ddot{z} + C\dot{z} + Kz = -M\ddot{y} \tag{3.14}$$

Substituting initial conditions $z(0) = \dot{z}(0) = 0$ into Laplace transform of equation (3.14), the equation can be written as

$$\left|\frac{Z(s)}{\ddot{Y}(s)}\right| = \frac{1}{s^2 + (2\xi\omega_n)s + \omega_n^2} \tag{3.15}$$

Where $\omega_n = \sqrt{\frac{K}{M}}$ is the first natural frequency of this structure, $\xi = \frac{C}{2\sqrt{KM}}$ is the damping ratio which can be calculated using half power method (3dB method) from the experiment data.

The electric output of the sensor can be considered as an electrical voltage generator model[26] as shown in Figure 3-9.

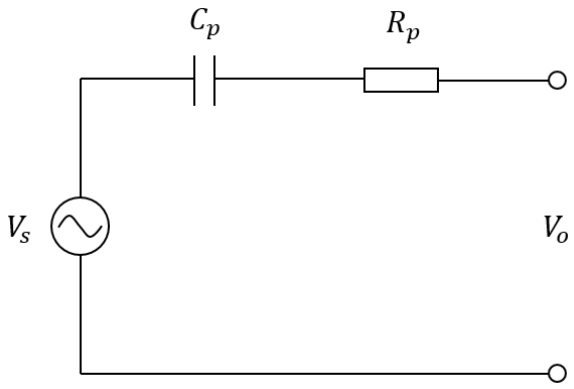

Figure 3-9 A voltage generator model for sensor circuit

The impedance of this voltage generator model in Figure 3-6 is given by

$$\mathrm{Im}(s) = \frac{R_p C_p s + 1}{C_p s} \tag{3.16}$$

For an ideal voltage generator model, the internal resistance R_p is equal to zero. Then the open circuit output voltage of this voltage generator model [27]is

$$V_0(s) = I(s)\,\mathrm{Im}(s) = \frac{Q(s)s}{C_p s} = \frac{Q(s)}{C_p} \tag{3.17}$$

From static constitutive Equation (2.1),

$$Q(t) = e_{42}F = e_{42}(K\delta) = e_{42}Kz(t) \tag{3.18}$$

Substituting Equation (2.68) and Equation (3.9) into Equation (3.18), gives

$$Q(t) = -\frac{3wY_c d_{31} h_c (h_c + h_p)}{2(h_p + 2h_c)L} z(t) = Q_d z(t) \tag{3.19}$$

Where Q_d is the charge coefficient representing the charge generated by unit tip displacement. Then Equation (3.17) can be rewritten as

$$\frac{V_0(s)}{Z(s)} = \frac{Q_d}{C_p} \tag{3.20}$$

Substituting Equation (3.20) into Equation (3.15), the mechanical electric model can be derived as

$$\left|\frac{V_0(s)}{\ddot{Y}(s)}\right| = \frac{Q_d}{C_p}\frac{1}{s^2 + (2\xi\omega_n)s + \omega_n^2} \tag{3.21}$$

If a sinusoidal base movement input $y(t) = Y_0 \sin\omega t$ is applied to the SDOF system, the peak voltage can be obtained as

$$V_0 = \frac{Q_d(\omega/\omega_n)^2}{C_p\sqrt{(\omega/\omega_n)^4 + 2(2\xi^2 - 1)(\omega/\omega_n)^2 + 1}} Y_0 \qquad (3.22)$$

An accelerometer experiment is conducted to verify the theoretical model. Figure 3-10(a) shows the illustrative block diagram of the experiment setup and actual experiment setup[28] is shown in Figure 3-10(b).

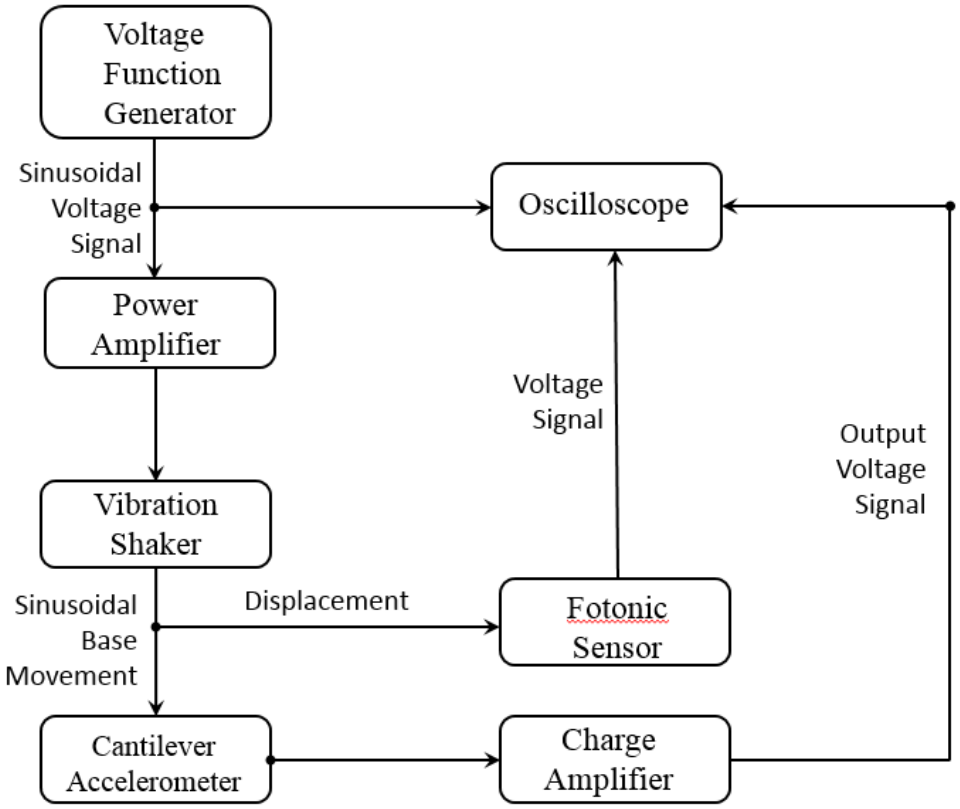

(a)

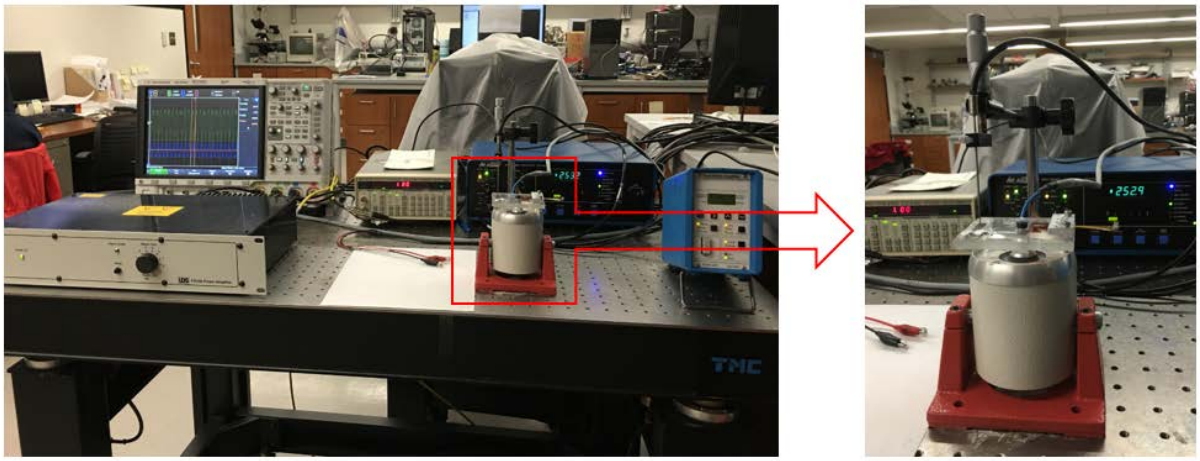

(b)

Figure 3-10 (a) illustrative block diagram of the experiment setup; (b) actual experiment setup for the accelerometer test

3.4 RESULTS OF CANTILEVER BEAM SENSOR EXPERIMENT

The first task of the experiment is to obtain the first natural frequency of the SDOF system. The proof mass (m_{acc}) glued at the tip of cantilever in this experiment is 0.15g. The theoretical first natural frequency can be calculated as $f_1 = \frac{1}{2\pi}\sqrt{\frac{K}{M}} = 57.75\text{Hz}$.

To find the first natural frequency of this system, we use the function generator to generate sinusoidal signal as the driving signal. The peak value of the displacement of the vibration base on the shaker is controlled as a constant (80um) by manually adjusting the gain knob of the power amplifier. The frequency of the driving signal is increased 2 Hz at a time from 0 Hz to 100 Hz, the output voltage of the fotonic sensor and output voltage of the charge amplifier are recorded and

observed by the oscilloscope. Then the plot of the output voltage of the accelerometer relates to frequency of input signal can be obtained from the experimental data as shown in Figure 3-11.

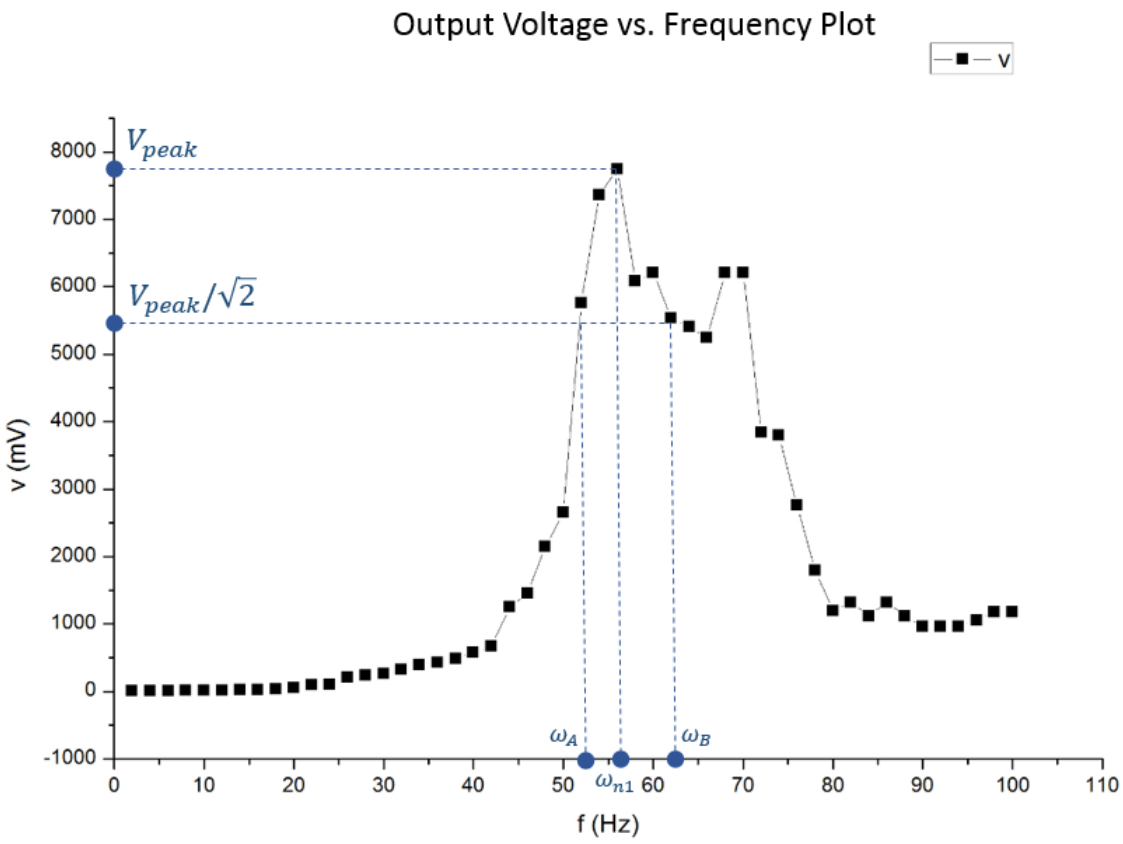

Figure 3-11 Plot of sensor output voltage vs. frequency

Figure 3-11 shows that the first natural frequency occurs at 56.4 Hz which is very close to the theoretical first natural frequency (57.75 Hz). The damping ratio can be determined from the experimental data using half-power method. The half-power point occurs when the output voltage drop by $1/\sqrt{2}$ or 0.707 of the maximum output voltage. The two half-power points ($f_A =$

$52.6\,Hz, f_B = 62.1\,Hz$) around the first natural frequency can be found on the sensor response curve as shown in Figure 3-8. The damping ratio can be calculated as follows

$$\xi = \frac{f_B - f_A}{2 f_{n1}} = \frac{62.1 - 52.6}{2 \times 56.4} = 0.0842 \tag{3.23}$$

This damping ratio can be used to obtain the theoretical response function curve for Equation (3.22) under sinusoidal base movement with constant peak value of the base displacement. Then comparison of the theoretical output function and experimental results under frequency range from 0 Hz to 100 Hz are shown in Figure 3-12. Figure 3-13 shows the comparison of the theoretical and experimental sensitivity curve.

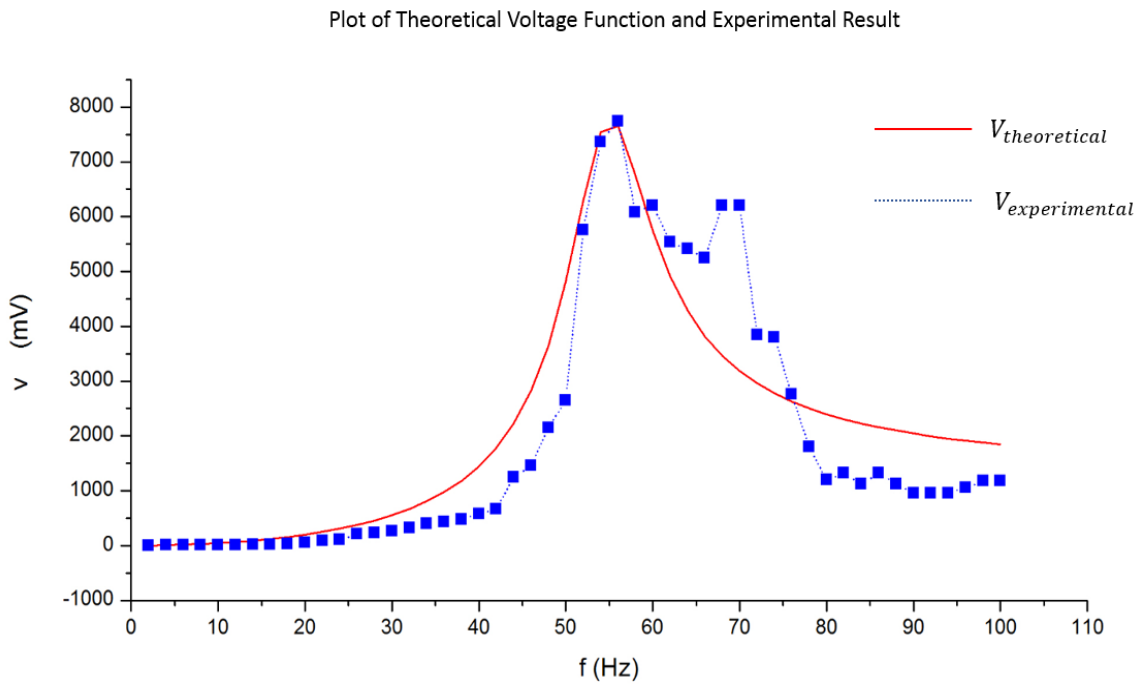

Figure 3-12 Comparison of theoretical model and experimental result

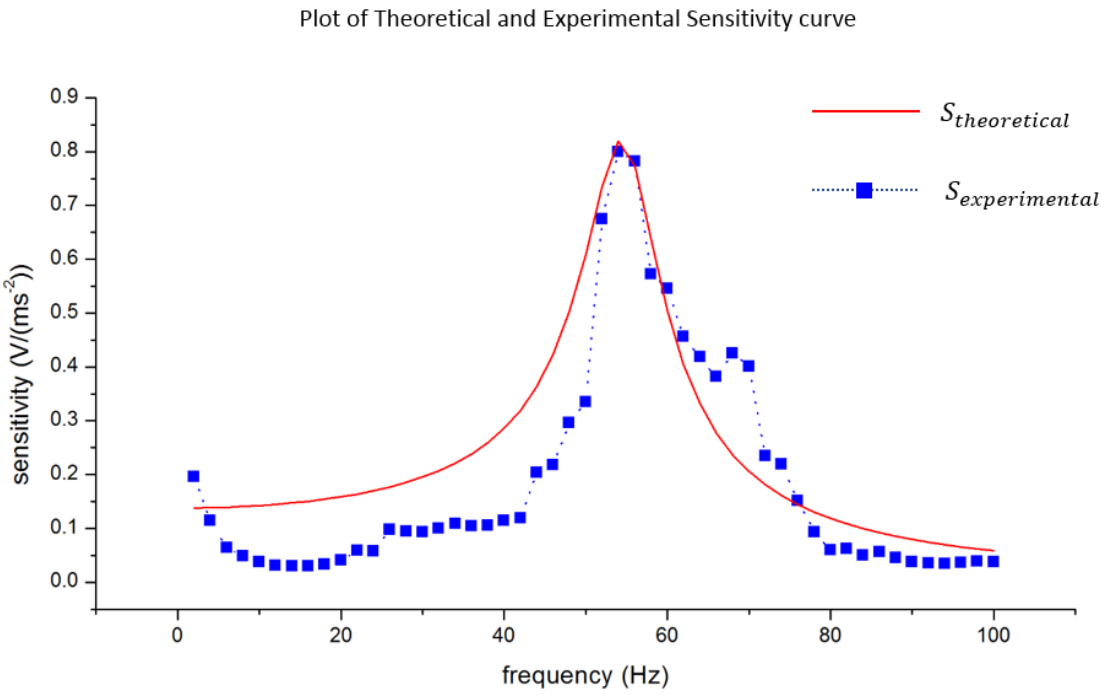

Figure 3-13 Comparison of theoretical and experimental sensitivity curve

It can be found from the figures that the experimental data matches theoretical model well. A second peak of the experimental data occurs around 67 Hz which is not appear in the theoretical model. Since the theoretical model is established by considering only the first natural frequency, the deviation is possibly be caused by the second and third natural frequency of the system. These two natural frequencies can be calculated from

$$\omega_{n2} = \sqrt{\frac{K}{M}} = \sqrt{\frac{K}{m_{eff\,2} + m_{acc}}} \tag{3.24}$$

$$\omega_{n3} = \sqrt{\frac{K}{M}} = \sqrt{\frac{K}{m_{eff\,3} + m_{acc}}} \tag{3.25}$$

Substituting

$$m_{eff\,2} = \frac{3R}{L^3} \frac{1}{(4.4961^2 \sqrt{\frac{R}{\rho L^4}})^2} \tag{3.26}$$

$$m_{eff\,3} = \frac{3R}{L^3} \frac{1}{(7.8547^2 \sqrt{\frac{R}{\rho L^4}})^2} \tag{3.27}$$

Into Equation (3.24) and (3.25), the second and third natural frequencies are

$$f_{n2} = \frac{\omega_{n2}}{2\pi} = 65.3688 Hz \tag{3.28}$$

$$f_{n3} = \frac{\omega_{n3}}{2\pi} = 65.5759 Hz \tag{3.29}$$

These natural frequencies are close to the second peak on the experimental data plot. To reduce this deviation between theoretical model and experiment result, larger end proof mass can be considered in future work for making all the output voltage peaks closer.

4.0 THEORETICAL ANALYSIS OF PZT-POLYMER COMPOSITE DOUBLE CLAMPED BEAM

4.1 A BRIEF INTRODUCTION OF THE DOUBLE CLAMPED COMPOSITE BEAM

In chapter 2, we have established a matrix form constitutive equations representing the reactions of the composite cantilever beam (including the slope at the tip α, the tip deflection δ, the volume displacement v and the charge generated Q) under different external excitations (including an external moment M , a tip force F, a uniformly distributed dynamic pressure P and a harmonic applied voltage V). To obtain the fourth column of elements in that matrix, we tried to transform the reaction caused by the electric field into the effect of the effective external moment. In the doubly clamped beam case we will introduce in this chapter, the effective external moment is very difficult to obtain. Therefore, we consider to use the energy method in the static analysis to establish a theoretical model for the doubly clamped beam.

The general structure of the doubly clamped beam is shown in Figure 4-1. The length of the beam is L, width is w, the thickness of each piezoelectric layer is h_c, the thickness of each polymer layer is h_p.

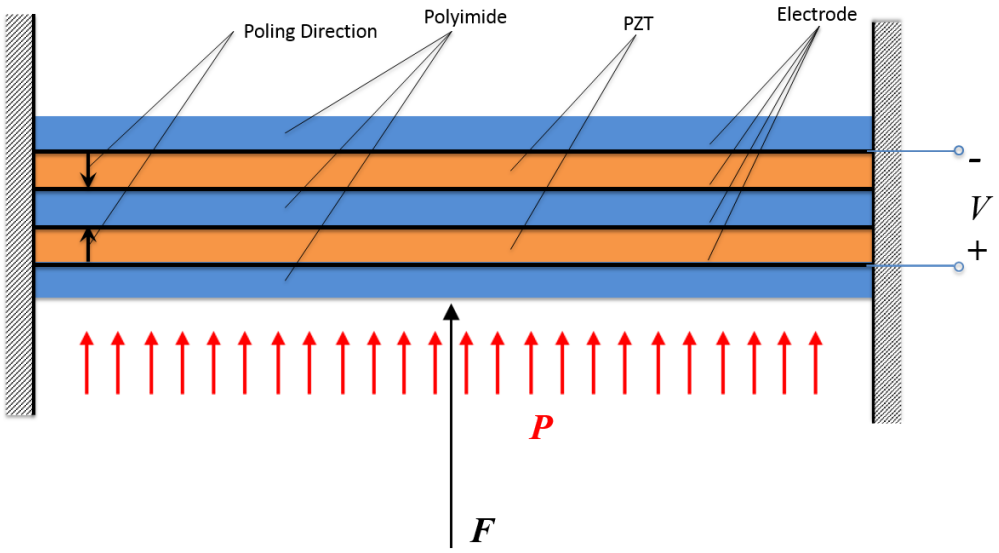

Figure 4-1 A schematic diagram of a PZT-polyimide composite bridge

In this chapter, we want to find a similar form in chapter 2 of a matrix equations of the constitutive equations of the beam. Since here we do not apply an external dynamic moment, we have a 3×3 matrix in the constitutive equations as

$$\begin{bmatrix} \delta \\ v \\ Q \end{bmatrix} = \begin{bmatrix} e_{11} & e_{12} & e_{13} \\ e_{21} & e_{22} & e_{23} \\ e_{31} & e_{32} & e_{33} \end{bmatrix} \begin{bmatrix} F \\ P \\ V \end{bmatrix} \tag{4.1}$$

Where the force F acts in the middle of the beam and P is the pressure acting on the lower surface of the beam. We have proved that the matrix in equation (4.1) is symmetric in chapter 2, so 6 independent elements need to be determined by using energy method [29] in the following sections. In thermodynamic theory, the internal energy density of an infinitesimal piezoelectric element can be defined as

$$u^c = \frac{1}{2} S_1^c \sigma_1^c + \frac{1}{2} D_3 E_3 \tag{4.2}$$

Where S_1^c is strain in length direction and σ_1^c is stress in length direction, D_3 is the electric displacement in thickness direction and E_3 is the electric field in thickness direction.

The internal energy density of the polymer layer is

$$u^p = \frac{1}{2} S_1^p \sigma_1^p = \frac{1}{2} Y_p (S_1^p)^2 \tag{4.3}$$

Where Y_p is the Young's modulus of the polyimide, σ_1^p is stress of the polyimide in length direction.

After determination of the internal energy density of each layer, the total energy of the five layers composite beam is the summation of the internal energy of each layer：

$$U = U^{(1)} + U^{(2)} + U^{(3)} + U^{(4)} + U^{(5)} \tag{4.4}$$

In the following sections, we will discuss the internal energy under different excitations and calculate the partial derivatives of the internal energy with respect to F, P, and V to determine the elements in matrix in equation (4.1).

4.2 THEORETICAL ANALYSIS OF THE BEAM SUBJECTED TO EXTERNAL VOLTAGE

If we apply an external voltage V across the middle three layers of the composite beam as shown in Figure 4-1. The voltage across the two layers of piezoelectric element will cause one of the element to expand along the length direction and the other to contract simultaneously.

Consider the direction of the electric field positive when it is parallel with the polarization direction of the lower piezoelectric element, the constitutive equations of each layer are

The first polymer layer:

$$\sigma_1^{(1)} = Y_p S_1^p = \frac{Y_p}{r(x,t)} z \tag{4.5}$$

The second piezoelectric layer:

$$S_x^{(2)} = s_{11}^E \sigma_x^{(2)} - d_{31} E_3 \tag{4.6}$$

$$-D_3^{(2)} = d_{31} \sigma_x^{(2)} - \varepsilon_{33}^T E_3 \tag{4.7}$$

The third polymer layer:

$$\sigma_1^{(3)} = Y_p S_1^{(3)} = \frac{Y_p}{r(x,t)} z \tag{4.8}$$

The fourth piezoelectric layer:

$$S_x^{(4)} = s_{11}^E \sigma_x^{(4)} + d_{31} E_3 \tag{4.9}$$

$$D_3^{(4)} = d_{31} \sigma_x^{(4)} + \varepsilon_{33}^T E_3 \tag{4.10}$$

The fifth polymer layer:

$$\sigma_1^{(5)} = Y_p S_1^{(5)} = \frac{Y_p}{r(x,t)} z \tag{4.11}$$

Then we can derive moment function of internal forces by integrating the product of stress and distance through the thickness direction as follows:

$$M = -\int_{\frac{h_p}{2}+h_c}^{\frac{3h_p}{2}+h_c} \sigma_x^{(1)} zwdz - \int_{\frac{h_p}{2}}^{\frac{h_p}{2}+h_c} \sigma_x^{(2)} zwdz - \int_{-\frac{h_p}{2}}^{\frac{h_p}{2}} \sigma_x^{(3)} zwdz - \int_{-\frac{h_p}{2}-h_c}^{-\frac{h_p}{2}} \sigma_x^{(4)} zwdz - \int_{-\frac{3h_p}{2}-h_c}^{-\frac{h_p}{2}-h_c} \sigma_x^{(5)} zwdz$$

$$= -\int_{\frac{h_p}{2}+h_c}^{\frac{3h_p}{2}+h_c} wY_p \frac{z^2}{r} dz - \int_{\frac{h_p}{2}}^{\frac{h_p}{2}+h_c} wY_c (\frac{z}{r} + d_{31}E_3) zdz - \int_{-\frac{h_p}{2}}^{\frac{h_p}{2}} wY_p \frac{z^2}{r} dz$$

$$-\int_{-\frac{h_p}{2}-h_c}^{-\frac{h_p}{2}} wY_c (\frac{z}{r} - d_{31}E_3) zdz - \int_{-\frac{3h_p}{2}-h_c}^{-\frac{h_p}{2}-h_c} wY_p \frac{z^2}{r} dz$$

$$= -\frac{w}{12r}[8h_c^3 Y_c + 27h_p^3 Y_p + 12h_c^2 h_p (Y_c + 2Y_p) + 6h_c h_p^2 (Y_c + 8Y_p)] - wh_c^2 d_{31} Y_c E_3 - wh_c h_p d_{31} Y_c E_3$$

$$= -\frac{R}{r} - wh_c^2 d_{31} Y_c E_3 - wh_c h_p d_{31} Y_c E_3 = R\frac{d^2 W}{dx^2} - wh_c^2 d_{31} Y_c E_3 - wh_c h_p d_{31} Y_c E_3 \qquad (4.12)$$

Since the structure of the beam is symmetric, we can simply analyze the deflection function for the left half part of the beam. The bending moment of the left part of the beam is equal to the moment on the left clamped end because of the absence of the external force and external moment as shown in figure 4-2.

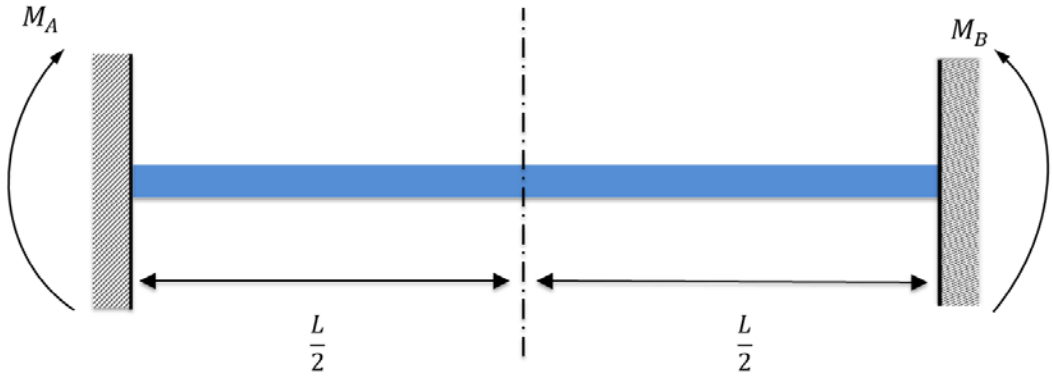

Figure 4-2 The bending moment of the beam

The bending moment of the beam at location x is

$$M(x) = M_A = M_B \tag{4.13}$$

The moment of internal forces is equal to the local bending moment, which gives

$$R\frac{d^2W(x)}{dx^2} - wh_c^2 d_{31} Y_c E_3 - wh_c h_p d_{31} Y_c E_3 = M(x) = M_A \tag{4.14}$$

The boundary conditions of deflection function are

$$W(0) = 0, \frac{dW(0)}{dx} = 0, \frac{dW(\frac{L}{2})}{dx} = 0 \tag{4.15}$$

Then we can solve for transverse deflection as

$$W(x) = 0 \tag{4.16}$$

Therefore, the transverse deflection is 0 under the external voltage V, which means this structure is not good working as an actuator. Since the electric field term is not explicitly appear in the governing deflection function, we have to change demensions of the electrode or the boundary conditions. We will try to use a partially covered electrode instead of fully covered electrode and see if we can get the desired equations.

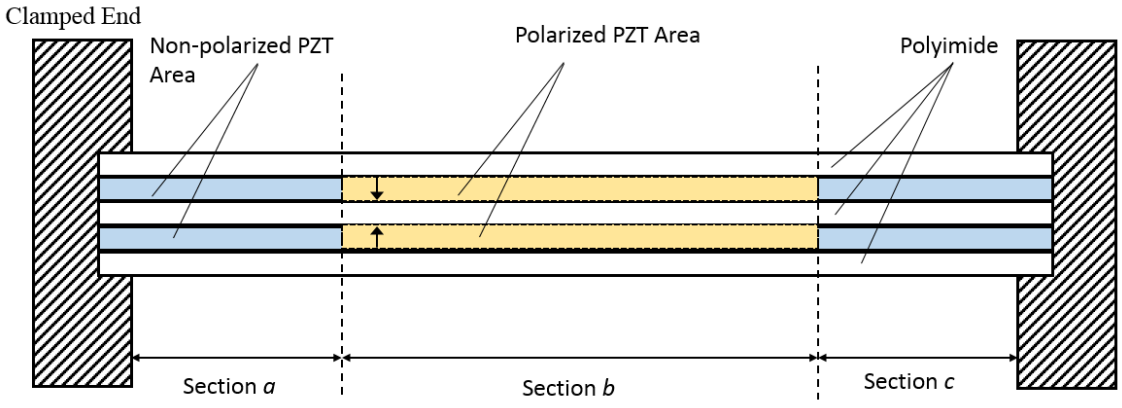

Figure 4-3 Partially polarized PZT layers in doubly clamped beam

Consider two piezoelectric elements in the composite beam with partially covered by the electrode[30]. Only the part of PZT under the covered electrode has been polarized. This structure is shown in Figure 4-3. Along the *x* axis, we divide the beam into three sections along length direction as section *a*, *b* and *c*. We consider the first and the third section which are section *a* and *c* as a non-piezoelectric section with the same length of l_1 and the middle section *b* as the piezoelectric section with the length $l_2 = L - 2l_1$. Since the structure is symmetric, we can analyze the left part of the beam instead of whole structure.

In section *a*, the stress in each layer is

$$\sigma_1^{(1a)} = Y_p \frac{z}{r} \tag{4.17}$$

$$\sigma_1^{(2a)} = Y_c \frac{z}{r} \tag{4.18}$$

$$\sigma_1^{(3a)} = Y_p \frac{z}{r} \tag{4.19}$$

$$\sigma_1^{(4a)} = Y_c \frac{z}{r} \tag{4.20}$$

$$\sigma_1^{(5a)} = Y_p \frac{z}{r} \tag{4.21}$$

The superscript (*ia*) denotes that the stress is in the *i*-th layer in section *a*. Then we can obtain the moment of internal forces by integration as follows:

$$M^{(a)} = -\int_{\frac{h_p}{2}+h_c}^{\frac{3h_p}{2}+h_c} \sigma_x^{(1a)} zwdz - \int_{\frac{h_p}{2}}^{\frac{h_p}{2}+h_c} \sigma_x^{(2a)} zwdz - \int_{-\frac{h_p}{2}}^{\frac{h_p}{2}} \sigma_x^{(3a)} zwdz - \int_{-\frac{h_p}{2}-h_c}^{-\frac{h_p}{2}} \sigma_x^{(4a)} zwdz - \int_{-\frac{3h_p}{2}-h_c}^{-\frac{h_p}{2}-h_c} \sigma_x^{(5a)} zwdz$$

$$= -\frac{w}{12r}[8h_c^3 Y_c + 27h_p^3 Y_p + 12h_c^2 h_p (Y_c + 2Y_p) + 6h_c h_p^2 (Y_c + 8Y_p)] = R\frac{d^2 W^{(a)}}{dx^2} \tag{4.22}$$

In section *b*, the constitutive equations for each layer are same as equation (4.5)-(4.11), then the moment of internal forces is same as (4.12):

$$M^{(b)} = R\frac{d^2W^{(b)}}{dx^2} - wh_c^2 d_{31}Y_c E_3 - wh_c h_p d_{31}Y_c E_3 \tag{4.23}$$

The governing equations of deflection functions of section *a* and section *b* are given by

$$R\frac{d^2W^{(a)}(x)}{dx^2} = M_A, 0 \le x \le l_1 \tag{4.24}$$

$$R\frac{d^2W^{(b)}(x)}{dx^2} - wh_c^2 d_{31}Y_c E_3 - wh_c h_p d_{31}Y_c E_3 = M_A, l_1 \le x \le \frac{L}{2} \tag{4.25}$$

The general solutions for equation (4.24) and equation (4.25) are

$$W^{(a)}(x) = \frac{M_A}{2R}x^2 + c_1 x + c_2, 0 \le x \le l_1 \tag{4.26}$$

$$W^{(b)}(x) = \frac{M_A + wh_c(h_c + h_p)Y_c d_{31}E_3}{2R}x^2 + c_3 x + c_4, l_1 \le x \le \frac{L}{2} \tag{4.27}$$

The boundary conditions are

$$W^{(a)}(0) = 0, \frac{dW^{(a)}(0)}{dx} = 0 \tag{4.28}$$

$$W^{(a)}(l_1) = W^{(b)}(l_1), \frac{dW^{(a)}(l_1)}{dx} = \frac{dW^{(b)}(l_1)}{dx} \tag{4.29}$$

$$\frac{dW^{(b)}(\frac{L}{2})}{dx} = 0 \tag{4.30}$$

Then we can obtain the deflection functions of two sections as follows

$$W^{(a)}(x) = -\frac{wh_c^2 LY_c d_{31}E_3 + wh_c h_p LY_c d_{31}E_3 - 2wh_c^2 l_1 Y_c d_{31}E_3 - 2wh_c h_p l_1 Y_c d_{31}E_3}{2RL}x^2 \tag{4.31}$$

$$W^{(b)}(x) = [-\frac{wh_c^2 LY_c d_{31}E_3 + wh_c h_p LY_c d_{31}E_3 - 2wh_c^2 l_1 Y_c d_{31}E_3 - 2wh_c h_p l_1 Y_c d_{31}E_3}{2RL}$$

$$+\frac{wh_c(h_c + h_p)Y_c d_{31}E_3}{2R}]x^2 - \frac{wh_c^2 l_1 Y_c d_{31}E_3 + wh_c h_p l_1 Y_c d_{31}E_3}{R}x$$

$$-\frac{-wh_c^2 l_1^2 Y_c d_{31} E_3 - wh_c h_p l_1^2 Y_c d_{31} E_3}{2R} \tag{4.32}$$

Now we have transverse deflection functions for two sections of the beam, then the deflection of midpoint of the beam can be found by substituting $x = \frac{L}{2}$ into equation (4.32):

$$\delta = W^{(b)}(\frac{L}{2}) = -\frac{wh_c(h_c + h_p)(L - 2l_1)l_1 Y_c d_{31} V}{4R(2h_c + h_p)} \tag{4.33}$$

$$e_{13} = -\frac{wh_c(h_c + h_p)(L - 2l_1)l_1 Y_c d_{31}}{4R(2h_c + h_p)} \tag{4.34}$$

From equation (4.33) we can see that when $l_1 = \frac{L}{4}$, the deflection has maximum value (d_{31} is negative) which is

$$\delta_{\max} = -\frac{wh_c(h_c + h_p)L^2 Y_c d_{31} V}{32R(2h_c + h_p)} \tag{4.35}$$

The volume displacement is given by

$$v = 2(\int_{-\frac{w}{2}}^{\frac{w}{2}} \int_0^{l_1} W^{(a)} dxdy + \int_{-\frac{w}{2}}^{\frac{w}{2}} \int_{l_1}^{\frac{L}{2}} W^{(b)} dxdy)$$

$$= -\frac{w^2 h_c(h_c + h_p)(L - 2l_1)(L - l_1)l_1 Y_c d_{31} V}{6R(2h_c + h_p)} \tag{4.36}$$

$$e_{23} = -\frac{w^2 h_c(h_c + h_p)(L - 2l_1)(L - l_1)l_1 Y_c d_{31}}{6R(2h_c + h_p)} \tag{4.37}$$

And from equation (4.36) we can see that when $l_1 = \frac{L}{4}$, the volumetric displacement has maximum value (d_{31} is negative) which is

$$v_{\max} = -\frac{w^2 h_c(h_c + h_p)L^3 Y_c d_{31} V}{64R(2h_c + h_p)} \tag{4.38}$$

To obtain the element e_{33}, first we need to find the total internal energy of the device. The total internal energy is the summation of the internal energy of three separated sections.

$$U = U^{(a)} + U^{(b)} + U^{(c)} \tag{4.39}$$

The internal energy of section *a* is strain energy which is given by

$$U^{(a)} = \int_0^{l_1} \int_{-\frac{w}{2}}^{\frac{w}{2}} (\int_{\frac{h_p}{2}+h_c}^{\frac{3h_p}{2}+h_c} \frac{1}{2}\sigma_1^{(1a)} S_1^{(1a)} dz + \int_{\frac{h_p}{2}}^{\frac{h_p}{2}+h_c} \frac{1}{2}\sigma_1^{(2a)} S_1^{(2a)} dz + \int_{-\frac{h_p}{2}}^{\frac{h_p}{2}} \frac{1}{2}\sigma_1^{(3a)} S_1^{(3a)} dz$$

$$+ \int_{-\frac{h_p}{2}-h_c}^{-\frac{h_p}{2}} \frac{1}{2}\sigma_1^{(4a)} S_1^{(4a)} dz + \int_{-\frac{3h_p}{2}-h_c}^{-\frac{h_p}{2}-h_c} \frac{1}{2}\sigma_1^{(5a)} S_1^{(5a)} dz) dy dx$$

$$= \int_0^{l_1} \int_{-\frac{w}{2}}^{\frac{w}{2}} (\int_{\frac{h_p}{2}+h_c}^{\frac{3h_p}{2}+h_c} [\frac{Y_p}{2}(\frac{d^2W^{(a)}(x)}{dx^2})^2 z^2] dz + \int_{\frac{h_p}{2}}^{\frac{h_p}{2}+h_c} [\frac{Y_c}{2}(\frac{d^2W^{(a)}(x)}{dx^2})^2 z^2] dz + \int_{-\frac{h_p}{2}}^{\frac{h_p}{2}} [\frac{Y_p}{2}(\frac{d^2W^{(a)}(x)}{dx^2})^2 z^2] dz$$

$$+ \int_{-\frac{h_p}{2}-h_c}^{-\frac{h_p}{2}} [\frac{Y_c}{2}(\frac{d^2W^{(a)}(x)}{dx^2})^2 z^2] dz + \int_{-\frac{3h_p}{2}-h_c}^{-\frac{h_p}{2}-h_c} [\frac{Y_p}{2}(\frac{d^2W^{(a)}(x)}{dx^2})^2 z^2] dz) dy dx \tag{4.40}$$

The expression of internal energy density of the piezoelectric element is given by equation (4.2), by substituting constitutive equations of each layer from (4.5) to (4.11) into equation (4.2), we can obtain the internal energy density of each layer in the middle section *b*:

$$u^{(1b)} = \frac{1}{2} Y_p (S_1^{(1b)})^2 = \frac{1}{2} Y_p [\frac{d^2W^{(b)}}{dx^2}]^2 z^2 \tag{4.41}$$

$$u^{(2b)} = \frac{1}{2} S_1^{(2b)} [Y_c (S_1^{(2b)} + d_{31} E_3)] + \frac{1}{2} \{\varepsilon_{33} E_3 - d_{31} [Y_c (S_1^{(2b)} + d_{31} E_3)]\} E_3$$

$$= \frac{1}{2} [Y_c (\frac{d^2W^{(b)}}{dx^2})^2 z^2 + \varepsilon_{33} E_3^2 - d_{31}^2 Y_c E_3^2] \tag{4.42}$$

$$u^{(3b)} = \frac{1}{2} Y_p (S_1^{(3b)})^2 = \frac{1}{2} Y_p [\frac{d^2W^{(b)}}{dx^2}]^2 z^2 \tag{4.43}$$

$$u^{(4b)} = \frac{1}{2} S_1^{(4b)} [Y_c (S_1^{(4b)} - d_{31} E_3)] + \frac{1}{2} \{d_{31} [Y_c (S_1^{(4b)} - d_{31} E_3)] + \varepsilon_{33} E_3\} E_3$$

$$= \frac{1}{2}[Y_c(\frac{d^2W^{(b)}}{dx^2})^2 z^2 + \varepsilon_{33}E_3^2 - Y_c d_{31}^2 E_3^2] \tag{4.44}$$

$$u^{(5b)} = \frac{1}{2}Y_p(S_1^{(5b)})^2 = \frac{1}{2}Y_p[\frac{d^2W^{(b)}}{dx^2}]^2 z^2 \tag{4.45}$$

The internal energy of the left half part of section *b* is

$$\frac{1}{2}U^{(b)} = \int_{l_1}^{\frac{L}{2}}\int_{-\frac{w}{2}}^{\frac{w}{2}}(\int_{\frac{h_p}{2}+h_c}^{\frac{3h_p}{2}+h_c} u^{(1b)}dz + \int_{\frac{h_p}{2}}^{\frac{h_p}{2}+h_c} u^{(2b)}dz$$

$$+\int_{-\frac{h_p}{2}}^{\frac{h_p}{2}} u^{(3b)}dz + \int_{-\frac{h_p}{2}-h_c}^{-\frac{h_p}{2}} u^{(4b)}dz + \int_{-\frac{3h_p}{2}-h_c}^{-\frac{h_p}{2}-h_c} u^{(5b)}dz)dydx \tag{4.46}$$

The total internal energy can be obtained by

$$U = 2(U^{(a)} + \frac{1}{2}U^{(b)})$$

$$= \frac{wh_c(L-2l_1)V^2}{LR(2h_c+h_p)^2}[(\varepsilon_{33} - d_{31}^2 Y_c)LR + d_{31}^2 Y_c^2 wh_c(h_c+h_p)^2 l_1] \tag{4.47}$$

The generated electric charge on the electrode then can be determined as

$$Q = \frac{\partial U}{\partial V} = \frac{2wh_c(L-2l_1)V}{LR(2h_c+h_p)^2}[(\varepsilon_{33} - d_{31}^2 Y_c)LR + d_{31}^2 Y_c^2 wh_c(h_c+h_p)^2 l_1] \tag{4.48}$$

The element e_{33} is

$$e_{33} = \frac{Q}{V} = \frac{2wh_c(L-2l_1)}{LR(2h_c+h_p)^2}[(\varepsilon_{33} - d_{31}^2 Y_c)LR + d_{31}^2 Y_c^2 wh_c(h_c+h_p)^2 l_1] \tag{4.49}$$

Therefore, we obtained all three elements in the third column in the matrix in constitutive equation (4.1).

4.3 THEORETICAL ANALYSIS OF THE BEAM UNDER APPLIED PRESSURE

In this case, we will apply an external pressure on the lower surface of the beam and try to establish a theoretical model for the constitutive equations[31]. Firstly, we will discuss a beam structure with fully covered electrode on the piezoelectric element. As discussed in the chapter 2, the governing equation for the transverse deflection function under a static pressure is

$$R\frac{d^4W(x)}{dx^4} = Pw \tag{4.50}$$

We impose the boundary conditions:

$$W(0) = W(L) = 0; \frac{dW(0)}{dx} = \frac{dW(L)}{dx} = 0 \tag{4.51}$$

We can obtain the deflection function:

$$W(x) = \frac{wPx^4 - 2wLPx^3 + wL^2Px^2}{24R} \tag{4.52}$$

The transverse deflection function can be used to characterize the internal energy density of each layer

$$u^{(1)} = \frac{1}{2}Y_p(S_1^{(1)})^2 = \frac{1}{2}Y_p[\frac{d^2W(x)}{dx^2}]^2 z^2 \tag{4.53}$$

$$u^{(2)} = \frac{1}{2}S_1^{(2)}[Y_c(S_1^{(2)} + d_{31}E_3)] + \frac{1}{2}\{\varepsilon_{33}E_3 - d_{31}[Y_c(S_1^{(2)} + d_{31}E_3)]\}E_3$$

$$= \frac{1}{2}[Y_c(\frac{d^2W(x)}{dx^2})^2 z^2 + \varepsilon_{33}E_3^2 - d_{31}^2 Y_c E_3^2] \tag{4.54}$$

$$u^{(3)} = \frac{1}{2}Y_p(S_1^{(3)})^2 = \frac{1}{2}Y_p[\frac{d^2W(x)}{dx^2}]^2 z^2 \tag{4.55}$$

$$u^{(4)} = \frac{1}{2}S_1^{(4)}[Y_c(S_1^{(4)} - d_{31}E_3)] + \frac{1}{2}\{d_{31}[Y_c(S_1^{(4)} - d_{31}E_3)] + \varepsilon_{33}E_3\}E_3$$

$$= \frac{1}{2}[Y_c(\frac{d^2W(x)}{dx^2})^2 z^2 + \varepsilon_{33}E_3^2 - Y_c d_{31}^2 E_3^2] \tag{4.56}$$

$$u^{(5)} = \frac{1}{2}Y_p(S_1^{(5)})^2 = \frac{1}{2}Y_p[\frac{d^2W(x)}{dx^2}]^2 z^2 \tag{4.57}$$

Therefore, the total system energy can be written in terms of applied pressure and electric field as follows.

$$U = \int_0^L \int_{-\frac{w}{2}}^{\frac{w}{2}} (\int_{\frac{h_p}{2}+h_c}^{\frac{3h_p}{2}+h_c} u^{(1)}dz + \int_{\frac{h_p}{2}}^{\frac{h_p}{2}+h_c} u^{(2)}dz + \int_{-\frac{h_p}{2}}^{\frac{h_p}{2}} u^{(3)}dz + \int_{-\frac{h_p}{2}-h_c}^{-\frac{h_p}{2}} u^{(4)}dz + \int_{-\frac{3h_p}{2}-h_c}^{-\frac{h_p}{2}-h_c} u^{(5)}dz)dydx$$

$$= wLh_c(\varepsilon_{33} - d_{31}^2 Y_c)E_3^2 + \frac{w^2L^5}{1440R}P^2 = \frac{wLh_c(\varepsilon_{33} - d_{31}^2 Y_c)}{(2h_c + h_p)^2}V^2 + \frac{w^2L^5}{1440R}P^2 \tag{4.58}$$

The generated charge from the external pressure can be derived by differentiating the total energy with respect to the voltage:

$$Q = \frac{\partial U}{\partial V} = \frac{2wLh_c(\varepsilon_{33} - d_{31}^2 Y_c)}{(2h_c + h_p)^2}V \tag{4.59}$$

In this case with pressure applied only, there is no applied voltage in equation (4.59), thus this model will not generate charge on the electrode, which means this model is not good to work as an sensor to convert mechanical energy to electrical energy[32]. From this perspective, we consider a similar model as described in Section 4.2 which divides the beam into three sections along the length direction as shown in Figure 4-3.Then we will try to establish a theoretical model for this beam with partially covered electrodes as follows.

We can use figure 4-4 to analyze the forces and moments of the doubly clamped beam.

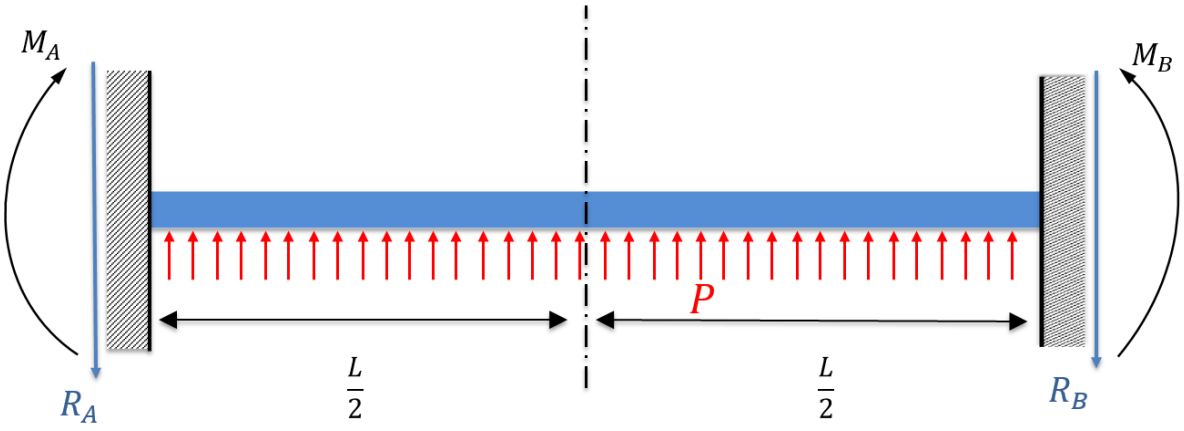

Figure 4-4 Reactions and moments on the beam under uniformly distributed load

Because of the symmetry, we have

$$R_A = R_B = \frac{wPL}{2}, M_A = M_B \tag{4.60}$$

The moment at point x is

$$M = M_A + \frac{wPx(x-L)}{2} \tag{4.61}$$

The moment of internal forces of each section is

$$M^{(a)} = R\frac{d^2W^{(a)}}{dx^2} \tag{4.62}$$

$$M^{(b)} = R\frac{d^2W^{(b)}}{dx^2} - wh_c^2 d_{31} Y_c E_3 - wh_c h_p d_{31} Y_c E_3 \tag{4.63}$$

$$M^{(c)} = R\frac{d^2W^{(c)}}{dx^2} \tag{4.64}$$

For symmetric structure we can focus on the left half part of the beam only, then we have

$$R\frac{d^2W^{(a)}}{dx^2} = M_A + \frac{wPx(x-L)}{2}, 0 \le x \le l_1 \tag{4.65}$$

$$R\frac{d^2W^{(b)}(x)}{dx^2} - wh_c^2 d_{31} Y_c E_3 - wh_c h_p d_{31} Y_c E_3 = M_A + \frac{wPx(x-L)}{2}, l_1 \le x \le \frac{L}{2} \tag{4.66}$$

The boundary conditions in this case are

$$W^{(a)}(0) = 0, \frac{dW^{(a)}(0)}{dx} = 0 \tag{4.67}$$

$$W^{(a)}(l_1) = W^{(b)}(l_1), \frac{dW^{(a)}(l_1)}{dx} = \frac{dW^{(b)}(l_1)}{dx} \tag{4.68}$$

$$\frac{dW^{(b)}(\frac{L}{2})}{dx} = 0 \tag{4.69}$$

Then we can solve for the deflection functions of two sections as follows

$$W^{(a)}(x) = \frac{wP}{24R}x^4 - \frac{wPL}{12R}x^3 + \frac{M_A}{2R}x^2, 0 \le x \le l_1 \tag{4.70}$$

$$W^{(b)}(x) = \frac{wP}{24R}x^4 - \frac{wPL}{12R}x^3 + \frac{M_A + wh_c(h_c + h_p)Y_c d_{31} E_3}{2R}x^2 + c_1 x + c_2, l_1 \le x \le \frac{L}{2} \tag{4.71}$$

Where

$$c_1 = -\frac{wh_c^2 l_1 Y_c d_{31} E_3 + wh_c h_p l_1 Y_c d_{31} E_3}{R} \tag{4.72}$$

$$c_2 = \frac{wh_c^2 l_1^2 Y_c d_{31} E_3 + wh_c h_p l_1^2 Y_c d_{31} E_3}{2R} \tag{4.73}$$

$$M_A = -\frac{1}{12L}(-wPL^3 + 12wh_c^2 LY_c d_{31} E_3 + 12wh_c h_p LY_c d_{31} E_3$$

$$-24wh_c^2 l_1 Y_c d_{31} E_3 - 24wh_c h_p l_1 Y_c d_{31} E_3) \tag{4.74}$$

The previous relations can be used to characterize the internal energy of the deformed beam of each section:

$$U^{(a)} = \int_0^{l_1} \int_{-\frac{w}{2}}^{\frac{w}{2}} (\int_{\frac{h_p}{2}+h_c}^{\frac{3h_p}{2}+h_c} \frac{1}{2}\sigma_1^{(1a)} S_1^{(1a)} dz + \int_{\frac{h_p}{2}}^{\frac{h_p}{2}+h_c} \frac{1}{2}\sigma_1^{(2a)} S_1^{(2a)} dz + \int_{-\frac{h_p}{2}}^{\frac{h_p}{2}} \frac{1}{2}\sigma_1^{(3a)} S_1^{(3a)} dz$$

$$+\int_{-\frac{h_p}{2}-h_c}^{-\frac{h_p}{2}} \frac{1}{2}\sigma_1^{(4a)} S_1^{(4a)} dz + \int_{-\frac{3h_p}{2}-h_c}^{-\frac{h_p}{2}-h_c} \frac{1}{2}\sigma_1^{(5a)} S_1^{(5a)} dz) dy dx$$

$$= \int_0^{l_1} \int_{-\frac{w}{2}}^{\frac{w}{2}} (\int_{\frac{h_p}{2}+h_c}^{\frac{3h_p}{2}+h_c} [\frac{Y_p}{2}(\frac{d^2W^{(a)}(x)}{dx^2})^2 z^2] dz + \int_{\frac{h_p}{2}}^{\frac{h_p}{2}+h_c} [\frac{Y_c}{2}(\frac{d^2W^{(a)}(x)}{dx^2})^2 z^2] dz + \int_{-\frac{h_p}{2}}^{\frac{h_p}{2}} [\frac{Y_p}{2}(\frac{d^2W^{(a)}(x)}{dx^2})^2 z^2] dz$$

$$+\int_{-\frac{h_p}{2}-h_c}^{-\frac{h_p}{2}} [\frac{Y_c}{2}(\frac{d^2W^{(a)}(x)}{dx^2})^2 z^2] dz + \int_{-\frac{3h_p}{2}-h_c}^{-\frac{h_p}{2}-h_c} [\frac{Y_p}{2}(\frac{d^2W^{(a)}(x)}{dx^2})^2 z^2] dz) dy dx \quad (4.75)$$

$$\frac{1}{2}U^{(b)} = \int_{l_1}^{\frac{L}{2}} \int_{-\frac{w}{2}}^{\frac{w}{2}} (\int_{\frac{h_p}{2}+h_c}^{\frac{3h_p}{2}+h_c} u^{(1b)} dz + \int_{\frac{h_p}{2}}^{\frac{h_p}{2}+h_c} u^{(2b)} dz$$

$$+\int_{-\frac{h_p}{2}}^{\frac{h_p}{2}} u^{(3b)} dz + \int_{-\frac{h_p}{2}-h_c}^{-\frac{h_p}{2}} u^{(4b)} dz + \int_{-\frac{3h_p}{2}-h_c}^{-\frac{h_p}{2}-h_c} u^{(5b)} dz) dy dx \quad (4.76)$$

The total internal energy is

$$U = 2(U^{(a)} + \frac{1}{2}U^{(b)})$$

$$= \frac{w^2 L^5 P^2}{1440R} - \frac{w^2 h_c (h_c + h_p) l_1 (L^2 - 3Ll_1 + 2l_1^2) Y_c d_{31} E_3 P}{6R}$$

$$+\frac{w h_c (L - 2l_1) E_3^2}{LR}[(\varepsilon_{33} - d_{31}^2 Y_c) LR + d_{31}^2 Y_c h_c (h_c + h_p)^2 l_1 w Y_c] \quad (4.77)$$

We can see that we have $U(E_3, P)$ term in energy equation, which means this structure can be used as sensor. The generated charge is

$$Q = \frac{\partial U}{\partial V} = -\frac{w^2 h_c (h_c + h_p) l_1 (L^2 - 3Ll_1 + 2l_1^2) Y_c d_{31} P}{6R(2h_c + h_p)}$$

$$+\frac{2w h_c (L - 2l_1) V}{LR(2h_c + h_p)^2}[(\varepsilon_{33} - d_{31}^2 Y_c) LR + d_{31}^2 Y_c h_c (h_c + h_p)^2 l_1 w Y_c] \quad (4.78)$$

Since no external voltage applied, the generated charge is

$$Q = -\frac{w^2 h_c (h_c + h_p) l_1 (L^2 - 3Ll_1 + 2l_1^2) Y_c d_{31} P}{6R(2h_c + h_p)} \tag{4.79}$$

Therefore, the element e_{32} in equation (4.1) is

$$e_{32} = -\frac{w^2 h_c (h_c + h_p) l_1 (L^2 - 3Ll_1 + 2l_1^2) Y_c d_{31}}{6R(2h_c + h_p)} \tag{4.80}$$

We can see that $e_{32} = e_{23}$ as the described symmetry property of the matrix in equation (4.1).

Now we have transverse deflection functions for two sections of the beam, then the deflection of midpoint of the beam can be found by substituting $x = \frac{L}{2}$ into equation (4.71):

$$\delta = W^{(b)}(\frac{L}{2}) = \frac{wPL^4 - 96wh_c(h_c + h_p)(L - 2l_1) l_1 Y_c d_{31} E_3}{384R} \tag{4.81}$$

In this case, there is no external voltage applied on the beam, so $E_3 = 0$, the element e_{12} can be obtained as

$$e_{12} = \frac{wL^4}{384R} \tag{4.82}$$

The volume displacement is given by

$$v = 2(\int_{-\frac{w}{2}}^{\frac{w}{2}} \int_0^{l_1} W^{(a)} dxdy + \int_{-\frac{w}{2}}^{\frac{w}{2}} \int_{l_1}^{\frac{L}{2}} W^{(b)} dxdy)$$

$$= \frac{w^2 L^5 P - 120w^2 h_c (h_c + h_p)(L - 2l_1)(L - l_1) l_1 Y_c d_{31} E_3}{720R} \tag{4.83}$$

Which will lead to e_{22}:

$$e_{22} = \frac{w^2 L^5}{720R} \tag{4.84}$$

4.4 THEORETICAL ANALYSIS OF THE BEAM UNDER APPLIED FORCE AT MIDPOINT

When the beam is subjected to a point load at midpoint perpendicular to the length direction as shown in figure 4-5, its transverse deflection function can be analyzed as follows.

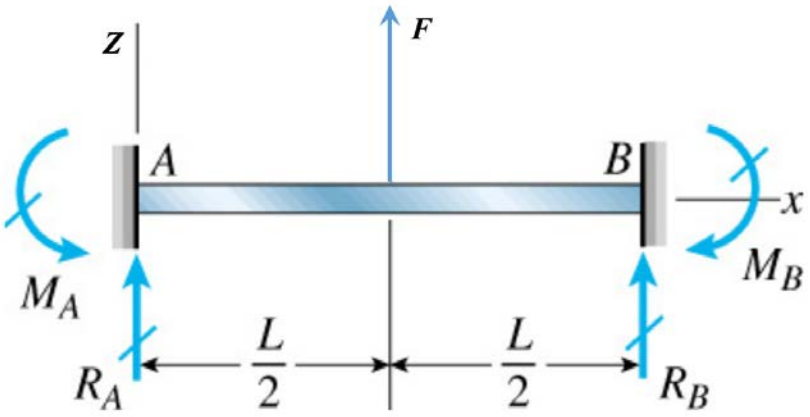

Figure 4-5 Doubly clamped beam subjected to a concentrated load F

Because the load F is in y direction and the structure is symmetric, we have:

$$R_A = R_b = -\frac{F}{2}, M_A = M_B \tag{4.85}$$

$$M(x) = R_A x - M_A = -M_A - \frac{F}{2}x, 0 \le x \le \frac{L}{2} \tag{4.86}$$

The moment of internal force from constitutive equations of each layer is

$$M = -\int_{\frac{h_p}{2}+h_c}^{\frac{3h_p}{2}+h_c} \sigma_x^{(1)} zwdz - \int_{\frac{h_p}{2}}^{\frac{h_p}{2}+h_c} \sigma_x^{(2)} zwdz - \int_{-\frac{h_p}{2}}^{\frac{h_p}{2}} \sigma_x^{(3)} zwdz - \int_{-\frac{h_p}{2}-h_c}^{-\frac{h_p}{2}} \sigma_x^{(4)} zwdz - \int_{-\frac{3h_p}{2}-h_c}^{-\frac{h_p}{2}-h_c} \sigma_x^{(5)} zwdz$$

$$= R\frac{d^2W}{dx^2} - wh_c^2 d_{31} Y_c E_3 - wh_c h_p d_{31} Y_c E_3 \tag{4.87}$$

Then we have

$$R\frac{d^2W}{dx^2} - wh_c^2 d_{31} Y_c E_3 - wh_c h_p d_{31} Y_c E_3 = -M_A - \frac{F}{2}x \tag{4.88}$$

After integration, it is

$$R\frac{dW}{dx} = -M_A x - \frac{F}{4}x^2 + wh_c(h_c + h_p) Y_c d_{31} E_3 x + c_1 \tag{4.89}$$

$$RW = -\frac{M_A}{2}x^2 - \frac{F}{12}x^3 + \frac{wh_c(h_c + h_p) Y_c d_{31} E_3}{2}x^2 + c_1 x + c_2 \tag{4.90}$$

The boundary conditions:

$$W(0) = 0, \frac{dW(0)}{dx} = 0, \frac{dW(\frac{L}{2})}{dx} = 0 \tag{4.91}$$

Then we have

$$M_A = -\frac{FL}{8} + wh_c(h_c + h_p) Y_c d_{31} E_3 \tag{4.92}$$

$$W(x) = \frac{FL}{16R}x^2 - \frac{F}{12R}x^3, 0 \le x \le \frac{L}{2} \tag{4.93}$$

Then we can obtain the total internal energy from transverse deflection function as

$$U = 2\int_0^{\frac{L}{2}} \int_{-\frac{w}{2}}^{\frac{w}{2}} (\int_{\frac{h_p}{2}+h_c}^{\frac{3h_p}{2}+h_c} u^{(1)} dz + \int_{\frac{h_p}{2}}^{\frac{h_p}{2}+h_c} u^{(2)} dz + \int_{-\frac{h_p}{2}}^{\frac{h_p}{2}} u^{(3)} dz + \int_{-\frac{h_p}{2}-h_c}^{-\frac{h_p}{2}} u^{(4)} dz + \int_{-\frac{3h_p}{2}-h_c}^{-\frac{h_p}{2}-h_c} u^{(5)} dz) dy dx$$

$$= wLh_c E_3^2(\varepsilon_{33} - d_{31}^2 Y_c) + \frac{L^3 F^2}{384R} = \frac{wLh_c(\varepsilon_{33} - d_{31}^2 Y_c)}{(2h_c + h_p)^2} V^2 + \frac{L^3 F^2}{384R} \tag{4.94}$$

The two terms indicates the electric potential $U(V^2)$ and mechanical strain energy $U(F^2)$ respectively. The absence of the electromechanically coupling energy means that this model

cannot transfer mechanical energy into electric energy. So we turn our attention to the structure with partially covered electrodes as described in the previous sections. Consider the non-polarized outer elastic zone *a* in the left part of the beam with length l_1, the piezoelectric zone *b* in the left part of the beam with length $\frac{L}{2} - l_1$.

The deflection functions of section *a* and section *b* are given by

$$W^{(a)}(x) = -\frac{F}{12R}x^3 - \frac{1}{2R}M_A x^2 + c_1 x + c_2 \tag{4.95}$$

$$W^{(b)}(x) = -\frac{F}{12R}x^3 - \frac{1}{2R}M_A x^2 + \frac{1}{2R}wh_c(h_c + h_p)d_{31}Y_c E_3 x^2 + c_3 x + c_4 \tag{4.96}$$

Then we impose boundary conditions:

$$W^{(a)}(0) = 0, \frac{dW^{(a)}(0)}{dx} = 0 \tag{4.97}$$

$$W^{(a)}(l_1) = W^{(b)}(l_1), \frac{dW^{(a)}(l_1)}{dx} = \frac{dW^{(b)}(l_1)}{dx} \tag{4.98}$$

$$\frac{dW^{(b)}(\frac{L}{2})}{dx} = 0 \tag{4.99}$$

Then we can obtain

$$c_1 = c_2 = 0 \tag{4.100}$$

$$c_3 = -\frac{h_c^2 l_1 w Y_c d_{31} E_3 + h_c h_p w l_1 Y_c d_{31} E_3}{R} \tag{4.101}$$

$$c_4 = \frac{h_c^2 w l_1^2 Y_c d_{31} E_3 + h_c h_p w l_1^2 Y_c d_{31} E_3}{2R} \tag{4.102}$$

$$M_A = -\frac{1}{8L}(FL^2 - 8wh_c^2 L Y_c d_{31} E_3 - 8wh_c h_p L Y_c d_{31} E_3$$

$$+16wh_c^2 l_1 Y_c d_{31} E_3 + 16wh_c h_p l_1 Y_c d_{31} E_3) \tag{4.103}$$

After obtaining the deflection function of the beam, we can try to solve for total internal energy of the beam:

$$U = 2(U^{(a)} + U^{(b)}) = \frac{L^3 F^2}{384R} - \frac{wh_c(h_c + h_p)(L - 2l_1)l_1 Y_c d_{31} E_3 F}{4R}$$

$$+ \frac{wh_c(L - 2l_1)E_3^2}{LR}[(\varepsilon_{33} - d_{31}^2 Y_c)LR + h_c(h_c + h_p)^2 l_1 w Y_c^2 d_{31}^2] \tag{4.104}$$

We can see that the electromechanical energy term $U(E_3, F)$ appears in the equation (4.104), thus we can use this model as a transformer.

The deflection amplitude of the midpoint of the beam is given by

$$W^{(b)}(\frac{L}{2}) = \frac{FL^3 - 48h_c(h_c + h_p)(L - 2l_1)l_1 w Y_c d_{31} E_3}{192R} \tag{4.105}$$

In this case, $E_3 = 0$, then we have

$$\delta = \frac{FL^3}{192R} \tag{4.106}$$

$$e_{11} = \frac{L^3}{192R} \tag{4.107}$$

5.0 EXPERIMENTAL STUDIES OF PZT-POLYMER COMPOSITE FIXED-FIXED BEAM

5.1 EXPERIMENTAL DESIGN AND PROCEDURE FOR DOUBLY CLAMPED BEAM ACCELEROMETER

In chapter 4, the static constitutive equations were derived for the PZT-polymer composite fixed-fixed beam. In this section, a doubly clamped beam based accelerometer is designed and tested based on the constitutive equations and the experimental results are compared to the simulation results. In order to make an doubly clamped beam based accelerometer, a partially polarized PZT-polymer laminated composite with length 30mm and width 4mm is fabricated. The structure of the doubly clamped beam with accelerometer mass at the midpoint is shown in Figure 5-1. All the properties of the composite is same as in Table 3.1.

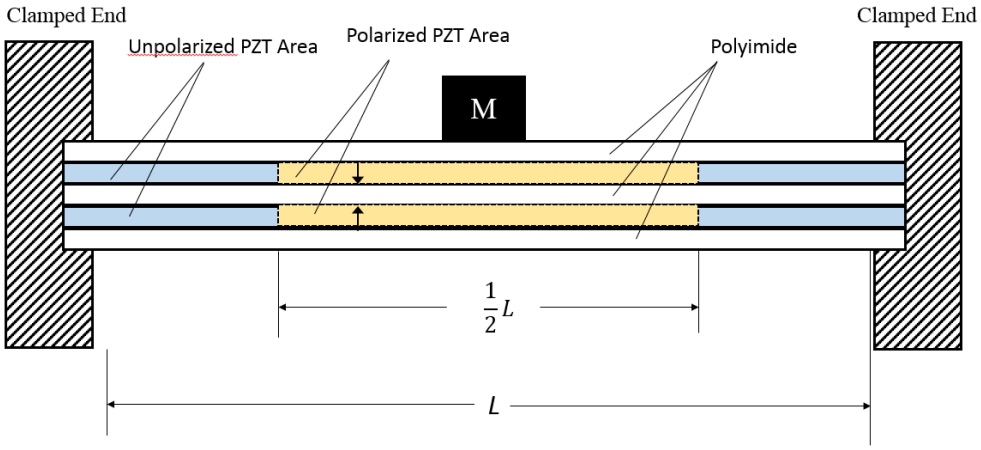

Figure 5-1 The structure of the PZT-polyimide fixed-fixed beam

In order to test the accelerometer, a function generator is used to generate sinusoidal signal to drive a vibration shaker. The base of the whole doubly clamped beam structure is mounted at the top of the shaker so that the beam will vibrate with the shaker. A fotonic sensor is used to measure the displacement of the vibrating base. The output voltage of the composite beam sensor is amplified by a charge amplifier. Both the output signal of the fotonic sensor and the output voltage of the charge amplifier is transferred to the oscilloscope for observation. The illustrative block diagram of the experiment setup is shown in Figure 5-2(a) and the actual experimental setup is shown in Figure 5-2(b).

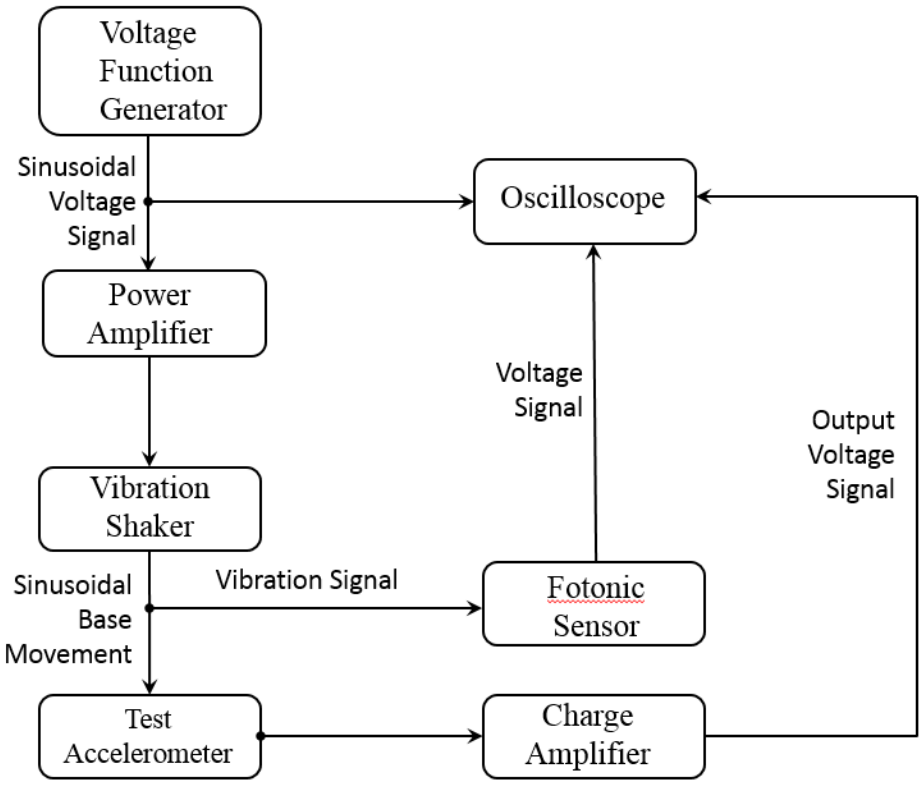

(a)

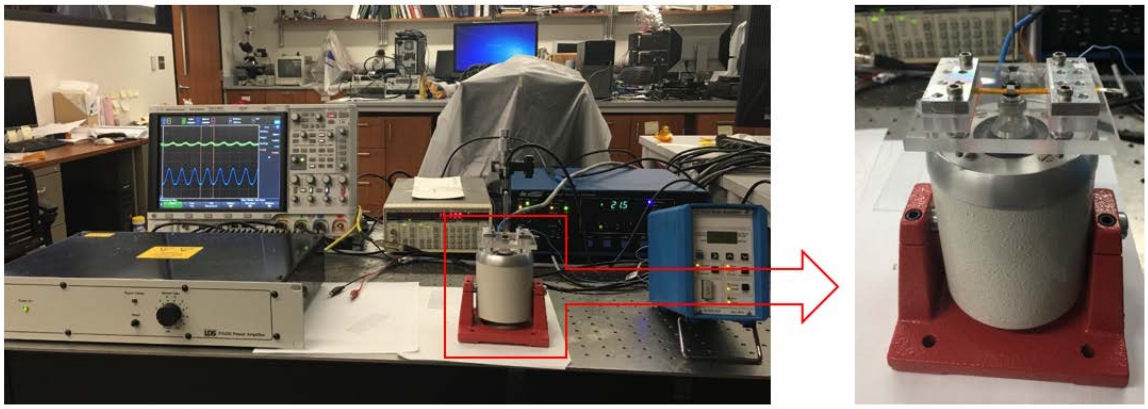

(b)

Figure 5-2 (a) illustrative block diagram of the experiment setup; (b) actual experiment setup for the accelerometer test

The first step of the experiment is to find the first natural frequency of the accelerometer. For the theoretical analysis, the theoretical first natural frequency of the doubly clamped beam without accelerometer mass can be solved from the transverse deflection function of a beam under free vibration as follows:

$$W(x,t) = (A\cos\omega t + B\sin\omega t)(c_1\cos\Omega x + c_2\sin\Omega x + c_3\cosh\Omega x + c_4\sinh\Omega x) \qquad (5.1)$$

The boundary conditions for doubly clamped beam are

$$W(0) = 0, \frac{dW(0)}{dx} = 0, W(L) = 0, \frac{dW(L)}{dx} = 0 \qquad (5.2)$$

Which lead to characteristic equation

$$\cos\Omega L\cosh\Omega L = 1 \qquad (5.3)$$

The infinite values of ΩL which satisfy the equation (5.3) can be relates to the different natural frequencies of the structure as

$$f_n = \frac{(\Omega_n L)^2}{2\pi}\sqrt{\frac{R}{\rho L^4}} \tag{5.4}$$

Therefore, the first three natural frequencies of the doubly clamped beam corresponding to the first three values of ΩL satisfy Equation (5.3) in this experiment can be solved as

$$f_1 = \frac{(4.73)^2}{2\pi}\sqrt{\frac{R}{\rho L^4}} = 774.1134Hz \tag{5.5}$$

$$f_2 = \frac{(7.8532)^2}{2\pi}\sqrt{\frac{R}{\rho L^4}} = 2133.9Hz \tag{5.6}$$

$$f_3 = \frac{(10.9956)^2}{2\pi}\sqrt{\frac{R}{\rho L^4}} = 4183.3Hz \tag{5.7}$$

To calculate the first natural frequency of the accelerometer, the same single degree of freedom mechanical system model as described in Section 3.2 which consists of a seismic mass *M*, a spring with constant *K* and a damper with damping coefficient *C* is used in this analysis. The equivalent spring constant can be obtained from the static constitutive equations of the beam as

$$K = \frac{\partial F}{\partial \delta} = \frac{1}{e_{11}} = \frac{192R}{L^3} \tag{5.8}$$

Then the seismic mass of the model can be calculated as

$$M = m_{eff1} + m_{acc} = \frac{K}{(2\pi f_1)^2} + m_{acc} \tag{5.9}$$

Where $m_{eff1} = \frac{K}{(2\pi f_1)^2}$.The proof mass added at the midpoint is $m_{acc} = 0.26g$. Therefore, the first natural frequency of the system is

$$f_{n1} = \frac{1}{2\pi}\sqrt{\frac{K}{M}} = 354.43Hz \tag{5.10}$$

Similarly, the second and third natural frequency of the system are

$$f_{n2} = \frac{1}{2\pi}\sqrt{\frac{K}{m_{eff\,2} + m_{acc}}} = 391.90Hz \tag{5.11}$$

$$f_{n3} = \frac{1}{2\pi}\sqrt{\frac{K}{m_{eff\,3} + m_{acc}}} = 396.88Hz \tag{5.12}$$

Since the theoretical first natural frequency occurs at 354.43 Hz, we can increase the frequency of driving voltage by 5 Hz at a time starting from 10 Hz to 450 Hz. The amplitude of the base vibration is controlled as a constant by adjusting the gain knob of the power amplifier. Then the amplitude of the output of the charge amplifier is recorded for the calculation of the output voltage of the accelerometer.

5.2 EXPERIMENTAL RESULTS AND COMPARISON WITH THEORETICAL SIMULATION

The relationship of the output voltage of the PZT-polymer composite and the frequencies of the driving voltage is firstly investigated to calculate the damping ratio of the SDOF system by using the half-power method mentioned previously in Section 3.4. The plot of the output voltage data versus frequency is shown in Figure 5-3.

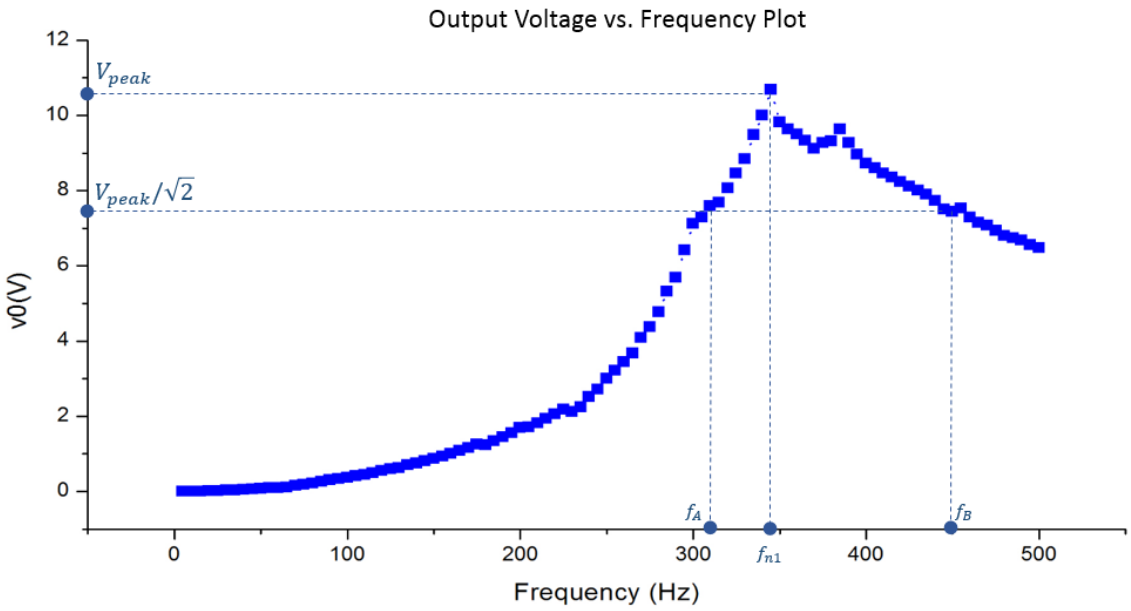

Figure 5-3 Plot of sensor output voltage vs. frequency

It can be found that the first natural frequency occurs at 345 Hz which matches the theoretical value (354.43 Hz) well. The damping ratio can be determined by half power method as follows:

$$\xi = \frac{f_B - f_A}{2 f_{n1}} = \frac{450 - 315}{2 \times 345} = 0.196 \tag{5.13}$$

Then substituting the damping ratio $\xi = 0.196$, the first natural frequency $f_{n1} = 345Hz$ into equation (3.22), the relationship between amplitude of the output voltage of sensor and input amplitude of base movement can be obtained. We can compare the experimental result with the theoretical model in the same plot as shown in Figure 5-4. From the plot we can see that there is a second smaller peak occurs around 385Hz which is close to the second theoretical natural frequency. Figure 5-5 shows the comparison of the theoretical and experimental sensitivity curve

versus frequencies. The sensitivity obtained from experimental data matches theoretical model quite well. The relatively flat sensitivity area occurs at low frequency range from 5-200 Hz which can be used to design accelerometer.

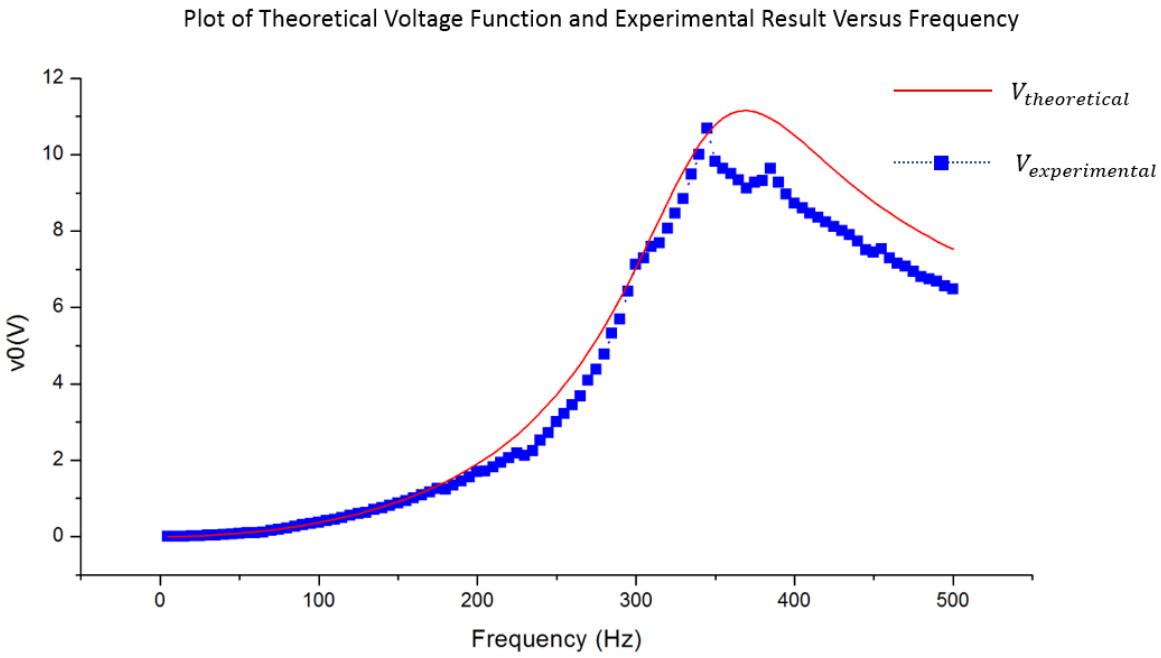

Figure 5-4 Comparison of theoretical model and experimental result

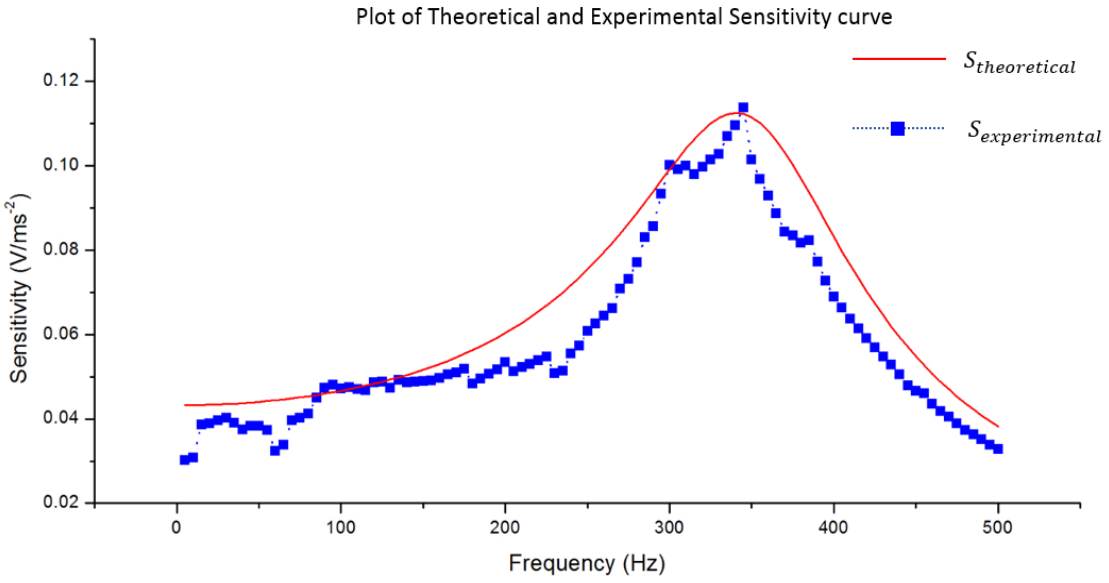

Figure 5-5 Comparison of theoretical and experimental sensitivity curve

6.0 CONCLUSION AND DISCUSSION FOR FUTURE WORK

6.1 CONCLUSION FOR PREVIOUS WORK

In this thesis, two major parts of work have been done: the first part of the work is the theoretical analysis part for establishing constitutive equations for cantilever beam and doubly clamped beam which are composed of PZT-polymer 5-layer composite; the second part of the work is experimental design and test for verifying the theoretical model and using the constitutive equations to do some accelerometer design works.

In Chapter 2, the static and dynamic analysis are introduced for PZT-polymer composite based cantilever beam. The matrix form constitutive equations are established to relate the responses of the cantilever to the different external excitations. Two experiments are conducted in Chapter 3 to verify the theoretical analysis. The first experiment tests the actuating mode at different frequency. The tip deflections are recorded under different frequencies. The experiment results show a good agreement with our dynamic constitutive equation when driving frequency is not too close to the natural frequency. The second experiment tests the sensor mode of the cantilever beam by adding a proof mass at the tip of the cantilever to construct an accelerometer. The static constitutive equations are introduced to establish the theoretical model of the accelerometer. During the experiment, the vibration movement of the base of the cantilever beam is transferred to voltage output of the sensor. The amplitude of the voltage and the displacement

of the base are recorded. The experimental data agrees with the theoretical model for the accelerometer test.

In Chapter 4, the static constitutive equations are established for the doubly clamped beam which is composed of PZT-polyimide composite. The two layers of PZT element in the composite is partially polarized in doubly clamped beam for effectively generating charge when bending. The optimal length of the polarization area is investigated in theoretical analysis. A sensor experiment similar with the cantilever beam accelerometer is conducted using the composite with optimal length of the polarized PZT area in Chapter 5. The theoretical model of the response of the accelerometer is analyzed by using the static constitutive equations derived in Chapter 4. The experiment results are compared to the theoretical analysis. The trend of the distribution of the measured data is close to the analytical model. The theoretical sensitivity matches the experimental data well.

6.2 DISCUSSION FOR FUTURE WORK

The main objective of this thesis is to establish the theoretical constitutive equations for cantilever beam and doubly clamped beam which are composed of PZT-polymer laminated composite. Since the theoretical analysis is based on the Euler-Bernoulli beam theories, which is restricted by the small transverse deflection, the theoretical model works inaccurately when the vibration frequency is close to the natural frequency of the beam. In the future work, new models such as large strain theory and Timoshenko beam theory can be introduced into the establishment of theoretical model, especially when the vibration frequency is close to natural frequency. Due to the nonlinear terms

of these models, some numerical methods such as finite element method can be used to do the theoretical analysis in the future work.

Second, the tape-casting process of fabrication of PZT thick film can provide different PZT film with thickness from tens to hundreds micrometers. These films can be used to make different types of PZT-polymer laminated composite with high flexibility without losing piezoelectricity. In this research, the main limitation is the number and types of PZT thick film are restricted. The only one type of rectangular PZT film with thickness of 80um is available for the experiments. More samples of PZT film should be produced and provided to do more test such as the effects of different thickness ratio of PZT and polyimide to the sensitivity of the device.

Third, some new experiment designs can be considered in the future research. The partially electrode covered and fully polarized PZT element can be used in doubly clamped beam and can be compared to the partially polarized PZT film we used in the accelerometer experiment. The larger proof mass can be used to make the first three natural frequencies closer to eliminate the second peak appeared in Figure 3-11 and Figure 5-4. The different value of damping ratio can be studied to explore different effects to the sensitivity curve of the accelerometer.

APPENDIX A

MATHEMATICA CODE FOR THEORETICAL MODELING

1. Cantilever

```
Solve[c7*L^2 + c8*L + c9 == 0 && 2*c7*L + c8 == 0 &&
  c1*L1^2 == c4*L1^2 + c5*L1 + c6 && 2*c1*L1 == 2*c4*L1 + c5 &&
  2*c1*R == 2*c4*R - w*hc^2*d31*Yc*E3 - w*hc*hp*d31*Yc*E3 &&
  c4*(L - L1)^2 + c5*(L - L1) + c6 ==
   c7*(L - L1)^2 + c8*(L - L1) + c9 &&
  2*c4*(L - L1) + c5 == 2*c7*(L - L1) + c8 &&
  2*c4*R - w*hc^2*d31*Yc*E3 - w*hc*hp*d31*Yc*E3 == 2*c7*R, {c1, c4,
  c5, c6, c7, c8, c9}]


{{c1 -> -1/(
     2 L R) (d31 E3 hc^2 L w Yc + d31 E3 hc hp L w Yc -
       2 d31 E3 hc^2 L1 w Yc - 2 d31 E3 hc hp L1 w Yc),
  c4 -> -((-d31 E3 hc^2 L1 w Yc - d31 E3 hc hp L1 w Yc)/(L R)),
  c5 -> -((d31 E3 hc^2 L1 w Yc + d31 E3 hc hp L1 w Yc)/R),
  c6 -> (L1^2 (d31 E3 hc^2 w Yc + d31 E3 hc hp w Yc))/(2 R),
  c7 -> -1/(
     2 L R) (d31 E3 hc^2 L w Yc + d31 E3 hc hp L w Yc -
       2 d31 E3 hc^2 L1 w Yc - 2 d31 E3 hc hp L1 w Yc),
  c8 -> -1/R (-d31 E3 hc^2 L w Yc - d31 E3 hc hp L w Yc +
       2 d31 E3 hc^2 L1 w Yc + 2 d31 E3 hc hp L1 w Yc),
```

```
 c9 -> -1/(
    2 R) (d31 E3 hc^2 L^2 w Yc + d31 E3 hc hp L^2 w Yc -
     2 d31 E3 hc^2 L L1 w Yc - 2 d31 E3 hc hp L L1 w Yc)}}

Simplify[-((-d31 E3 hc^2 L1 w Yc - d31 E3 hc hp L1 w Yc)/(
   L R))*(L/2)^2 + (-((d31 E3 hc^2 L1 w Yc + d31 E3 hc hp L1 w Yc)/
    R))*L/2 + (L1^2 (d31 E3 hc^2 w Yc + d31 E3 hc hp w Yc))/(2 R)]

-((d31 E3 hc (hc + hp) (L - 2 L1) L1 w Yc)/(4 R))

Integrate[c1*x^2, {x, 0, L1}]

(c1 L1^3)/3

Integrate[c4*x^2 + c5*x + c6, {x, L1, L - L1}]

c6 L + (c5 L^2)/2 + (c4 L^3)/3 - 2 c6 L1 - c5 L L1 - c4 L^2 L1 +
 c4 L L1^2 - (2 c4 L1^3)/3

Integrate[c7*x^2 + c8*x + c9, {x, L - L1, L}]

c9 L1 + c8 L L1 + c7 L^2 L1 - (c8 L1^2)/2 - c7 L L1^2 + (c7 L1^3)/3

In[67]

-1/(6 R) d31 E3 hc (hc + hp) L1 (L^2 - 3 L L1 + 2 L1 (-3 + 4 L1)) w Yc

Simplify[-(1/(
   2 L R)) (d31 E3 hc^2 L w Yc + d31 E3 hc hp L w Yc -
    2 d31 E3 hc^2 L1 w Yc - 2 d31 E3 hc hp L1 w Yc)*L1^3/3 + (
```

```
L1^2 (d31 E3 hc^2 w Yc + d31 E3 hc hp w Yc))/(2 R)*
L + (-((d31 E3 hc^2 L1 w Yc + d31 E3 hc hp L1 w Yc)/R))/2*
L^2 + (-((-d31 E3 hc^2 L1 w Yc - d31 E3 hc hp L1 w Yc)/(L R)))*
L^3/3 - 2*(L1^2 (d31 E3 hc^2 w Yc + d31 E3 hc hp w Yc))/(2 R)*
L1 - (-((d31 E3 hc^2 L1 w Yc + d31 E3 hc hp L1 w Yc)/R))*L*
L1 - (-((-d31 E3 hc^2 L1 w Yc - d31 E3 hc hp L1 w Yc)/(L R)))*L^2*
L1 + (-((-d31 E3 hc^2 L1 w Yc - d31 E3 hc hp L1 w Yc)/(L R)))*L*
L1^2 - 2*(-((-d31 E3 hc^2 L1 w Yc - d31 E3 hc hp L1 w Yc)/(L R)))*
L1^3/3 + (-(1/(
   2 R)) (d31 E3 hc^2 L^2 w Yc + d31 E3 hc hp L^2 w Yc -
    2 d31 E3 hc^2 L L1 w Yc - 2 d31 E3 hc hp L L1 w Yc))*
L1 + (-(1/
   R) (-d31 E3 hc^2 L w Yc - d31 E3 hc hp L w Yc +
    2 d31 E3 hc^2 L1 w Yc + 2 d31 E3 hc hp L1 w Yc))*L*
L1 + (-(1/(
   2 L R)) (d31 E3 hc^2 L w Yc + d31 E3 hc hp L w Yc -
    2 d31 E3 hc^2 L1 w Yc - 2 d31 E3 hc hp L1 w Yc))*L^2*
L1 - (-(1/
   R) (-d31 E3 hc^2 L w Yc - d31 E3 hc hp L w Yc +
    2 d31 E3 hc^2 L1 w Yc + 2 d31 E3 hc hp L1 w Yc))*
L1^2/2 - (-(1/(
   2 L R)) (d31 E3 hc^2 L w Yc + d31 E3 hc hp L w Yc -
    2 d31 E3 hc^2 L1 w Yc - 2 d31 E3 hc hp L1 w Yc))*L*
L1^2 + (-(1/(
   2 L R)) (d31 E3 hc^2 L w Yc + d31 E3 hc hp L w Yc -
    2 d31 E3 hc^2 L1 w Yc - 2 d31 E3 hc hp L1 w Yc))*L1^3/3]

-((d31 E3 hc (hc + hp) L1 (L^2 - 3 L L1 + 2 L1^2) w Yc)/(6 R))
```

Out[60]

```
{{c1 -> -1/(
    2 L R) (d31 E3 hc^2 L w Yc + d31 E3 hc hp L w Yc -
     2 d31 E3 hc^2 L1 w Yc - 2 d31 E3 hc hp L1 w Yc),
  c4 -> -((-d31 E3 hc^2 L1 w Yc - d31 E3 hc hp L1 w Yc)/(L R)),
  c5 -> -((d31 E3 hc^2 L1 w Yc + d31 E3 hc hp L1 w Yc)/R),
  c6 -> (L1^2 (d31 E3 hc^2 w Yc + d31 E3 hc hp w Yc))/(2 R),
  c7 -> -1/(
    2 L R) (d31 E3 hc^2 L w Yc + d31 E3 hc hp L w Yc -
     2 d31 E3 hc^2 L1 w Yc - 2 d31 E3 hc hp L1 w Yc),
  c8 -> -1/R (-d31 E3 hc^2 L w Yc - d31 E3 hc hp L w Yc +
     2 d31 E3 hc^2 L1 w Yc + 2 d31 E3 hc hp L1 w Yc),
  c9 -> -1/(
    2 R) (d31 E3 hc^2 L^2 w Yc + d31 E3 hc hp L^2 w Yc -
     2 d31 E3 hc^2 L L1 w Yc - 2 d31 E3 hc hp L L1 w Yc)}}

Simplify[-1/(
    2 L R) (d31 E3 hc^2 L w Yc + d31 E3 hc hp L w Yc -
     2 d31 E3 hc^2 L1 w Yc - 2 d31 E3 hc hp L1 w Yc)*L1^3/3 + (
  L1^2 (d31 E3 hc^2 w Yc + d31 E3 hc hp w Yc))/(2 R)*
  L + (-((d31 E3 hc^2 L1 w Yc + d31 E3 hc hp L1 w Yc)/R))/2*
  L^2 + (-((-d31 E3 hc^2 L1 w Yc - d31 E3 hc hp L1 w Yc)/(L R)))/3*
  L^3 - 2*(L1^2 (d31 E3 hc^2 w Yc + d31 E3 hc hp w Yc))/(2 R)*
  L1 - (-((d31 E3 hc^2 L1 w Yc + d31 E3 hc hp L1 w Yc)/R))*L*
  L1 - (-((-d31 E3 hc^2 L1 w Yc - d31 E3 hc hp L1 w Yc)/(L R)))*L^2*
  L1 + (-((-d31 E3 hc^2 L1 w Yc - d31 E3 hc hp L1 w Yc)/(L R)))*L1^2*
  L - 2/3*(-((-d31 E3 hc^2 L1 w Yc - d31 E3 hc hp L1 w Yc)/(L R)))*
  L1^3 + (-1/(
    2 R) (d31 E3 hc^2 L^2 w Yc + d31 E3 hc hp L^2 w Yc -
     2 d31 E3 hc^2 L L1 w Yc - 2 d31 E3 hc hp L L1 w Yc))*
```

L1 + (-1/
R (-d31 E3 hc^2 L w Yc - d31 E3 hc hp L w Yc +
2 d31 E3 hc^2 L1 w Yc + 2 d31 E3 hc hp L1 w Yc))*L*
L1 + (-1/(
2 L R) (d31 E3 hc^2 L w Yc + d31 E3 hc hp L w Yc -
2 d31 E3 hc^2 L1 w Yc - 2 d31 E3 hc hp L1 w Yc))*L^2*L1 -
1/2*(-1/
R (-d31 E3 hc^2 L w Yc - d31 E3 hc hp L w Yc +
2 d31 E3 hc^2 L1 w Yc + 2 d31 E3 hc hp L1 w Yc))*
L1^2 - (-1/(
2 L R) (d31 E3 hc^2 L w Yc + d31 E3 hc hp L w Yc -
2 d31 E3 hc^2 L1 w Yc - 2 d31 E3 hc hp L1 w Yc))*L*L1^2 +
1/3*(-1/(2 L R) (d31 E3 hc^2 L w Yc + d31 E3 hc hp L w Yc -
2 d31 E3 hc^2 L1 w Yc - 2 d31 E3 hc hp L1 w Yc))*L1^3]

-((d31 E3 hc (hc + hp) L1 (L^2 - 3 L L1 + 2 L1^2) w Yc)/(6 R))

Integrate[Yp/2*(2*c1)^2*z^2, {z, hp/2 + hc, 3*hp/2 + hc}]

2 c1^2 hc^2 hp Yp + 4 c1^2 hc hp^2 Yp + 13/6 c1^2 hp^3 Yp

Integrate[Yc/2*(2*c1)^2*z^2, {z, hp/2, hp/2 + hc}]

2/3 c1^2 hc^3 Yc + c1^2 hc^2 hp Yc + 1/2 c1^2 hc hp^2 Yc

Integrate[Yp/2*(2*c1)^2*z^2, {z, -hp/2, hp/2}]

1/6 c1^2 hp^3 Yp

Integrate[Yc/2*(2*c1)^2*z^2, {z, -hp/2 - hc, -hp/2}]

```
2/3 c1^2 hc^3 Yc + c1^2 hc^2 hp Yc + 1/2 c1^2 hc hp^2 Yc
```

```
Integrate[Yp/2*(2*c1)^2*z^2, {z, -3 hp/2 - hc, -hp/2 - hc}]
```

```
2 c1^2 hc^2 hp Yp + 4 c1^2 hc hp^2 Yp + 13/6 c1^2 hp^3 Yp
```

```
Simplify[Out[72] + Out[73] + Out[74] + Out[75] + Out[76]]
```

```
1/6 c1^2 (8 hc^3 Yc + 27 hp^3 Yp + 12 hc^2 hp (Yc + 2 Yp) +
  6 hc hp^2 (Yc + 8 Yp))
```

```
Integrate[
 1/6 c1^2 (8 hc^3 Yc + 27 hp^3 Yp + 12 hc^2 hp (Yc + 2 Yp) +
   6 hc hp^2 (Yc + 8 Yp)), {x, 0, L1}, {y, -w/2, w/2}]
```

```
1/6 c1^2 L1 w (8 hc^3 Yc + 27 hp^3 Yp + 12 hc^2 hp (Yc + 2 Yp) +
  6 hc hp^2 (Yc + 8 Yp))
```

```
Simplify[(-(1/(
    2 L R)) (d31 E3 hc^2 L w Yc + d31 E3 hc hp L w Yc -
     2 d31 E3 hc^2 L1 w Yc - 2 d31 E3 hc hp L1 w Yc))^2]
```

```
(d31^2 E3^2 hc^2 (hc + hp)^2 (L - 2 L1)^2 w^2 Yc^2)/(4 L^2 R^2)
```

```
Integrate[2*Yp*c7^2*z^2, {z, hp/2 + hc, 3*hp/2 + hc}]
```

```
2 c7^2 hc^2 hp Yp + 4 c7^2 hc hp^2 Yp + 13/6 c7^2 hp^3 Yp
```

```
Integrate[2*Yc*c7^2*z^2, {z, hp/2, hp/2 + hc}]
```

2/3 c7^2 hc^3 Yc + c7^2 hc^2 hp Yc + 1/2 c7^2 hc hp^2 Yc

Integrate[2*Yp*c7^2*z^2, {z, -hp/2, hp/2}]

1/6 c7^2 hp^3 Yp

Integrate[2*Yc*c7^2*z^2, {z, -hp/2 - hc, -hp/2}]

2/3 c7^2 hc^3 Yc + c7^2 hc^2 hp Yc + 1/2 c7^2 hc hp^2 Yc

Integrate[2*Yp*c7^2*z^2, {z, -3*hp/2 - hc, -hp/2 - hc}]

2 c7^2 hc^2 hp Yp + 4 c7^2 hc hp^2 Yp + 13/6 c7^2 hp^3 Yp

Simplify[Out[80] + Out[81] + Out[82] + Out[83] + Out[84]]

1/6 c7^2 (8 hc^3 Yc + 27 hp^3 Yp + 12 hc^2 hp (Yc + 2 Yp) +
  6 hc hp^2 (Yc + 8 Yp))

Simplify[2*R*
 L1*(-(1/(2 L R)) (d31 E3 hc^2 L w Yc + d31 E3 hc hp L w Yc -
     2 d31 E3 hc^2 L1 w Yc - 2 d31 E3 hc hp L1 w Yc))^2]

(d31^2 E3^2 hc^2 (hc + hp)^2 (L - 2 L1)^2 L1 w^2 Yc^2)/(2 L^2 R)

Integrate[2*Yp*c4^2*z^2, {z, hp/2 + hc, 3*hp/2 + hc}]

2 c4^2 hc^2 hp Yp + 4 c4^2 hc hp^2 Yp + 13/6 c4^2 hp^3 Yp

```
Integrate[
 1/2*(4*Yc*c4^2*z^2 + epson*E3^2 - d31^2*Yc*E3^2), {z, hp/2,
  hp/2 + hc}]

1/2 E3^2 epson hc - 1/2 d31^2 E3^2 hc Yc + 2/3 c4^2 hc^3 Yc +
 c4^2 hc^2 hp Yc + 1/2 c4^2 hc hp^2 Yc

Integrate[2*Yp*c4^2*z^2, {z, -hp/2, hp/2}]

1/6 c4^2 hp^3 Yp

Integrate[
 1/2*(4*Yc*c4^2*z^2 + epson*E3^2 - Yc*d31^2*E3^2), {z, -hp/2 -
   hc, -hp/2}]

1/2 E3^2 epson hc - 1/2 d31^2 E3^2 hc Yc + 2/3 c4^2 hc^3 Yc +
 c4^2 hc^2 hp Yc + 1/2 c4^2 hc hp^2 Yc

Integrate[2*Yp*c4^2*z^2, {z, -3*hp/2 - hc, -hp/2 - hc}]

2 c4^2 hc^2 hp Yp + 4 c4^2 hc hp^2 Yp + 13/6 c4^2 hp^3 Yp

Simplify[Out[87] + Out[88] + Out[89] + Out[90] + Out[91]]

E3^2 hc (epson - d31^2 Yc) +
 1/6 c4^2 (8 hc^3 Yc + 27 hp^3 Yp + 12 hc^2 hp (Yc + 2 Yp) +
    6 hc hp^2 (Yc + 8 Yp))

Integrate[(epson - d31^2*Yc)*hc*E3^2 + 2*R/w*c4^2, {x, L1,
  L - L1}, {y, -w/2, w/2}]
```

(L - 2 L1) w ((2 c4^2 R)/w + E3^2 hc (epson - d31^2 Yc))

Simplify[(L - 2 L1) w ((
2 (-((-d31 E3 hc^2 L1 w Yc - d31 E3 hc hp L1 w Yc)/(L R)))^2 R)/
w + E3^2 hc (epson - d31^2 Yc))]

1/(L^2 R) E3^2 hc (L - 2 L1) w (epson L^2 R +
d31^2 Yc (-L^2 R + 2 hc (hc + hp)^2 L1^2 w Yc))

2. Fixed-Fixed Beam

Wa[x_] = w*P/(24*R)*x^4 + c1*x^3

c1 x^3 + (P w x^4)/(24 R)

Wb[x_] = w*P/(24*R)*x^4 + c5*x^3 + c6*x^2 + c7*x + c8

c8 + c7 x + c6 x^2 + c5 x^3 + (P w x^4)/(24 R)

Wc[x_] = w*P/(24*R)*x^4 + c9*x^3 + c10*x^2 + c11*x + c12

c12 + c11 x + c10 x^2 + c9 x^3 + (P w x^4)/(24 R)

ua1[x_, z_] = 1/2*Yp*(D[Wa[x], {x, 2}])^2*z^2

1/2 (6 c1 x + (P w x^2)/(2 R))^2 Yp z^2

```
ua2[x_, z_] = 1/2*Yc*(D[Wa[x], {x, 2}])^2*z^2
```

```
1/2 (6 c1 x + (P w x^2)/(2 R))^2 Yc z^2
```

```
ua3[x_, z_] = 1/2*Yp*(D[Wa[x], {x, 2}])^2*z^2
```

```
1/2 (6 c1 x + (P w x^2)/(2 R))^2 Yp z^2
```

```
ua4[x_, z_] = 1/2*Yc*(D[Wa[x], {x, 2}])^2*z^2
```

```
1/2 (6 c1 x + (P w x^2)/(2 R))^2 Yc z^2
```

```
ua5[x_, z_] = 1/2*Yp*(D[Wa[x], {x, 2}])^2*z^2
```

```
1/2 (6 c1 x + (P w x^2)/(2 R))^2 Yp z^2
```

```
Integrate[
 ua1[x, z], {x, 0, L1}, {y, -w/2, w/2}, {z, hp/2 + hc, 3*hp/2 + hc}]
```

```
(hp (12 hc^2 + 24 hc hp + 13 hp^2) L1^3 w (240 c1^2 R^2 +
   30 c1 L1 P R w + L1^2 P^2 w^2) Yp)/(480 R^2)
```

```
Integrate[ua2[x, z], {x, 0, L1}, {y, -w/2, w/2}, {z, hp/2, hp/2 + hc}]
```

```
(hc (4 hc^2 + 6 hc hp + 3 hp^2) L1^3 w (240 c1^2 R^2 +
   30 c1 L1 P R w + L1^2 P^2 w^2) Yc)/(480 R^2)
```

```
Integrate[ua3[x, z], {x, 0, L1}, {y, -w/2, w/2}, {z, -hp/2, hp/2}]
```

```
(hp^3 L1^3 w (240 c1^2 R^2 + 30 c1 L1 P R w +
```

```
  L1^2 P^2 w^2) Yp)/(480 R^2)

Integrate[
 ua4[x, z], {x, 0, L1}, {y, -w/2, w/2}, {z, -hp/2 - hc, -hp/2}]

(hc (4 hc^2 + 6 hc hp + 3 hp^2) L1^3 w (240 c1^2 R^2 +
  30 c1 L1 P R w + L1^2 P^2 w^2) Yc)/(480 R^2)

Integrate[
 ua5[x, z], {x, 0, L1}, {y, -w/2, w/2}, {z, -3*hp/2 - hc, -hp/2 - hc}]

(hp (12 hc^2 + 24 hc hp + 13 hp^2) L1^3 w (240 c1^2 R^2 +
  30 c1 L1 P R w + L1^2 P^2 w^2) Yp)/(480 R^2)

Simplify[Out[21] + Out[23] + Out[24] + Out[25] + Out[26]]

(L1^3 w (240 c1^2 R^2 + 30 c1 L1 P R w + L1^2 P^2 w^2) (8 hc^3 Yc +
  27 hp^3 Yp + 12 hc^2 hp (Yc + 2 Yp) +
  6 hc hp^2 (Yc + 8 Yp)))/(480 R^2)



Simplify[1/(480 R^2)
  L1^3 w (240 (-(1/(
      72 (L - L1) L1 R)) (-L^3 P w + 6 L^2 L1 P w - 6 L L1^2 P w +
       12 d31 E3 hc^2 L w Yc + 12 d31 E3 hc hp L w Yc -
       24 d31 E3 hc^2 L1 w Yc - 24 d31 E3 hc hp L1 w Yc))^2 R^2 +
   30 (-(1/(
      72 (L - L1) L1 R)) (-L^3 P w + 6 L^2 L1 P w - 6 L L1^2 P w +
       12 d31 E3 hc^2 L w Yc + 12 d31 E3 hc hp L w Yc -
```

```
      24 d31 E3 hc^2 L1 w Yc - 24 d31 E3 hc hp L1 w Yc)) L1 P R w +
   L1^2 P^2 w^2) (8 hc^3 Yc + 27 hp^3 Yp + 12 hc^2 hp (Yc + 2 Yp) +
  6 hc hp^2 (Yc + 8 Yp))]

1/(51840 R^2)
 L1^3 w^3 (108 L1^2 P^2 + (
  45 P (L^3 P - 6 L^2 L1 P + 24 d31 E3 hc (hc + hp) L1 Yc +
    6 L (L1^2 P - 2 d31 E3 hc (hc + hp) Yc)))/(L - L1) + (
  5 (L^3 P - 6 L^2 L1 P + 24 d31 E3 hc (hc + hp) L1 Yc +
    6 L (L1^2 P - 2 d31 E3 hc (hc + hp) Yc))^2)/((L -
    L1)^2 L1^2)) (8 hc^3 Yc + 27 hp^3 Yp +
  12 hc^2 hp (Yc + 2 Yp) + 6 hc hp^2 (Yc + 8 Yp))

Collect[Out[28], P]

(L1^3 ((240 L^4)/(L - L1)^2 + (45 L^3)/(L - L1) + (
  5 L^6)/((L - L1)^2 L1^2) - (60 L^5)/((L - L1)^2 L1) - (
  360 L^3 L1)/(L - L1)^2 - (270 L^2 L1)/(L - L1) + 108 L1^2 + (
  180 L^2 L1^2)/(L - L1)^2 + (270 L L1^2)/(
  L - L1)) P^2 w^3 (8 hc^3 Yc + 27 hp^3 Yp +
  12 hc^2 hp (Yc + 2 Yp) + 6 hc hp^2 (Yc + 8 Yp)))/(51840 R^2) +
 1/(51840 R^2)
  L1^3 P w^3 (-((2160 d31 E3 hc (hc + hp) L^2 Yc)/(L - L1)^2) - (
   540 d31 E3 hc (hc + hp) L Yc)/(L - L1) - (
   120 d31 E3 hc (hc + hp) L^4 Yc)/((L - L1)^2 L1^2) + (
   960 d31 E3 hc (hc + hp) L^3 Yc)/((L - L1)^2 L1) + (
   1440 d31 E3 hc (hc + hp) L L1 Yc)/(L - L1)^2 + (
   1080 d31 E3 hc (hc + hp) L1 Yc)/(L - L1)) (8 hc^3 Yc +
   27 hp^3 Yp + 12 hc^2 hp (Yc + 2 Yp) + 6 hc hp^2 (Yc + 8 Yp)) + (
 L1^3 w^3 ((2880 d31^2 E3^2 hc^2 (hc + hp)^2 Yc^2)/(L - L1)^2 + (
```

720 d31^2 E3^2 hc^2 (hc + hp)^2 L^2 Yc^2)/((L - L1)^2 L1^2) - (
2880 d31^2 E3^2 hc^2 (hc + hp)^2 L Yc^2)/((L -
L1)^2 L1)) (8 hc^3 Yc + 27 hp^3 Yp + 12 hc^2 hp (Yc + 2 Yp) +
6 hc hp^2 (Yc + 8 Yp)))/(51840 R^2)

FullSimplify[%29]

1/(51840 (L - L1)^2 R^2)
L1 w^3 ((5 L^6 - 60 L^5 L1 + 285 L^4 L1^2 - 675 L^3 L1^3 +
828 L^2 L1^4 - 486 L L1^5 + 108 L1^6) P^2 -
60 d31 E3 hc (hc + hp) (L - 3 L1) (L - 2 L1) (2 L^2 - 6 L L1 +
3 L1^2) P Yc +
720 d31^2 E3^2 hc^2 (hc + hp)^2 (L - 2 L1)^2 Yc^2) (8 hc^3 Yc +
27 hp^3 Yp + 12 hc^2 hp (Yc + 2 Yp) + 6 hc hp^2 (Yc + 8 Yp))

ub1[x_, z_] = 1/2*Yp*(D[Wb[x], {x, 2}])^2*z^2

1/2 (2 c6 + 6 c5 x + (P w x^2)/(2 R))^2 Yp z^2

ub2[x_, z_] =
1/2*(Yc*(D[Wb[x], {x, 2}])^2*z^2 + epson*E3^2 - d31^2*Yc*E3^2)

1/2 (E3^2 epson -
d31^2 E3^2 Yc + (2 c6 + 6 c5 x + (P w x^2)/(2 R))^2 Yc z^2)

ub3[x_, z_] = 1/2*Yp*(D[Wb[x], {x, 2}])^2*z^2

1/2 (2 c6 + 6 c5 x + (P w x^2)/(2 R))^2 Yp z^2

ub4[x_, z_] =

```
 1/2*(Yc*(D[Wb[x], {x, 2}])^2*z^2 + epson*E3^2 - Yc*d31^2*E3^2)

1/2 (E3^2 epson -
   d31^2 E3^2 Yc + (2 c6 + 6 c5 x + (P w x^2)/(2 R))^2 Yc z^2)

ub5[x_, z_] = 1/2*Yp*(D[Wb[x], {x, 2}])^2*z^2

1/2 (2 c6 + 6 c5 x + (P w x^2)/(2 R))^2 Yp z^2

Integrate[
 ub1[x, z], {x, L1, L - L1}, {y, -w/2, w/2}, {z, hp/2 + hc,
  3*hp/2 + hc}]

1/(1440 R^2)
  hp (12 hc^2 + 24 hc hp + 13 hp^2) (L -
    2 L1) w (240 (c6^2 + 3 c5 c6 L +
       3 c5^2 (L^2 - L L1 + L1^2)) R^2 +
    10 (4 c6 (L^2 - L L1 + L1^2) +
       9 c5 L (L^2 - 2 L L1 + 2 L1^2)) P R w +
    3 (L^4 - 3 L^3 L1 + 4 L^2 L1^2 - 2 L L1^3 + L1^4) P^2 w^2) Yp

Integrate[
 ub2[x, z], {x, L1, L - L1}, {y, -w/2, w/2}, {z, hp/2, hp/2 + hc}]

1/1440 hc w (720 E3^2 epson L - 1440 E3^2 epson L1 -
    720 d31^2 E3^2 L Yc + 720 c6^2 hp^2 L Yc +
    2160 c5 c6 hp^2 L^2 Yc + 960 c6^2 hc^2 (L - 2 L1) Yc +
    1440 c6^2 hc hp (L - 2 L1) Yc + 2880 c5 c6 hc^2 L (L - 2 L1) Yc +
    4320 c5 c6 hc hp L (L - 2 L1) Yc + 1440 d31^2 E3^2 L1 Yc -
    1440 c6^2 hp^2 L1 Yc - 4320 c5 c6 hp^2 L L1 Yc +
```

```
   2880 c5^2 hc^2 ((L - L1)^3 - L1^3) Yc +
   4320 c5^2 hc hp ((L - L1)^3 - L1^3) Yc +
   2160 c5^2 hp^2 ((L - L1)^3 - L1^3) Yc + (
   160 c6 hc^2 ((L - L1)^3 - L1^3) P w Yc)/R + (
   240 c6 hc hp ((L - L1)^3 - L1^3) P w Yc)/R + (
   120 c6 hp^2 ((L - L1)^3 - L1^3) P w Yc)/R + (
   360 c5 hc^2 ((L - L1)^4 - L1^4) P w Yc)/R + (
   540 c5 hc hp ((L - L1)^4 - L1^4) P w Yc)/R + (
   270 c5 hp^2 ((L - L1)^4 - L1^4) P w Yc)/R + (
   12 hc^2 ((L - L1)^5 - L1^5) P^2 w^2 Yc)/R^2 + (
   18 hc hp ((L - L1)^5 - L1^5) P^2 w^2 Yc)/R^2 + (
   9 hp^2 ((L - L1)^5 - L1^5) P^2 w^2 Yc)/R^2)

Integrate[ub3[x, z], {x, L1, L - L1}, {y, -w/2, w/2}, {z, -hp/2, hp/2}]

1/(1440 R^2)
  hp^3 (L -
   2 L1) w (240 (c6^2 + 3 c5 c6 L +
      3 c5^2 (L^2 - L L1 + L1^2)) R^2 +
   10 (4 c6 (L^2 - L L1 + L1^2) +
      9 c5 L (L^2 - 2 L L1 + 2 L1^2)) P R w +
   3 (L^4 - 3 L^3 L1 + 4 L^2 L1^2 - 2 L L1^3 + L1^4) P^2 w^2) Yp

Integrate[
 ub4[x, z], {x, L1, L - L1}, {y, -w/2, w/2}, {z, -hp/2 - hc, -hp/2}]

1/1440 hc w (720 E3^2 epson L - 1440 E3^2 epson L1 -
   720 d31^2 E3^2 L Yc + 720 c6^2 hp^2 L Yc +
   2160 c5 c6 hp^2 L^2 Yc + 960 c6^2 hc^2 (L - 2 L1) Yc +
   1440 c6^2 hc hp (L - 2 L1) Yc + 2880 c5 c6 hc^2 L (L - 2 L1) Yc +
```

```
   4320 c5 c6 hc hp L (L - 2 L1) Yc + 1440 d31^2 E3^2 L1 Yc -
   1440 c6^2 hp^2 L1 Yc - 4320 c5 c6 hp^2 L L1 Yc +
   2880 c5^2 hc^2 ((L - L1)^3 - L1^3) Yc +
   4320 c5^2 hc hp ((L - L1)^3 - L1^3) Yc +
   2160 c5^2 hp^2 ((L - L1)^3 - L1^3) Yc + (
   160 c6 hc^2 ((L - L1)^3 - L1^3) P w Yc)/R + (
   240 c6 hc hp ((L - L1)^3 - L1^3) P w Yc)/R + (
   120 c6 hp^2 ((L - L1)^3 - L1^3) P w Yc)/R + (
   360 c5 hc^2 ((L - L1)^4 - L1^4) P w Yc)/R + (
   540 c5 hc hp ((L - L1)^4 - L1^4) P w Yc)/R + (
   270 c5 hp^2 ((L - L1)^4 - L1^4) P w Yc)/R + (
   12 hc^2 ((L - L1)^5 - L1^5) P^2 w^2 Yc)/R^2 + (
   18 hc hp ((L - L1)^5 - L1^5) P^2 w^2 Yc)/R^2 + (
   9 hp^2 ((L - L1)^5 - L1^5) P^2 w^2 Yc)/R^2)

Integrate[
 ub5[x, z], {x, L1, L - L1}, {y, -w/2,
  w/2}, {z, -3*hp/2 - hc, -hp/2 - hc}]

1/(1440 R^2)
  hp (12 hc^2 + 24 hc hp + 13 hp^2) (L -
   2 L1) w (240 (c6^2 + 3 c5 c6 L +
      3 c5^2 (L^2 - L L1 + L1^2)) R^2 +
   10 (4 c6 (L^2 - L L1 + L1^2) +
      9 c5 L (L^2 - 2 L L1 + 2 L1^2)) P R w +
   3 (L^4 - 3 L^3 L1 + 4 L^2 L1^2 - 2 L L1^3 + L1^4) P^2 w^2) Yp

Simplify[Out[36] + Out[37] + Out[38] + Out[40] + Out[45]]

1/1440 w (2 hc (720 E3^2 epson L - 1440 E3^2 epson L1 -
```

```
  720 d31^2 E3^2 L Yc + 720 c6^2 hp^2 L Yc +
  2160 c5 c6 hp^2 L^2 Yc + 960 c6^2 hc^2 (L - 2 L1) Yc +
  1440 c6^2 hc hp (L - 2 L1) Yc +
  2880 c5 c6 hc^2 L (L - 2 L1) Yc +
  4320 c5 c6 hc hp L (L - 2 L1) Yc + 1440 d31^2 E3^2 L1 Yc -
  1440 c6^2 hp^2 L1 Yc - 4320 c5 c6 hp^2 L L1 Yc +
  2880 c5^2 hc^2 ((L - L1)^3 - L1^3) Yc +
  4320 c5^2 hc hp ((L - L1)^3 - L1^3) Yc +
  2160 c5^2 hp^2 ((L - L1)^3 - L1^3) Yc + (
  160 c6 hc^2 ((L - L1)^3 - L1^3) P w Yc)/R + (
  240 c6 hc hp ((L - L1)^3 - L1^3) P w Yc)/R + (
  120 c6 hp^2 ((L - L1)^3 - L1^3) P w Yc)/R + (
  360 c5 hc^2 ((L - L1)^4 - L1^4) P w Yc)/R + (
  540 c5 hc hp ((L - L1)^4 - L1^4) P w Yc)/R + (
  270 c5 hp^2 ((L - L1)^4 - L1^4) P w Yc)/R + (
  12 hc^2 ((L - L1)^5 - L1^5) P^2 w^2 Yc)/R^2 + (
  18 hc hp ((L - L1)^5 - L1^5) P^2 w^2 Yc)/R^2 + (
  9 hp^2 ((L - L1)^5 - L1^5) P^2 w^2 Yc)/R^2) +
1/R^2 hp^3 (L -
   2 L1) (240 (c6^2 + 3 c5 c6 L +
     3 c5^2 (L^2 - L L1 + L1^2)) R^2 +
   10 (4 c6 (L^2 - L L1 + L1^2) +
     9 c5 L (L^2 - 2 L L1 + 2 L1^2)) P R w +
   3 (L^4 - 3 L^3 L1 + 4 L^2 L1^2 - 2 L L1^3 +
     L1^4) P^2 w^2) Yp +
1/R^2 2 hp (12 hc^2 + 24 hc hp + 13 hp^2) (L -
   2 L1) (240 (c6^2 + 3 c5 c6 L +
     3 c5^2 (L^2 - L L1 + L1^2)) R^2 +
   10 (4 c6 (L^2 - L L1 + L1^2) +
     9 c5 L (L^2 - 2 L L1 + 2 L1^2)) P R w +
```

3 (L^4 - 3 L^3 L1 + 4 L^2 L1^2 - 2 L L1^3 + L1^4) P^2 w^2) Yp)

Ub[c5_, c6_] = Out[48]

1/1440 w (2 hc (720 E3^2 epson L - 1440 E3^2 epson L1 -
720 d31^2 E3^2 L Yc + 720 c6^2 hp^2 L Yc +
2160 c5 c6 hp^2 L^2 Yc + 960 c6^2 hc^2 (L - 2 L1) Yc +
1440 c6^2 hc hp (L - 2 L1) Yc +
2880 c5 c6 hc^2 L (L - 2 L1) Yc +
4320 c5 c6 hc hp L (L - 2 L1) Yc + 1440 d31^2 E3^2 L1 Yc -
1440 c6^2 hp^2 L1 Yc - 4320 c5 c6 hp^2 L L1 Yc +
2880 c5^2 hc^2 ((L - L1)^3 - L1^3) Yc +
4320 c5^2 hc hp ((L - L1)^3 - L1^3) Yc +
2160 c5^2 hp^2 ((L - L1)^3 - L1^3) Yc + (
160 c6 hc^2 ((L - L1)^3 - L1^3) P w Yc)/R + (
240 c6 hc hp ((L - L1)^3 - L1^3) P w Yc)/R + (
120 c6 hp^2 ((L - L1)^3 - L1^3) P w Yc)/R + (
360 c5 hc^2 ((L - L1)^4 - L1^4) P w Yc)/R + (
540 c5 hc hp ((L - L1)^4 - L1^4) P w Yc)/R + (
270 c5 hp^2 ((L - L1)^4 - L1^4) P w Yc)/R + (
12 hc^2 ((L - L1)^5 - L1^5) P^2 w^2 Yc)/R^2 + (
18 hc hp ((L - L1)^5 - L1^5) P^2 w^2 Yc)/R^2 + (
9 hp^2 ((L - L1)^5 - L1^5) P^2 w^2 Yc)/R^2) +
1/R^2 hp^3 (L -
2 L1) (240 (c6^2 + 3 c5 c6 L +
3 c5^2 (L^2 - L L1 + L1^2)) R^2 +
10 (4 c6 (L^2 - L L1 + L1^2) +
9 c5 L (L^2 - 2 L L1 + 2 L1^2)) P R w +
3 (L^4 - 3 L^3 L1 + 4 L^2 L1^2 - 2 L L1^3 +
L1^4) P^2 w^2) Yp +

```
   1/R^2 2 hp (12 hc^2 + 24 hc hp + 13 hp^2) (L -
      2 L1) (240 (c6^2 + 3 c5 c6 L +
        3 c5^2 (L^2 - L L1 + L1^2)) R^2 +
      10 (4 c6 (L^2 - L L1 + L1^2) +
        9 c5 L (L^2 - 2 L L1 + 2 L1^2)) P R w +
      3 (L^4 - 3 L^3 L1 + 4 L^2 L1^2 - 2 L L1^3 + L1^4) P^2 w^2) Yp)

Ub[0, 0]

1/1440 w (2 hc (720 E3^2 epson L - 1440 E3^2 epson L1 -
      720 d31^2 E3^2 L Yc + 1440 d31^2 E3^2 L1 Yc + (
      12 hc^2 ((L - L1)^5 - L1^5) P^2 w^2 Yc)/R^2 + (
      18 hc hp ((L - L1)^5 - L1^5) P^2 w^2 Yc)/R^2 + (
      9 hp^2 ((L - L1)^5 - L1^5) P^2 w^2 Yc)/R^2) + (
   3 hp^3 (L - 2 L1) (L^4 - 3 L^3 L1 + 4 L^2 L1^2 - 2 L L1^3 +
      L1^4) P^2 w^2 Yp)/R^2 + (
   6 hp (12 hc^2 + 24 hc hp + 13 hp^2) (L - 2 L1) (L^4 - 3 L^3 L1 +
      4 L^2 L1^2 - 2 L L1^3 + L1^4) P^2 w^2 Yp)/R^2)

Ub[-((L P w)/(
  12 R)), -((-L^3 P w - 12 d31 E3 hc^2 L1 w Yc -
  12 d31 E3 hc hp L1 w Yc)/(24 (L - L1) R))]

1/1440 w (2 hc (720 E3^2 epson L - 1440 E3^2 epson L1 -
      720 d31^2 E3^2 L Yc + 1440 d31^2 E3^2 L1 Yc + (
      20 hc^2 L^2 ((L - L1)^3 - L1^3) P^2 w^2 Yc)/R^2 + (
      30 hc hp L^2 ((L - L1)^3 - L1^3) P^2 w^2 Yc)/R^2 + (
      15 hp^2 L^2 ((L - L1)^3 - L1^3) P^2 w^2 Yc)/R^2 - (
      30 hc^2 L ((L - L1)^4 - L1^4) P^2 w^2 Yc)/R^2 - (
      45 hc hp L ((L - L1)^4 - L1^4) P^2 w^2 Yc)/R^2 - (
```

```
45 hp^2 L ((L - L1)^4 - L1^4) P^2 w^2 Yc)/(2 R^2) + (
12 hc^2 ((L - L1)^5 - L1^5) P^2 w^2 Yc)/R^2 + (
18 hc hp ((L - L1)^5 - L1^5) P^2 w^2 Yc)/R^2 + (
9 hp^2 ((L - L1)^5 - L1^5) P^2 w^2 Yc)/R^2 + (
15 hp^2 L^3 P w Yc (-L^3 P w - 12 d31 E3 hc^2 L1 w Yc -
  12 d31 E3 hc hp L1 w Yc))/(2 (L - L1) R^2) + (
10 hc^2 L^2 (L - 2 L1) P w Yc (-L^3 P w -
  12 d31 E3 hc^2 L1 w Yc - 12 d31 E3 hc hp L1 w Yc))/((L -
  L1) R^2) + (
15 hc hp L^2 (L - 2 L1) P w Yc (-L^3 P w -
  12 d31 E3 hc^2 L1 w Yc - 12 d31 E3 hc hp L1 w Yc))/((L -
  L1) R^2) - (
15 hp^2 L^2 L1 P w Yc (-L^3 P w - 12 d31 E3 hc^2 L1 w Yc -
  12 d31 E3 hc hp L1 w Yc))/((L - L1) R^2) - (
20 hc^2 ((L - L1)^3 - L1^3) P w Yc (-L^3 P w -
  12 d31 E3 hc^2 L1 w Yc - 12 d31 E3 hc hp L1 w Yc))/(
3 (L - L1) R^2) - (
10 hc hp ((L - L1)^3 - L1^3) P w Yc (-L^3 P w -
  12 d31 E3 hc^2 L1 w Yc - 12 d31 E3 hc hp L1 w Yc))/((L -
  L1) R^2) - (
5 hp^2 ((L - L1)^3 - L1^3) P w Yc (-L^3 P w -
  12 d31 E3 hc^2 L1 w Yc - 12 d31 E3 hc hp L1 w Yc))/((L -
  L1) R^2) + (
5 hp^2 L Yc (-L^3 P w - 12 d31 E3 hc^2 L1 w Yc -
  12 d31 E3 hc hp L1 w Yc)^2)/(4 (L - L1)^2 R^2) + (
5 hc^2 (L - 2 L1) Yc (-L^3 P w - 12 d31 E3 hc^2 L1 w Yc -
  12 d31 E3 hc hp L1 w Yc)^2)/(3 (L - L1)^2 R^2) + (
5 hc hp (L - 2 L1) Yc (-L^3 P w - 12 d31 E3 hc^2 L1 w Yc -
  12 d31 E3 hc hp L1 w Yc)^2)/(2 (L - L1)^2 R^2) - (
5 hp^2 L1 Yc (-L^3 P w - 12 d31 E3 hc^2 L1 w Yc -
```

```
      12 d31 E3 hc hp L1 w Yc)^2)/(2 (L - L1)^2 R^2)) +
  1/R^2 hp^3 (L -
    2 L1) (3 (L^4 - 3 L^3 L1 + 4 L^2 L1^2 - 2 L L1^3 +
      L1^4) P^2 w^2 +
    10 P R w (-((3 L^2 (L^2 - 2 L L1 + 2 L1^2) P w)/(
       4 R)) - ((L^2 - L L1 + L1^2) (-L^3 P w -
         12 d31 E3 hc^2 L1 w Yc - 12 d31 E3 hc hp L1 w Yc))/(
      6 (L - L1) R)) +
    240 R^2 ((L^2 (L^2 - L L1 + L1^2) P^2 w^2)/(48 R^2) + (

      L^2 P w (-L^3 P w - 12 d31 E3 hc^2 L1 w Yc -
        12 d31 E3 hc hp L1 w Yc))/(
      96 (L - L1) R^2) + (-L^3 P w - 12 d31 E3 hc^2 L1 w Yc -
        12 d31 E3 hc hp L1 w Yc)^2/(576 (L - L1)^2 R^2))) Yp +
  1/R^2 2 hp (12 hc^2 + 24 hc hp + 13 hp^2) (L -
    2 L1) (3 (L^4 - 3 L^3 L1 + 4 L^2 L1^2 - 2 L L1^3 +
      L1^4) P^2 w^2 +
    10 P R w (-((3 L^2 (L^2 - 2 L L1 + 2 L1^2) P w)/(
       4 R)) - ((L^2 - L L1 + L1^2) (-L^3 P w -
         12 d31 E3 hc^2 L1 w Yc - 12 d31 E3 hc hp L1 w Yc))/(
      6 (L - L1) R)) +
    240 R^2 ((L^2 (L^2 - L L1 + L1^2) P^2 w^2)/(48 R^2) + (
      L^2 P w (-L^3 P w - 12 d31 E3 hc^2 L1 w Yc -
        12 d31 E3 hc hp L1 w Yc))/(
      96 (L - L1) R^2) + (-L^3 P w - 12 d31 E3 hc^2 L1 w Yc -
        12 d31 E3 hc hp L1 w Yc)^2/(576 (L - L1)^2 R^2))) Yp)

Collect[Out[51], P]

1/1440 P^2 w ((5 hc hp^2 L^7 w^2 Yc)/(2 (L - L1)^2 R^2) + (
```

10 hc^3 L^6 (L - 2 L1) w^2 Yc)/(3 (L - L1)^2 R^2) + (

5 hc^2 hp L^6 (L - 2 L1) w^2 Yc)/((L - L1)^2 R^2) - (

15 hc hp^2 L^6 w^2 Yc)/((L - L1) R^2) - (

20 hc^3 L^5 (L - 2 L1) w^2 Yc)/((L - L1) R^2) - (

30 hc^2 hp L^5 (L - 2 L1) w^2 Yc)/((L - L1) R^2) - (

5 hc hp^2 L^6 L1 w^2 Yc)/((L - L1)^2 R^2) + (

30 hc hp^2 L^5 L1 w^2 Yc)/((L - L1) R^2) + (

40 hc^3 L^2 ((L - L1)^3 - L1^3) w^2 Yc)/R^2 + (

60 hc^2 hp L^2 ((L - L1)^3 - L1^3) w^2 Yc)/R^2 + (

30 hc hp^2 L^2 ((L - L1)^3 - L1^3) w^2 Yc)/R^2 + (

40 hc^3 L^3 ((L - L1)^3 - L1^3) w^2 Yc)/(3 (L - L1) R^2) + (

20 hc^2 hp L^3 ((L - L1)^3 - L1^3) w^2 Yc)/((L - L1) R^2) + (

10 hc hp^2 L^3 ((L - L1)^3 - L1^3) w^2 Yc)/((L - L1) R^2) - (

60 hc^3 L ((L - L1)^4 - L1^4) w^2 Yc)/R^2 - (

90 hc^2 hp L ((L - L1)^4 - L1^4) w^2 Yc)/R^2 - (

45 hc hp^2 L ((L - L1)^4 - L1^4) w^2 Yc)/R^2 + (

24 hc^3 ((L - L1)^5 - L1^5) w^2 Yc)/R^2 + (

36 hc^2 hp ((L - L1)^5 - L1^5) w^2 Yc)/R^2 + (

18 hc hp^2 ((L - L1)^5 - L1^5) w^2 Yc)/R^2 + (

5 hp^3 L^6 (L - 2 L1) w^2 Yp)/(12 (L - L1)^2 R^2) + (

5 hp (12 hc^2 + 24 hc hp + 13 hp^2) L^6 (L - 2 L1) w^2 Yp)/(

6 (L - L1)^2 R^2) - (5 hp^3 L^5 (L - 2 L1) w^2 Yp)/(

2 (L - L1) R^2) - (

5 hp (12 hc^2 + 24 hc hp + 13 hp^2) L^5 (L - 2 L1) w^2 Yp)/((L -

L1) R^2) + (5 hp^3 L^2 (L - 2 L1) (L^2 - L L1 + L1^2) w^2 Yp)/

R^2 + (10 hp (12 hc^2 + 24 hc hp + 13 hp^2) L^2 (L - 2 L1) (L^2 -

L L1 + L1^2) w^2 Yp)/R^2 + (

5 hp^3 L^3 (L - 2 L1) (L^2 - L L1 + L1^2) w^2 Yp)/(

3 (L - L1) R^2) + (

10 hp (12 hc^2 + 24 hc hp + 13 hp^2) L^3 (L - 2 L1) (L^2 - L L1 +

```
    L1^2) w^2 Yp)/(3 (L - L1) R^2) - (
  15 hp^3 L^2 (L - 2 L1) (L^2 - 2 L L1 + 2 L1^2) w^2 Yp)/(
  2 R^2) - (
  15 hp (12 hc^2 + 24 hc hp + 13 hp^2) L^2 (L - 2 L1) (L^2 -
    2 L L1 + 2 L1^2) w^2 Yp)/R^2 + (
  3 hp^3 (L - 2 L1) (L^4 - 3 L^3 L1 + 4 L^2 L1^2 - 2 L L1^3 +
    L1^4) w^2 Yp)/R^2 + (
  6 hp (12 hc^2 + 24 hc hp + 13 hp^2) (L - 2 L1) (L^4 - 3 L^3 L1 +
    4 L^2 L1^2 - 2 L L1^3 + L1^4) w^2 Yp)/R^2) +
1/1440 P w ((
  60 d31 E3 hc^3 hp^2 L^4 L1 w^2 Yc^2)/((L - L1)^2 R^2) + (
  60 d31 E3 hc^2 hp^3 L^4 L1 w^2 Yc^2)/((L - L1)^2 R^2) + (
  80 d31 E3 hc^5 L^3 (L - 2 L1) L1 w^2 Yc^2)/((L - L1)^2 R^2) + (
  200 d31 E3 hc^4 hp L^3 (L - 2 L1) L1 w^2 Yc^2)/((L -
    L1)^2 R^2) + (
  120 d31 E3 hc^3 hp^2 L^3 (L - 2 L1) L1 w^2 Yc^2)/((L -
    L1)^2 R^2) - (
  180 d31 E3 hc^3 hp^2 L^3 L1 w^2 Yc^2)/((L - L1) R^2) - (
  180 d31 E3 hc^2 hp^3 L^3 L1 w^2 Yc^2)/((L - L1) R^2) - (
  240 d31 E3 hc^5 L^2 (L - 2 L1) L1 w^2 Yc^2)/((L - L1) R^2) - (
  600 d31 E3 hc^4 hp L^2 (L - 2 L1) L1 w^2 Yc^2)/((L - L1) R^2) - (
  360 d31 E3 hc^3 hp^2 L^2 (L - 2 L1) L1 w^2 Yc^2)/((L -
    L1) R^2) - (
  120 d31 E3 hc^3 hp^2 L^3 L1^2 w^2 Yc^2)/((L - L1)^2 R^2) - (
  120 d31 E3 hc^2 hp^3 L^3 L1^2 w^2 Yc^2)/((L - L1)^2 R^2) + (
  360 d31 E3 hc^3 hp^2 L^2 L1^2 w^2 Yc^2)/((L - L1) R^2) + (
  360 d31 E3 hc^2 hp^3 L^2 L1^2 w^2 Yc^2)/((L - L1) R^2) + (
  160 d31 E3 hc^5 L1 ((L - L1)^3 - L1^3) w^2 Yc^2)/((L -
    L1) R^2) + (
  400 d31 E3 hc^4 hp L1 ((L - L1)^3 - L1^3) w^2 Yc^2)/((L -
```

L1) R^2) + (

360 d31 E3 hc^3 hp^2 L1 ((L - L1)^3 - L1^3) w^2 Yc^2)/((L -

L1) R^2) + (

120 d31 E3 hc^2 hp^3 L1 ((L - L1)^3 - L1^3) w^2 Yc^2)/((L -

L1) R^2) + (

10 d31 E3 hc^2 hp^3 L^3 (L - 2 L1) L1 w^2 Yc Yp)/((L -

L1)^2 R^2) + (

10 d31 E3 hc hp^4 L^3 (L - 2 L1) L1 w^2 Yc Yp)/((L -

L1)^2 R^2) + (

20 d31 E3 hc^2 hp (12 hc^2 + 24 hc hp + 13 hp^2) L^3 (L -

2 L1) L1 w^2 Yc Yp)/((L - L1)^2 R^2) + (

20 d31 E3 hc hp^2 (12 hc^2 + 24 hc hp + 13 hp^2) L^3 (L -

2 L1) L1 w^2 Yc Yp)/((L - L1)^2 R^2) - (

30 d31 E3 hc^2 hp^3 L^2 (L - 2 L1) L1 w^2 Yc Yp)/((L -

L1) R^2) - (

30 d31 E3 hc hp^4 L^2 (L - 2 L1) L1 w^2 Yc Yp)/((L - L1) R^2) - (

60 d31 E3 hc^2 hp (12 hc^2 + 24 hc hp + 13 hp^2) L^2 (L -

2 L1) L1 w^2 Yc Yp)/((L - L1) R^2) - (

60 d31 E3 hc hp^2 (12 hc^2 + 24 hc hp + 13 hp^2) L^2 (L -

2 L1) L1 w^2 Yc Yp)/((L - L1) R^2) + (

20 d31 E3 hc^2 hp^3 (L - 2 L1) L1 (L^2 - L L1 +

L1^2) w^2 Yc Yp)/((L - L1) R^2) + (

20 d31 E3 hc hp^4 (L - 2 L1) L1 (L^2 - L L1 +

L1^2) w^2 Yc Yp)/((L - L1) R^2) + (

40 d31 E3 hc^2 hp (12 hc^2 + 24 hc hp + 13 hp^2) (L -

2 L1) L1 (L^2 - L L1 + L1^2) w^2 Yc Yp)/((L - L1) R^2) + (

40 d31 E3 hc hp^2 (12 hc^2 + 24 hc hp + 13 hp^2) (L -

2 L1) L1 (L^2 - L L1 + L1^2) w^2 Yc Yp)/((L - L1) R^2)) +

1/1440 w (1440 E3^2 epson hc L - 2880 E3^2 epson hc L1 -

1440 d31^2 E3^2 hc L Yc + 2880 d31^2 E3^2 hc L1 Yc + (

```
360 d31^2 E3^2 hc^5 hp^2 L L1^2 w^2 Yc^3)/((L - L1)^2 R^2) + (
720 d31^2 E3^2 hc^4 hp^3 L L1^2 w^2 Yc^3)/((L - L1)^2 R^2) + (
360 d31^2 E3^2 hc^3 hp^4 L L1^2 w^2 Yc^3)/((L - L1)^2 R^2) + (
480 d31^2 E3^2 hc^7 (L - 2 L1) L1^2 w^2 Yc^3)/((L -
  L1)^2 R^2) + (
1680 d31^2 E3^2 hc^6 hp (L - 2 L1) L1^2 w^2 Yc^3)/((L -
  L1)^2 R^2) + (
1920 d31^2 E3^2 hc^5 hp^2 (L - 2 L1) L1^2 w^2 Yc^3)/((L -
  L1)^2 R^2) + (
720 d31^2 E3^2 hc^4 hp^3 (L - 2 L1) L1^2 w^2 Yc^3)/((L -
  L1)^2 R^2) - (
720 d31^2 E3^2 hc^5 hp^2 L1^3 w^2 Yc^3)/((L - L1)^2 R^2) - (
1440 d31^2 E3^2 hc^4 hp^3 L1^3 w^2 Yc^3)/((L - L1)^2 R^2) - (
720 d31^2 E3^2 hc^3 hp^4 L1^3 w^2 Yc^3)/((L - L1)^2 R^2) + (
60 d31^2 E3^2 hc^4 hp^3 (L - 2 L1) L1^2 w^2 Yc^2 Yp)/((L -
  L1)^2 R^2) + (
120 d31^2 E3^2 hc^3 hp^4 (L - 2 L1) L1^2 w^2 Yc^2 Yp)/((L -
  L1)^2 R^2) + (
60 d31^2 E3^2 hc^2 hp^5 (L - 2 L1) L1^2 w^2 Yc^2 Yp)/((L -
  L1)^2 R^2) + (
120 d31^2 E3^2 hc^4 hp (12 hc^2 + 24 hc hp + 13 hp^2) (L -
  2 L1) L1^2 w^2 Yc^2 Yp)/((L - L1)^2 R^2) + (
240 d31^2 E3^2 hc^3 hp^2 (12 hc^2 + 24 hc hp + 13 hp^2) (L -
  2 L1) L1^2 w^2 Yc^2 Yp)/((L - L1)^2 R^2) + (
120 d31^2 E3^2 hc^2 hp^3 (12 hc^2 + 24 hc hp + 13 hp^2) (L -
  2 L1) L1^2 w^2 Yc^2 Yp)/((L - L1)^2 R^2))
```

```
Simplify[2*Out[30] + Out[52]]
```

```
1/(51840 (L - L1)^2 R^2)
```

```
 w (L^3 (3 L^4 - 26 L^3 L1 + 78 L^2 L1^2 - 90 L L1^3 +
      30 L1^4) P^2 w^2 (8 hc^3 Yc + 27 hp^3 Yp +
      12 hc^2 hp (Yc + 2 Yp) + 6 hc hp^2 (Yc + 8 Yp)) -
    120 d31 E3 hc (hc + hp) L1 (2 L^4 - 13 L^3 L1 + 27 L^2 L1^2 -
      21 L L1^3 + 6 L1^4) P w^2 Yc (8 hc^3 Yc + 27 hp^3 Yp +
      12 hc^2 hp (Yc + 2 Yp) + 6 hc hp^2 (Yc + 8 Yp)) +
    720 E3^2 hc (L - 2 L1) (72 epson (L - L1)^2 R^2 +
      d31^2 Yc (-72 L^2 R^2 +
        2 L L1 (72 R^2 +
          hc (hc + hp)^2 w^2 Yc (8 hc^3 Yc + 27 hp^3 Yp +
            12 hc^2 hp (Yc + 2 Yp) + 6 hc hp^2 (Yc + 8 Yp))) -
        L1^2 (72 R^2 +
          hc (hc + hp)^2 w^2 Yc (8 hc^3 Yc + 27 hp^3 Yp +
            12 hc^2 hp (Yc + 2 Yp) + 6 hc hp^2 (Yc + 8 Yp))))))

Collect[Out[53], P]

(L^3 (3 L^4 - 26 L^3 L1 + 78 L^2 L1^2 - 90 L L1^3 +
    30 L1^4) P^2 w^3 (8 hc^3 Yc + 27 hp^3 Yp +
    12 hc^2 hp (Yc + 2 Yp) + 6 hc hp^2 (Yc + 8 Yp)))/(
 51840 (L - L1)^2 R^2) - (
 d31 E3 hc (hc + hp) L1 (2 L^4 - 13 L^3 L1 + 27 L^2 L1^2 -
    21 L L1^3 + 6 L1^4) P w^3 Yc (8 hc^3 Yc + 27 hp^3 Yp +
    12 hc^2 hp (Yc + 2 Yp) + 6 hc hp^2 (Yc + 8 Yp)))/(
 432 (L - L1)^2 R^2) +
 1/(72 (L - L1)^2 R^2)
   E3^2 hc (L - 2 L1) w (72 epson (L - L1)^2 R^2 +
     d31^2 Yc (-72 L^2 R^2 +
       2 L L1 (72 R^2 +
         hc (hc + hp)^2 w^2 Yc (8 hc^3 Yc + 27 hp^3 Yp +
```

```
            12 hc^2 hp (Yc + 2 Yp) + 6 hc hp^2 (Yc + 8 Yp))) -
        L1^2 (72 R^2 +
          hc (hc + hp)^2 w^2 Yc (8 hc^3 Yc + 27 hp^3 Yp +
            12 hc^2 hp (Yc + 2 Yp) + 6 hc hp^2 (Yc + 8 Yp)))))

Simplify[1/(51840 (L - L1)^2 R^2)
  w (L^3 (3 L^4 - 26 L^3 L1 + 78 L^2 L1^2 - 90 L L1^3 +
      30 L1^4) P^2 w^2 (12*R/w) -
    120 d31 E3 hc (hc + hp) L1 (2 L^4 - 13 L^3 L1 + 27 L^2 L1^2 -
      21 L L1^3 + 6 L1^4) P w^2 Yc (12*R/w) +
    720 E3^2 hc (L - 2 L1) (72 epson (L - L1)^2 R^2 +
      d31^2 Yc (-72 L^2 R^2 +
        2 L L1 (72 R^2 + hc (hc + hp)^2 w^2 Yc (12*R/w)) -
        L1^2 (72 R^2 + hc (hc + hp)^2 w^2 Yc (12*R/w)))))]

1/(4320 (L - L1)^2 R)
  w (L^3 (3 L^4 - 26 L^3 L1 + 78 L^2 L1^2 - 90 L L1^3 +
      30 L1^4) P^2 w -
    120 d31 E3 hc (hc + hp) L1 (2 L^4 - 13 L^3 L1 + 27 L^2 L1^2 -
      21 L L1^3 + 6 L1^4) P w Yc +
    720 E3^2 hc (L - 2 L1) (6 epson (L - L1)^2 R +
      d31^2 Yc (-6 L^2 R + 2 L L1 (6 R + hc (hc + hp)^2 w Yc) -
        L1^2 (6 R + hc (hc + hp)^2 w Yc))))

Simplify[(2*L^4 - 13*L^3*L1 + 27*L^2*L1^2 - 21*L*L1^3 +
   6*L1^4)/(L - L1)^2]

(2 L^4 - 13 L^3 L1 + 27 L^2 L1^2 - 21 L L1^3 + 6 L1^4)/(L - L1)^2

Expand[(2 L^4 - 13 L^3 L1 + 27 L^2 L1^2 - 21 L L1^3 +
```

6 L1^4)/(L - L1)^2]

(2 L^4)/(L - L1)^2 - (13 L^3 L1)/(L - L1)^2 + (
27 L^2 L1^2)/(L - L1)^2 - (21 L L1^3)/(L - L1)^2 + (6 L1^4)/(L - L1)^2

Denominator[(
2 L^4 - 13 L^3 L1 + 27 L^2 L1^2 - 21 L L1^3 + 6 L1^4)/(L - L1)^2]

(L - L1)^2

Expand[(L - L1)^2]

L^2 - 2 L L1 + L1^2

(L - L1)^2*(L^2 - 3*L1*L + 2*L1^2)

(L - L1)^2 (L^2 - 3 L L1 + 2 L1^2)

Expand[(L - L1)^2 (L^2 - 3 L L1 + 2 L1^2)]

L^4 - 5 L^3 L1 + 9 L^2 L1^2 - 7 L L1^3 + 2 L1^4

Wb[L/2]

c8 + (c7 L)/2 + (c6 L^2)/4 + (c5 L^3)/8 + (L^4 P w)/(384 R)

delta[c5_, c6_, c7_, c8_] = Out[63]

c8 + (c7 L)/2 + (c6 L^2)/4 + (c5 L^3)/8 + (L^4 P w)/(384 R)

```
delta[-((L P w)/(
  12 R)), -((-L^3 P w - 12 d31 E3 hc^2 L1 w Yc -
   12 d31 E3 hc hp L1 w Yc)/(24 (L - L1) R)), -((
  L^3 L1 P w + 12 d31 E3 hc^2 L L1 w Yc + 12 d31 E3 hc hp L L1 w Yc)/(
  24 (L - L1) R)), -(1/(
   72 (L - L1) R)) (-L^3 L1^2 P w - 24 d31 E3 hc^2 L L1^2 w Yc -
    24 d31 E3 hc hp L L1^2 w Yc + 12 d31 E3 hc^2 L1^3 w Yc +
    12 d31 E3 hc hp L1^3 w Yc)]

-((L^4 P w)/(128 R)) - (
 L^2 (-L^3 P w - 12 d31 E3 hc^2 L1 w Yc - 12 d31 E3 hc hp L1 w Yc))/(
 96 (L - L1) R) - (
 L (L^3 L1 P w + 12 d31 E3 hc^2 L L1 w Yc +
    12 d31 E3 hc hp L L1 w Yc))/(
 48 (L - L1) R) - (-L^3 L1^2 P w - 24 d31 E3 hc^2 L L1^2 w Yc -
  24 d31 E3 hc hp L L1^2 w Yc + 12 d31 E3 hc^2 L1^3 w Yc +
  12 d31 E3 hc hp L1^3 w Yc)/(72 (L - L1) R)

FullSimplify[%65]

(L^3 (3 L^2 - 15 L L1 + 16 L1^2) P w -
 48 d31 E3 hc (hc + hp) (L - 2 L1) (3 L - 2 L1) L1 w Yc)/(1152 (L -
   L1) R)

f[L1_] = (L^3 (3 L^2 - 15 L L1 + 16 L1^2) P w)/(1152 (L - L1) R)

(L^3 (3 L^2 - 15 L L1 + 16 L1^2) P w)/(1152 (L - L1) R)

f'[L1]
```

```
(L^3 (-15 L + 32 L1) P w)/(1152 (L - L1) R) + (
 L^3 (3 L^2 - 15 L L1 + 16 L1^2) P w)/(1152 (L - L1)^2 R)

Solve[(L^3 (-15 L + 32 L1) P w)/(1152 (L - L1) R) + (
   L^3 (3 L^2 - 15 L L1 + 16 L1^2) P w)/(1152 (L - L1)^2 R) == 0, L1]

{{L1 -> L/2}, {L1 -> (3 L)/2}}

f[0]

(L^4 P w)/(384 R)

f[L/2]

-((L^4 P w)/(1152 R))

f[L/4]

(L^4 P w)/(3456 R)

Integrate[Wa[x], {x, 0, L1}]

(c1 L1^4)/4 + (L1^5 P w)/(120 R)

Integrate[Wb[x], {x, L1, L - L1}]

c8 L + (c7 L^2)/2 - 2 c8 L1 - c7 L L1 + 1/3 c6 ((L - L1)^3 - L1^3) +
 1/4 c5 ((L - L1)^4 - L1^4) + (((L - L1)^5 - L1^5) P w)/(120 R)

Integrate[Wc[x], {x, L - L1, L}]
```

```
1/4 c9 (L^4 - (L - L1)^4) + c12 L1 + c11 L L1 + c10 L^2 L1 - (
 c11 L1^2)/2 - c10 L L1^2 + (c10 L1^3)/3 + ((L^5 - (L - L1)^5) P w)/(
 120 R)

Simplify[Out[73] + Out[74] + Out[75]]

(c6 L^3)/3 + (c5 L^4)/4 + c8 (L - 2 L1) + 1/2 c7 L (L - 2 L1) +
 c12 L1 + c11 L L1 + c10 L^2 L1 - c6 L^2 L1 - c5 L^3 L1 +
 c9 L^3 L1 - (c11 L1^2)/2 - c10 L L1^2 + c6 L L1^2 +
 3/2 c5 L^2 L1^2 - 3/2 c9 L^2 L1^2 + (c10 L1^3)/3 - (2 c6 L1^3)/3 -
 c5 L L1^3 + c9 L L1^3 + (c1 L1^4)/4 - (c9 L1^4)/4 + (L^5 P w)/(120 R)

v[c1_, c5_, c6_, c7_, c8_, c9_, c10_, c11_, c12_] = Out[76]

(c6 L^3)/3 + (c5 L^4)/4 + c8 (L - 2 L1) + 1/2 c7 L (L - 2 L1) +
 c12 L1 + c11 L L1 + c10 L^2 L1 - c6 L^2 L1 - c5 L^3 L1 +
 c9 L^3 L1 - (c11 L1^2)/2 - c10 L L1^2 + c6 L L1^2 +
 3/2 c5 L^2 L1^2 - 3/2 c9 L^2 L1^2 + (c10 L1^3)/3 - (2 c6 L1^3)/3 -
 c5 L L1^3 + c9 L L1^3 + (c1 L1^4)/4 - (c9 L1^4)/4 + (L^5 P w)/(120 R)

v[-(1/(72 (L - L1) L1 R)) (-L^3 P w + 6 L^2 L1 P w - 6 L L1^2 P w +
    12 d31 E3 hc^2 L w Yc + 12 d31 E3 hc hp L w Yc -
    24 d31 E3 hc^2 L1 w Yc - 24 d31 E3 hc hp L1 w Yc), -((L P w)/(
  12 R)), -((-L^3 P w - 12 d31 E3 hc^2 L1 w Yc -
   12 d31 E3 hc hp L1 w Yc)/(24 (L - L1) R)), -((
  L^3 L1 P w + 12 d31 E3 hc^2 L L1 w Yc + 12 d31 E3 hc hp L L1 w Yc)/(
  24 (L - L1) R)), -(1/(
   72 (L - L1) R)) (-L^3 L1^2 P w - 24 d31 E3 hc^2 L L1^2 w Yc -
    24 d31 E3 hc hp L L1^2 w Yc + 12 d31 E3 hc^2 L1^3 w Yc +
```

12 d31 E3 hc hp L1^3 w Yc), -(1/(
72 (L - L1) L1 R)) (L^3 P w + 6 L^2 L1 P w - 6 L L1^2 P w -
12 d31 E3 hc^2 L w Yc - 12 d31 E3 hc hp L w Yc +
24 d31 E3 hc^2 L1 w Yc + 24 d31 E3 hc hp L1 w Yc), -(1/(
24 (L - L1) L1 R)) (-L^4 P w + 12 d31 E3 hc^2 L^2 w Yc +
12 d31 E3 hc hp L^2 w Yc - 24 d31 E3 hc^2 L L1 w Yc -
24 d31 E3 hc hp L L1 w Yc), -(1/(
24 (L - L1) L1 R)) (L^5 P w - 2 L^4 L1 P w + 2 L^3 L1^2 P w -
12 d31 E3 hc^2 L^3 w Yc - 12 d31 E3 hc hp L^3 w Yc +
24 d31 E3 hc^2 L^2 L1 w Yc + 24 d31 E3 hc hp L^2 L1 w Yc), -(1/(
72 (L - L1) L1 R)) (-L^6 P w + 3 L^5 L1 P w - 3 L^4 L1^2 P w +
12 d31 E3 hc^2 L^4 w Yc + 12 d31 E3 hc hp L^4 w Yc -
24 d31 E3 hc^2 L^3 L1 w Yc - 24 d31 E3 hc hp L^3 L1 w Yc)]

-((L^5 P w)/(80 R)) + (L^4 L1 P w)/(12 R) - (L^3 L1^2 P w)/(8 R) + (
L^2 L1^3 P w)/(12 R) - (
L1^3 (-L^3 P w + 6 L^2 L1 P w - 6 L L1^2 P w +
12 d31 E3 hc^2 L w Yc + 12 d31 E3 hc hp L w Yc -
24 d31 E3 hc^2 L1 w Yc - 24 d31 E3 hc hp L1 w Yc))/(
288 (L - L1) R) - (
L^3 (-L^3 P w - 12 d31 E3 hc^2 L1 w Yc - 12 d31 E3 hc hp L1 w Yc))/(
72 (L - L1) R) + (
L^2 L1 (-L^3 P w - 12 d31 E3 hc^2 L1 w Yc -
12 d31 E3 hc hp L1 w Yc))/(24 (L - L1) R) - (
L L1^2 (-L^3 P w - 12 d31 E3 hc^2 L1 w Yc -
12 d31 E3 hc hp L1 w Yc))/(24 (L - L1) R) + (
L1^3 (-L^3 P w - 12 d31 E3 hc^2 L1 w Yc - 12 d31 E3 hc hp L1 w Yc))/(
36 (L - L1) R) - (
L^3 (L^3 P w + 6 L^2 L1 P w - 6 L L1^2 P w - 12 d31 E3 hc^2 L w Yc -
12 d31 E3 hc hp L w Yc + 24 d31 E3 hc^2 L1 w Yc +

24 d31 E3 hc hp L1 w Yc))/(72 (L - L1) R) + (

L^2 L1 (L^3 P w + 6 L^2 L1 P w - 6 L L1^2 P w -

12 d31 E3 hc^2 L w Yc - 12 d31 E3 hc hp L w Yc +

24 d31 E3 hc^2 L1 w Yc + 24 d31 E3 hc hp L1 w Yc))/(

48 (L - L1) R) - (

L L1^2 (L^3 P w + 6 L^2 L1 P w - 6 L L1^2 P w -

12 d31 E3 hc^2 L w Yc - 12 d31 E3 hc hp L w Yc +

24 d31 E3 hc^2 L1 w Yc + 24 d31 E3 hc hp L1 w Yc))/(

72 (L - L1) R) + (

L1^3 (L^3 P w + 6 L^2 L1 P w - 6 L L1^2 P w -

12 d31 E3 hc^2 L w Yc - 12 d31 E3 hc hp L w Yc +

24 d31 E3 hc^2 L1 w Yc + 24 d31 E3 hc hp L1 w Yc))/(

288 (L - L1) R) - (

L^2 (-L^4 P w + 12 d31 E3 hc^2 L^2 w Yc + 12 d31 E3 hc hp L^2 w Yc -

24 d31 E3 hc^2 L L1 w Yc - 24 d31 E3 hc hp L L1 w Yc))/(

24 (L - L1) R) + (

L L1 (-L^4 P w + 12 d31 E3 hc^2 L^2 w Yc +

12 d31 E3 hc hp L^2 w Yc - 24 d31 E3 hc^2 L L1 w Yc -

24 d31 E3 hc hp L L1 w Yc))/(24 (L - L1) R) - (

L1^2 (-L^4 P w + 12 d31 E3 hc^2 L^2 w Yc +

12 d31 E3 hc hp L^2 w Yc - 24 d31 E3 hc^2 L L1 w Yc -

24 d31 E3 hc hp L L1 w Yc))/(72 (L - L1) R) - (

L (L - 2 L1) (L^3 L1 P w + 12 d31 E3 hc^2 L L1 w Yc +

12 d31 E3 hc hp L L1 w Yc))/(48 (L - L1) R) - (

L (L^5 P w - 2 L^4 L1 P w + 2 L^3 L1^2 P w -

12 d31 E3 hc^2 L^3 w Yc - 12 d31 E3 hc hp L^3 w Yc +

24 d31 E3 hc^2 L^2 L1 w Yc + 24 d31 E3 hc hp L^2 L1 w Yc))/(

24 (L - L1) R) + (

L1 (L^5 P w - 2 L^4 L1 P w + 2 L^3 L1^2 P w -

12 d31 E3 hc^2 L^3 w Yc - 12 d31 E3 hc hp L^3 w Yc +

```
   24 d31 E3 hc^2 L^2 L1 w Yc + 24 d31 E3 hc hp L^2 L1 w Yc))/(
 48 (L - L1) R) - (-L^6 P w + 3 L^5 L1 P w - 3 L^4 L1^2 P w +
  12 d31 E3 hc^2 L^4 w Yc + 12 d31 E3 hc hp L^4 w Yc -
  24 d31 E3 hc^2 L^3 L1 w Yc - 24 d31 E3 hc hp L^3 L1 w Yc)/(
 72 (L - L1) R) - ((L - 2 L1) (-L^3 L1^2 P w -
    24 d31 E3 hc^2 L L1^2 w Yc - 24 d31 E3 hc hp L L1^2 w Yc +
    12 d31 E3 hc^2 L1^3 w Yc + 12 d31 E3 hc hp L1^3 w Yc))/(
 72 (L - L1) R)
```

FullSimplify[%78]

```
(L^3 (L^2 - 5 L L1 + 5 L1^2) P w -
 60 d31 E3 hc (hc + hp) (L - 2 L1) (L - L1) L1 w Yc)/(720 R)
```

APPENDIX B

MATLAB CODE FOR MODEL CALCULATION AND SIMULATION

```
% Flexural rigidity
hc=80*10^(-6);
hp=70*10^(-6);
h=2*hc+3*hp;
L=30*10^(-3);
w=4*10^(-3);
yc=50*10^(9);
yp=2.5*10^(9);
R=w*(8*hc^3*yc+27*hp^3*yp+12*hc^2*hp*(yc+2*yp)+6*hc*hp^2*(yc+8*yp))/12;
d31=-190*10^(-12);
e33=1.1281*10^(-8);

% mass density per unit length
densityp=1420;
densityc=7500;
rho=densityp*3*hp*w+densityc*2*hc*w;

% a
a=sqrt(R/rho);

% epson
epson33=(d31)^2*yc/((0.4)^2)

% natural frequency
omega1=(1.875104/L)^2*a;
f1=omega1/(2*pi)
omega2=(4.694091/L)^2*a;
f2=omega2/(2*pi)
omega3=(7.854757/L)^2*a;
f3=omega3/(2*pi)



% tip deflection under V(6V 80Hz)

V=5;
```

```
omega=120*2*pi;

delta=-
(sin(sqrt(omega/a)*L)*sinh(sqrt(omega/a)*L))/(R*(sqrt(omega/a))^2*(1+cos(sqrt(omega/a)*L)*cosh(sqrt
(omega/a)*L)))*w*yc*d31*hc*(hc+hp)/(hp+2*hc)*V
vo=delta*10^6/0.16

% disp vs frequency

f=zeros(3000,1);
disp=zeros(3000,1);
for i=1:1:3000
   f(i)=i;
disp(i)=-
(sin(sqrt(2*pi*f(i)/a)*L)*sinh(sqrt(2*pi*f(i)/a)*L))/((sqrt(2*pi*f(i)/a))^2*(1+cos(sqrt(2*pi*f(i)/a)*L)*cos
h(sqrt(2*pi*f(i)/a)*L)))/R*w*yc*d31*hc*(hc+hp)/(hc+2*hp);
end
% %plot(f,disp)


% theoretical tip disp vs frequency
V1=2;
V2=5;
V3=10;
Delta1=zeros(151,1);
Delta2=zeros(151,1);
Delta3=zeros(151,1);
fre=zeros(151,1);
for i=1:151
   fre(i)=50+i-1;
   Delta1(i)=abs(-
(sin(sqrt(2*pi*fre(i)/a)*L)*sinh(sqrt(2*pi*fre(i)/a)*L))/((sqrt(2*pi*fre(i)/a))^2*(1+cos(sqrt(2*pi*fre(i)/a)
*L)*cosh(sqrt(2*pi*fre(i)/a)*L)))/R*w*yc*d31*hc*(hc+hp)/(hc+2*hp)*V1);
   Delta2(i)=abs(-
(sin(sqrt(2*pi*fre(i)/a)*L)*sinh(sqrt(2*pi*fre(i)/a)*L))/((sqrt(2*pi*fre(i)/a))^2*(1+cos(sqrt(2*pi*fre(i)/a)
*L)*cosh(sqrt(2*pi*fre(i)/a)*L)))/R*w*yc*d31*hc*(hc+hp)/(hc+2*hp)*V2);
   Delta3(i)=abs(-
(sin(sqrt(2*pi*fre(i)/a)*L)*sinh(sqrt(2*pi*fre(i)/a)*L))/((sqrt(2*pi*fre(i)/a))^2*(1+cos(sqrt(2*pi*fre(i)/a)
*L)*cosh(sqrt(2*pi*fre(i)/a)*L)))/R*w*yc*d31*hc*(hc+hp)/(hc+2*hp)*V3);
end

% figure;
% plot(fre,Delta1,'g',fre,Delta2,'b',fre,Delta3,'r');


% Sensor
if 0
   K=3*R/L^3;
meff=K/omega1^2;
mend=0.15*10^(-3);
Mtotal=meff+mend;
```

```
Omeganew=sqrt(K/Mtotal);
fnew=Omeganew/(2*pi)

meff2=K/omega2^2;
Mtotal2=meff2+mend;
Omeganew2=sqrt(K/Mtotal2);
fnew2=Omeganew2/(2*pi)

meff3=K/omega3^2;
Mtotal3=meff3+mend;
Omeganew3=sqrt(K/Mtotal3);
fnew3=Omeganew3/(2*pi)

% Qd and Cp
Qd=-3*w*yc*d31*hc*(hc+hp)/(2*(hp+2*hc)*L)
Cp=w*L/(hp+2*hc)*(e33-d31^2*yc)+w^2*L*d31^2*hc*(hc+hp)*yc^2/(2*R)

end


% frequency function
f=zeros(101,1);
Omega=zeros(101,1);
v=zeros(101,1);
Sensitivity=zeros(101,1);
y0=80*10^(-6);
wn=54.7464*2*pi;
Qd=9.913*10^(-5);
Cp=6.0769*10^(-9);

for i=1:1:101
   f(i)=-1+i;
   Omega(i)=2*pi*f(i);
   v(i)=Qd/Cp*y0*(Omega(i)/wn)^2/(sqrt((Omega(i)/wn)^4+2*(2*0.0842^2-1)*(Omega(i)/wn)^2+1));
   Sensitivity(i)=Qd/Cp*(1/wn)^2/(sqrt((Omega(i)/wn)^4+2*(2*0.0842^2-1)*(Omega(i)/wn)^2+1));
end

figure
plot(f,v)
figure
plot(f,Sensitivity)


% Calculation for doubly clamped beam

% Flexural rigidity
hc=80*10^(-6);
hp=70*10^(-6);
h=2*hc+3*hp;
L=30*10^(-3);
w=4*10^(-3);
```

```
yc=50*10^(9);
yp=2.5*10^(9);
R=w*(8*hc^3*yc+27*hp^3*yp+12*hc^2*hp*(yc+2*yp)+6*hc*hp^2*(yc+8*yp))/12;
d31=-190*10^(-12);
epson33=1.1281*10^(-8);
L1=L/4;

% mass density per unit length
densityp=1420;
densityc=7500;
rho=densityp*3*hp*w+densityc*2*hc*w;

% a
a=sqrt(R/rho);

% delta
v0=10;
delta=-w*hc*(hc+hp)*L^2*yc*d31/(32*R*(2*hc+hp))*v0

% natural frequencies
omega1=(4.73/L)^2*a;
f1=omega1/(2*pi)
omega2=(7.8532/L)^2*a;
f2=omega2/(2*pi)
omega3=(10.9956/L)^2*a;
f3=omega3/(2*pi)

K=192*R/L^3;
meff1=K/(2*pi*f1)^2;
meff2=K/omega2^2;
meff3=K/omega3^2;
macc=0.26*10^(-3);
fn1=1/(2*pi)*sqrt(K/(meff1+macc))
fn2=1/(2*pi)*sqrt(K/(meff2+macc))
fn3=1/(2*pi)*sqrt(K/(meff3+macc))

Qd=-6*w*yc*d31*hc*(hc+hp)/((hp+2*hc)*L)
Cp=2*w*hc*(L-2*L1)/(L*R*(2*hc+hp)^2)*((epson33-
d31^2*yc)*L*R+d31^2*yc^2*w*hc*(hc+hp)^2*L1)


% frequency responce for fixed-fixed beam
f=zeros(501,1);
Omega=zeros(101,1);
v=zeros(501,1);
sensitivity=zeros(501,1);
y0=20*10^(-6);
wn=354.43*2*pi;
Qd=3.9652*10^(-4);
Cp=1.8482*10^(-9);
```

```
for i=1:1:501
   f(i)=-1+i;
   Omega(i)=2*pi*f(i);
   v(i)=Qd/Cp*y0*(Omega(i)/wn)^2/(sqrt((Omega(i)/wn)^4+2*(2*0.196^2-1)*(Omega(i)/wn)^2+1));
   sensitivity(i)=(1/wn)^2/(sqrt((Omega(i)/wn)^4+2*(2*0.196^2-1)*(Omega(i)/wn)^2+1));
end
figure
plot(f,v)
figure
plot(f,sensitivity)
```

BIBLIOGRAPHY

1. Walter Heywang, et al. Piezoelectricity. Springer-Verlag, Berlin Heidelberg, 2008
2. D.A. Berlincourt, et al. “Piezoelectric and piezomagnetic materials and their function in transducers”, Physical Acoustics, New York, 1964
3. S. O. R. Moheimani and A. J. Fleming, Fundamentals of Piezoelectricity. Piezoelectric Transducers for Vibration Control and Damping, Springer, London, UK, 2006.
4. T.L. Jordan. “Piezoelectric Ceramics Characterization”. ICASE Report No. 2001-28, 2001.
5. https://en.wikipedia.org/wiki/Piezoelectricity
6. Alper Erturk, et al. Piezoelectric energy harvesting. Wiley, 2011
7. Paul A. Lagace. Unit M4.4-Simple Beam Theory. MIT - 16.003/16.004, 2008
8. https://en.wikipedia.org/wiki/Euler-Bernoulli_beam_theory
9. Ansel C. Ugural, et al. Advanced Strength and Applied Elasticity. Prentice Hall, 4th Edition, 2003
10. T. Bailey, et al. “ Distributed piezoelectric-polymer active vibration control of a cantilever”, AIAA J. Guidance Contr., Vol.6, pp. 605-611,1985
11. Y. Sugawara, et al. “Metal-ceramic composite actuators”, J. Amer, Cerm. Soc, Vol. 75, No. 4, pp.996-998, 1992
12. Y. Liao, et al. “Model of a single mode energy harvester and properties for optimal power generation”. Smart Materials and Structures. 17 (6) (2008) 065026.
13. R. Xu, et al. “Screen printed PZT/PZT thick film bimorph MEMS cantilever device for vibration energy harvesting”. Sensors and Actuators A, 188 (2012) 383–388
14. Lim, C.W. “Three Dimensional Electromechanical Responses of a Parallel Piezoelectric Bimorph”. International Journal of Solids and Structures, 38(16):2833-2849, 2001

15. Qin, Lifeng, et al. “Fabrication and characterization of thick-film piezoelectric lead zirconate titanate ceramic resonators by tape-casting”. Ultrasonics, Ferroelectrics and Frequency Control, IEEE Transactions on 59.12 (2012): 2803-2812.

16. S.-L. Kok, et al. “Fabrication and characterization of free-standing thick-film piezoelectric cantilevers for energy harvesting”, Measurement Science and Technology 20 (2009).

17. A. Erturk, et al. An experimentally validated bimorph cantilever model for piezoelectric energy harvesting from base excitations, Smart Materials and Structures 18 (2) (2009) 025009.

18. H.-B. Fang, et al. “Fabrication and performance of MEMS-based piezoelectric power generator for vibration energy harvesting”, Microelectronics Journal 37 (2006) 1280–1284.

19. Lee A. Christel, et al. “Vibration Rectification in Silicon Micromachined Accelerometers”. IEEE, 1991

20. Kovacs, A. “Structural Parameter Sensitivity Analysis of Cantilever- and Bridge-type Accelerometers”. Sensors and Actuators A, 89:197-205, 2001

21. Liao, W.H., et al. “Wireless Monitoring of Cable Tension of Cable-Stayed Bridges Using PVDF Piezoelectric Films”. Journal of Intelligent Material Systems and Structures, 12:331-339, 2001

22. Jan G. Smits, et al. “The constituent equations of piezoelectric bimorphs”. Ultrasonics Symposium, IEEE, 1989

23. Chang, Wenyang,et al. “Physical characteristics of polyimide films for flexible sensors”, Applied Physics A (2008) 92: 693–701

24. Jan G. Smits. “Dynamic Admittance Matrix of Piezoelectric Cantilever Bimorphs”, Journal of Microelectromechanical Systems, IEEE, 1994

25. J Ajitsaria, et al. “Modeling and analysis of a bimorph piezoelectric cantilever beam for voltage generation”. Smart Materials and Structures. 16 (2007) 447–454

26. Park, C.H. “On the Circuit Model of Piezoceramics”, Journal of Intelligent Material Systems and Structures, 12(2001):515-522

27. T.H NG, et al. “Sensitivity Analysis and Energy Harvesting for a Self-powered Piezoelectric Sensor”. Journal of Intelligent Material Systems and Structures, Vol.16, 2005

28. S Roundy, et al. “A piezoelectric vibration based generator for wireless electronics”. Smart Materials and Structures. 13(2004) 1131-1142

29. Wang, Q.M. and Cross, L.E. 1999. “Constitutive Equations of Symmetrical Triple Layer Piezoelectric Benders,” IEEE Transactions on Ultrasonics, Ferroelectrics, and Frequency Control, 46(6):1343-1351

30. Mo, Changki, et al. “Behaviour of a unimorph circular piezoelectric actuator”. Smart Materials and Structures. 15(2006) 1094-1102

31. Sungwan Kim, et al. “Piezoelectric Energy Harvesting with a Clamped Circular Plate: Analysis” , Journal of Intelligent Material Systems and Structures, Vol.16, 2005

32. R.G. Ballas, Piezoelectric Multilayer Beam Bending Actuators, Springer, 2007.